

COMPUTER AIDED DESIGN
FOR
COLOR APPEARANCE

A DISSERTATION
SUBMITTED TO THE FACULTY OF THE GRADUATE SCHOOL
OF THE UNIVERSITY OF MINNESOTA
BY

Clement Shimizu

IN PARTIAL FULFILLMENT OF THE REQUIREMENTS
FOR THE FINAL DEFENSE OF DEGREE OF
DOCTOR OF PHILOSOPHY

Advisor: Gary W. Meyer

SUMMER 2009

Acknowledgements

First, I can't thank my advisor, Gary Meyer, enough for taking a chance on me. Thank you for revealing the symbiosis between art, design, color, and science to me. Most of all, thanks for giving me a long leash. My heartfelt gratitude goes to Ford, DuPont, Benjamin Moore, the UMN Office for Technology Commercialization, the DTC, and the University of Minnesota Computer Science Department for generously funding my education. I am grateful to Victoria Interrante, Barbara Martinson, and John Riedl for participating in the thesis committee. I would like to recognize my classmates including Seth Berrier, Joseph Cherlin, Andrew Drenner, Jonathan Konieczny, Natalie Linnell, Brian Riese, Collin Scott, Jared Windsheimer, and the everyone from the graphics group.

My utmost appreciation goes to Patrick Chong, Alan Eggly, Kevin Ellwood, David Fischer, Jon Hall, Jim King, Susan Lampinen, Carl Minchew, Mark Nichols, Jeffery Nowak, Allan Rodriguez, and Erika Woelfel for granting me the rare opportunity to see first hand the secret inner workings of the color and appearance industry. Much credit to NVIDIA for supplying me with the excellent graphics hardware and sample code that made my research possible. Highest praise goes to Nick Golfis, Kate Iverson, and Molly Roark for producing the fantastic art and designs in Chapter 3.

Outside of school and research, I am deeply indebted to my family especially Agnes, Michio, Dominique, and Jerome for supporting me financially. Finally, high fives to my friends for their encouragement and support over the years, including Renee Bartley, Bucho, Catherine Campion, David Donnelly, Erik Holtzapple, Matt Kneen, Dave Krazzan, Ben Merrill, Numi Bunny, Valarie Quintana, Kari Rightfoot, Michelle Speidel, Stephen Stephens, Carrie Shanahan, Jimmy Sommerfeld and family, Terri Swan, Timesquid, Jane Vevea and family, and Levi Yourchuck. Special thanks goes to D'nardo Colucci and the Elumenati.

Dedication

This dissertation is dedicated to the artists, designers, and other creative people in my life.

Abstract

This research documents the creation and application of the first complete computer aided design system for color appearance. Although computer graphics and computer aided design are commonly used for geometric shape design, there are few computer tools for the design of color appearance and surface finish. Advances in computer graphics technology make it possible to create color appearance design tools analogous to those available for object and surface design. In this thesis, the fundamental components of computer aided geometric design (CAD) are applied to computer aided color appearance design (CACAD) including visualization, design, analysis/optimization, and scanning/prototyping tools. The problem domain was metallic and pearlescent automotive finishes, but the system architecture could be applied to other problems in color appearance design.

We develop a CACAD program for designing hypothetical goniochromatic colors by creating a design interface for a model of appearance. This interface controls all of the aspects of a metallic surface finish relevant to the designer including gloss and color shift. We suggest a rendering engine that combines the interactive control of a reflection model with the complex real-time lighting provided by an environment map. This allows the user to interactive design a reflection model and see the changes immediately on a fully lit 3D

object. Creative design interfaces are proposed that allow color stylists to take advantage of their training in the fashion, art, and other design industries. We illustrate the power of creative BRDF design interfaces by creating a virtual mood board that allows direct selection of the reflection model parameters from pictures, an image based BRDF tweaker for adjusting color appearance directly on a 3D object, and a sketch based design interface that can work with hand drawn concept art.

We study the color mismatches that result from geometric misalignment and why they are accentuated by the use of metallic and pearlescent paints with goniochromatic properties. We propose a metric for determining when the color difference is large enough for the misalignment to become apparent and illustrate a technique for selecting a paint that matches the adjacent part and creates the illusion of geometric continuity even though the two parts are misaligned. Finally, the CACAD system was connected to a paint formulation system to formulate and generate physical samples of color and surface finish designs in the same fashion that 3D printers can fabricate physical objects from CAD specifications. A series of experiments demonstrate the CACAD system’s maturity by showing that it is effective at designing and formulating paints in a wide variety of real world situations.

Table of Contents

Acknowledgements	i
Dedication	ii
Abstract	iii
Table of Contents	v
List of Figures	viii
1 Introduction	1
1.1 CAD vs. CACAD	3
1.2 Thesis overview	6
1.2.1 Computer aided color appearance design using environment map based lighting	6
1.2.2 Color styling tools	7
1.2.3 Geometric color matching issues in metallic paints	8
1.2.4 Rapid color prototyping	9
2 Computer aided color appearance design using environment map based lighting	10
2.1 Introduction	11
2.2 Background work	13
2.2.1 Rendering the metallic reflection model under point light illumination using shaders	13
2.2.2 Background on environment map based lighting	15
2.3 BRDF Representation	17
2.3.1 Basis BRDFs	18
2.3.2 Optimal basis functions	19
2.4 Real-time BRDF fitting	24
2.5 Rendering	28

2.5.1	Prefiltered environment maps	29
2.5.2	Realtime shader	30
2.5.3	Anisotropic Gaussian model	32
2.6	Remarks	35
3	Color styling tools	37
3.1	Introduction	39
3.2	Relevant work	42
3.3	Hierarchy of reflection models	43
3.3.1	Face/Flop/Travel/Gloss form	44
3.3.2	Parametric form	46
3.3.3	Aspecular measurements	48
3.3.4	Conversions between models	49
3.4	Interactive goniochromatic color design interface	50
3.4.1	Data point editor	52
3.4.2	Hue, saturation, and brightness control	53
3.4.3	Face, flop, and travel color picker	54
3.4.4	Variations control	56
3.4.5	Gloss control	57
3.4.6	Color pallet	58
3.5	Virtual mood board	59
3.5.1	Interface	63
3.5.2	Face/flop eyedropper	65
3.5.3	Gloss eyedropper	67
3.6	Image based BRDF tweaker	68
3.6.1	Tools and mode of operation	69
3.6.2	Making adjustments	71
3.7	Sketch based color styling	75
3.7.1	Setup	78
3.7.2	Artist interaction	78
3.7.3	Fitting	79
3.7.4	Results	81
3.7.5	Extension to environment mapped based lighting	83
3.8	Evaluation	84
3.9	Conclusions	86
4	Predicting and fixing geometric color mismatches	88
4.1	Introduction	90
4.2	Background	90
4.3	Goniogeometric index	91
4.3.1	Formulation	92

4.3.2	Application to solid paints	94
4.3.3	Application to metallic paints	95
4.4	Inverse trompe l’oeil	97
4.4.1	Diffuse paints	98
4.4.2	Metallic paints	100
4.5	Conclusion	103
5	CACAD for rapid color prototyping	104
5.1	Introduction	105
5.2	Background	108
5.2.1	Shading hardware/software	108
5.2.2	BRDF/Envmap	109
5.2.3	CACAD/automotive rendering	110
5.2.4	Color styling tools	110
5.3	Tools	111
5.3.1	XML file format	112
5.3.2	SpectraMaster book	112
5.3.3	Virtual SpectraMaster color library	113
5.3.4	ColorNet	120
5.3.5	ColorSnap	120
5.4	Results	123
5.4.1	Ford Design	124
5.4.2	College for Creative Studies	126
5.4.3	Automotive Engineering	130
5.4.4	UM Architecture/HouMinn Practice	130
5.5	Conclusions	132
6	Conclusions	134
	Bibliography	138

List of Figures

1.1	The major components of CAD.	2
1.2	The major components of CACAD.	4
1.3	An interactive design program was developed that allows the user to manipulate the parameters of a metallic paint reflection model. The program has an interface that provides the user with intuitive color controls (left) and permits them to see the appearance of the paint, as it is modified, in a complex lighting environment (right).	6
2.1	The software presented in this chapter is the main visualization component of the CACAD package.	10
2.2	Because of the metallic nature of automotive paint, three or more tristimulus measurements are necessary to characterize its appearance. Traditional methods of picking color are extended to deal with metallic paint as a trajectory through color space instead of a single point.	18
2.3	The diffuse lobe plus the five basis lobes chosen to be the optimal basis lobes in approximating the BRDF database.	20
2.4	The cosine exponents chosen by the nonlinear optimization routine to be the optimal basis functions.	21
2.5	The error in the choice of basis functions used to fit the BRDFs in the database.	23
2.6	Three slices of the target BRDF (above) are compared to the approximation using seven basis lobes(below) are lit from 10, 40, and 70 degrees(left to right).	27
2.7	The photographically acquired HDR environment map is prefiltered by the set of cosine lobe basis functions shown in Figure 2.3.	28
2.8	Rendering measured and designed automotive paint BRDFs.	30
2.9	Graph of an anisotropic BRDF viewed from 45 degrees off normal.	33

2.10	Reconstructing the reflection using multiple off specular cosine lobes: 15 lobes, 35 lobes, 81 lobes, actual(left to right).	33
2.11	Designed anisotropic reflections.	36
3.1	The software presented in this chapter is the design interface component of the CACAD package.	37
3.2	A diagram illustrating how the four components of the metallic reflection model relate to the shape of the BRDF. The light L is at 45° from normal N. The specular direction is labeled S.	45
3.3	An interface for directly manipulating face, flop, travel, and gloss. The L vs. aspecular angle plot illustrates how the parametric form interpolates face at 15° and flop at θ_{clamp}	46
3.4	This figure summarizes the three reflectance representations, their primary uses, and conversion pathways between representations.	50
3.5	The user interface.	51
3.6	Hue and saturation control.	53
3.7	Modifying a color by its control points.	54
3.8	The color corresponding to Figure 3.7.	55
3.9	Variations on the face color.	56
3.10	Variations on the flop color.	57
3.11	A three dimensional color pallet.	58
3.12	The automotive speed shape's color and travel were directly selected from a Dior fashion advertisement.	60
3.13	In the aesthetic design fields, mood boards are used extensively for material and color selection. The process might start out with a stylist collecting images from fashion magazines and other visually appealing artifacts. The art director of a style and fashion magazine was invited to participate in the user study. She proposed "Orange Ball of Paris" that appeals to a young and fashionable audience.	61
3.14	Inspired by the sporty fashion trends of California's Orange County, another mood board was created for a color called "Hydrogen Blue in the OC" for a hydrogen powered concept car.	62

3.15	A designer was instructed to create a virtual mood board relevant to a hydrogen concept vehicle (left). Designers arrange inspirational images for material concepts on the mood board. They select the 15° face color and θ_{clamp} flop color using eyedroppers. The rendering on the right is of a material seeded by the colors in the butterfly's wings.	63
3.16	Although the spatial distribution of velvet is not captured from this image, the system still duplicates the color appearance.	66
3.17	The original color looks a little too dull on the bottom left edge of the object. The stylist positions the crosshair over this area and increases saturation and brightness (left). A shader renders aspecular angle to an off screen buffer to assist mapping adjustments from image-space to BRDF space (center). By indexing into the buffer with the crosshair coordinates, the system calculates that the color should be adjusted at 78.3° (right).	70
3.18	The left shows the heads up display over an auto speed shape. Specific aspecular angles in image space are correlated to positions on a graph of the BRDF for this illustration (right).	72
3.19	The concept artist traced the outlines of a rendering onto a new sheet of paper. Next, he used colored markers to fill in the outlines with his concept color. This artwork was scanned back into the system using a flatbed scanner, and Photoshop was used to align the scanned artwork with the existing scene. The algorithm matched a pink pearlescent color to his concept art.	76
3.20	The initial image (left) was manipulated in Photoshop by rotating the hue to create the goal image (middle left). The least squares fitting routine found a close match (middle right). A contrast enhanced difference image visualizes the error (right).	81
3.21	The initial image (not shown) was printed to a hardcopy. The artist created his concept art by tracing the image and filling in with markers onto a new sheet of paper (top). A rendering of the final match is shown (bottom). Color samples in Lab space show that the computer's fit to the hand drawn image is not perfect, however it is a good match visually.	82
4.1	The software presented in this chapter are the design by optimization and computer aided analysis components of the CACAD package.	88

4.2	Color difference occurs between misaligned body panels. Because color and intensity vary with reflection angle for metallic and pearlescent paints, the effect is stronger for these goniochromatic colors (right) than for solid colors (center).	89
4.3	Variation of color difference between panels as a function of viewing position, light source position, and geometric misalignment.	96
4.4	Determining a solid color for the bottom half of each panel that matches the top half of the panel even though the two halves are misaligned by 3 degrees. Each row represents a different light source direction and each column a different solution technique. See text for details.	98
4.5	Finding a silver color that matches another silver color even though the two paints are on panels that are misaligned by 3 degrees. Color difference A results when the paints are identical, and the decreased color difference B occurs when there are dissimilarities between the face color and the travel for the two paints.	100
4.6	Bumper and fender misaligned by 8 degrees. Identical metallic paints cause a color mismatch (left) while painting the bumper a different color, determined using the inverse trompe l'oeil technique, eliminates the problem (right). . .	101
4.7	(left) Goniogeometric mismatch between the misaligned fender and the bumper in Figure 5 when they are both painted the same color. (right) Comparison between the BRDF for the original paint (top) and the BRDF for paint found using the inverse trompe l'oeil technique (bottom).	102
5.1	The research presented in this chapter connects the CACAD software package to and from the physical world.	104
5.2	The Virtual SpectraMaster Color Library shown as a thumbnail preview, rendered with environment map based lighting, along with the paint code. The entire collection of over 3,000 metallic and pearlescent paints is shown on the left. Sliders allow the user to filter the selection of colors to, for example, colors with high chroma travel(right).	113
5.3	The Virtual SpectraMaster Color Library follows the intuitive hierarchical organization the physical book uses to categorize six thousand solids, metallics, and pearls.	114

5.4	The distribution of flop indices for the solids, metallics, and pearls in the SpectraMaster database. Solid colors have a Flop Index of 0. Ignoring solids, the average Flop Index in the database is 11.38. Over 96% of colors have a Flop Index between 0 and 20.	116
5.5	This shows GM044 that has a Chroma Index of 46 Δ Es.	117
5.6	This shows YM144 that has a fairly high Hue Shift Index of 12.6 Δ Es. . . .	118
5.7	This shows BM304 that has a higher Flop Index of 16.6 but a low Chroma Index of 5.6 Δ Es.	119
5.8	This shows GM027 that has an extreme Hue Shift Index of 19.8 Δ Es. . . .	119
5.9	Screen shots of ColorSnap: A designed metallic red is shown relative to the nearest metallic color in the SpectraMaster database (left). A bright diffuse yellow color design is shown relative to the nearest solid color in the SpectraMaster database (right).	121
5.10	ColorSnap's visualization exposes two problematic color designs. The designed color on the left is too deep in saturation and shows up hanging far outside range of colors in the collection. The nearest match, RM209, is the correct hue, but not chromatic enough. The designed color on the right has a unusual off-radial travel. The closest match does not capture the hue-shifting nature of the design.	122
5.11	ColorSnap's visualization reveals that the designed color has a brighter face and a darker flop than the nearest match (left image). The rendering shows the designed color on the left side of the cylinder and the closest match, RM331, on the right side of the cylinder (right image).	123
5.12	Experimental setup for the rapid color prototyping experiment at DuPont. .	124
5.13	Ford Design Center color test.	125
5.14	Ryan Abellera's gold truck.	126
5.15	Sarah Montgomery's mood board.	127
5.16	Sarah Montgomery's car with color selected to match fashion stockings. . .	127
5.17	Victor Fernandez's concept art	129
5.18	Victor Fernandez's car with custom paint.	129
5.19	The BRDF Design Suite was employed by a paint engineering group at a major automotive manufacturer to redesign an old silver paint (left) to a new silver paint (right) to better compete with their competitor's selection. .	130
5.20	UM architecture façade.	131

Chapter 1

Introduction

Since their inception, computer graphics and computer aided design have been used to define the shapes of surfaces and the geometry of objects. These computer programs have made it possible to almost completely virtualize the mechanical design of automobiles, airplanes, and buildings. However, similar computer tools are not yet available to assist in the design of new color appearances and surface finishes for the exterior and interior components of these geometric systems.

Traditionally, the design and color forecasting of industrial surface finishes, like automotive paint, requires mixing physical samples of paint, applying the paint to evaluation surfaces, tweaking the paint formulations, and remixing until the desired appearance is achieved. This is an expensive and time consuming process. Computer tools were not used for two reasons. First, the standard reflection models employed in computer graphics tools were too limited to approximate complex surface finishes realistically. Second, any system capable of generating realistic images was unsuitable for use as an interactive design tool – the image took too long to generate once a new color was selected.

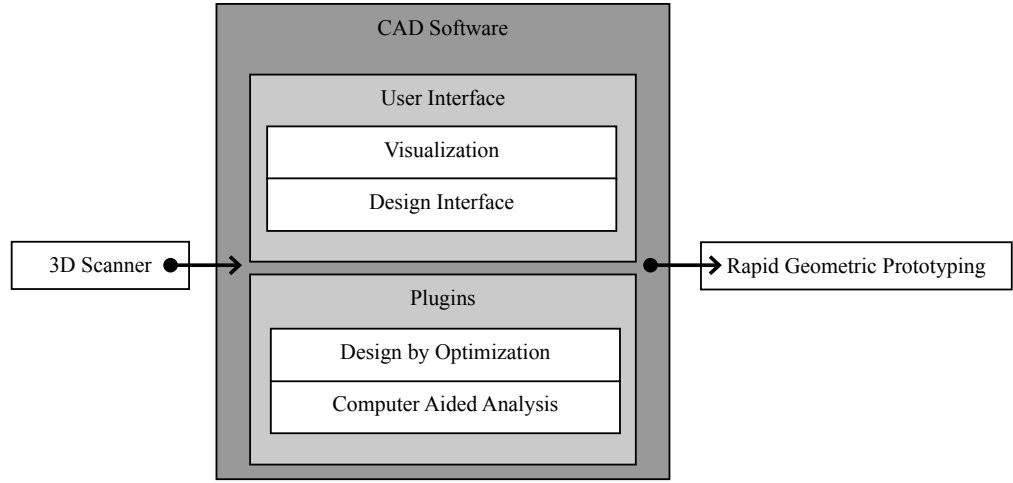


Figure 1.1: The major components of CAD.

Recent advances in computer graphics hardware and software are making computer aided color appearance design (CACAD) possible [37]. CACAD is computer aided design for color appearance. CACAD tools have the potential to help the color appearance industry in the same way that CAD tools have helped engineers. Yet color and material designs are still often done with non electronic tools because CAD packages for color appearance design are not currently available.

A complete computer aided color appearance design package would have all of the types of tools that are available for geometric CAD, but tuned for designing color. The contribution of this thesis work is a complete working CAD system for color appearance design. This was tackled by breaking the problem down and creating the separate components of a CACAD system one at a time. Along the way, this approach allowed for contributions to both color science and computer graphics.

1.1 CAD vs. CACAD

Computer aided design (CAD) describes the use of computer workstations to design objects. CAD was the original killer application of computer graphics and has since become a mature and feature rich technology. The most common application of CAD is to design the geometrical shape of objects. Therefore, in CAD software it is important for the software to be able to depict the important geometric characteristics realistically and visualize those changes as the shape is interactively designed. Once a design is represented digitally, computer aided analysis is employed by some advanced components of CAD, like finite element analysis, to detect potential issues with the cost or safety of a product. Design by optimization is also used to minimize or maximize aspects of a design, such as efficiency. 3D surface scanners, like 3D laser range finders, are used to import geometric data from the physical world. Finally, rapid prototyping machines, like CNC milling machines or 3D plotters, are used to create physical mockups. See Figure 1.1 for an illustration of the major components of CAD.

We illustrate the CACAD analogs to CAD in Figure 1.2. In CACAD the design software must manipulate appearance rather than shape. In CACAD, it is important for the software's rendering engine to be able to depict the important color appearance characteristics realistically and visualize those changes as the material is interactively designed. Instead of using computer aided analysis to detect potential issues with the efficiency or safety of a product, CACAD must detect potential undesirable aesthetic issues. Instead of using design by optimization to minimize or maximize aspects of a design, such as cost or

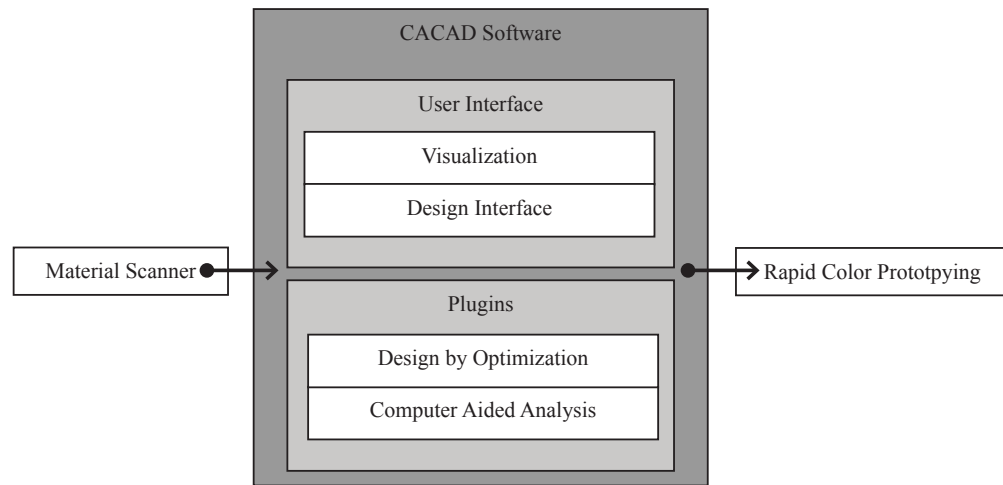


Figure 1.2: The major components of CACAD.

efficiency, CACAD applies computer optimization to minimize or maximize factors affecting aesthetics. Instead of 3D surface scanners, the system must import appearance data from hardware such as goniospectrophotometers or gloss meters. Finally, instead of creating physical mockups with rapid prototyping machines, CACAD must create prototypes of designed appearance by using paint formulation and mixing systems.

The combined components of the research presented in this thesis are the first complete working CACAD system. At the beginning of Chapters 2 through 5 we duplicate Figure 1.2 and highlight the component of the CACAD system that the chapter represents. To limit the scope of the problem, this research focuses on the aesthetic challenges facing the automotive industry. Automotive styling is, along with art, graphic design, and fashion, one of the most important color design problems. In the automotive industry, interior and exterior styling are equal to engine performance and handling as a driving force of sales. A significant amount of research and development costs for automobiles are in the aesthetics of color and

materials. Automobile designers sculpt character and evoke emotional response by how they differentiate aesthetic design. Finally, avant garde designs of concept cars are frequently embraced as a new trend, and their influence can eventually trickle down into other consumer product designs such as housewares and appliances. In addition a CACAD software package for the design of automotive finishes is directly applicable to other consumer design problems because the range of solid and metallic finishes that are used in automobile design represent a large fraction of the types of surface finishes found on most consumer products. Although automotive aesthetics is a very specific problem domain, it is also a far reaching and open groundwork from which the concepts of CAD for color appearance design, applied to many consumer products, can be fully explored.

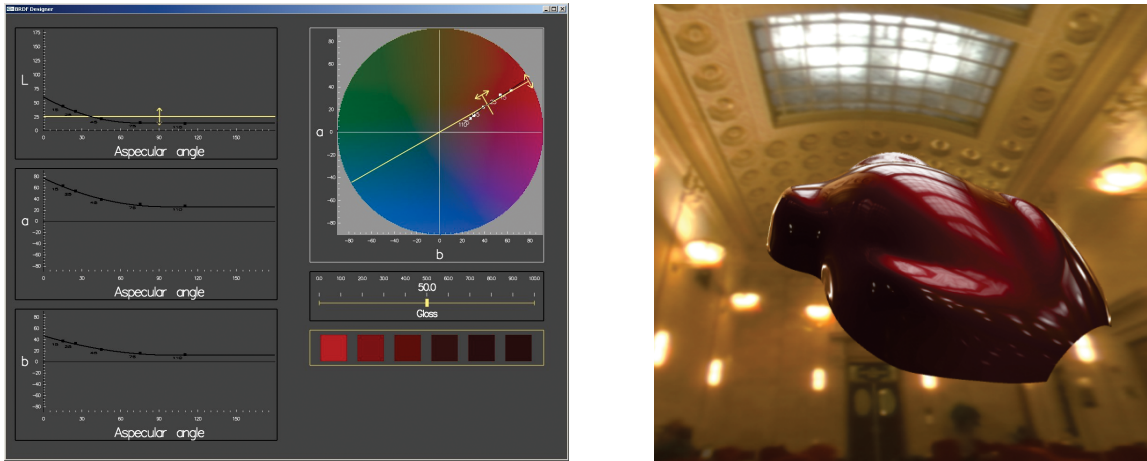


Figure 1.3: An interactive design program was developed that allows the user to manipulate the parameters of a metallic paint reflection model. The program has an interface that provides the user with intuitive color controls (left) and permits them to see the appearance of the paint, as it is modified, in a complex lighting environment (right).

1.2 Thesis overview

This section gives an overview of the thesis components related to the creation and application of a complete working CACAD suite for automotive finishes, the *BRDF Design Suite*. The BRDF Design Suite is a set of interactive programs that have been developed to assist in the design, visualization, analysis, and manufacture of new goniochromatic paints. Although the programs themselves are a subset of the work described in this dissertation, the BRDF Design Suite showcases the research results that have been achieved.

1.2.1 Computer aided color appearance design using environment map based lighting

Lighting is important for evaluating the aesthetic appearance of gloss, metallic, pearlescent, and color-shifting effects. A component of the design suite titled the *BRDF Viewer* employs complicated lighting environments for evaluating these paint effects.

At the time the BRDF Viewer was created, there was no way for doing interactive design of BRDFs in complex lighting environments. In Chapter 2 we develop a BRDF approximation suitable for interactive color appearance design in direct lighting provided by environment maps. The BRDFs are approximated as a linear combination of cosine lobes with a fixed set of specular exponents. A nonlinear optimization routine is used to fit the cosine lobes to BRDFs appropriate for a specific color appearance design application: automotive paint. Modification and rendering of the BRDF is made possible by linearly combining prefiltered environment maps for each cosine lobe in real time. This algorithm is implemented as a rendering engine for the BRDF Viewer to produce images of an automobile at the same time that the surface color of the car is being interactively designed.

1.2.2 Color styling tools

The first half of Chapter 3 describes a program titled the *BRDF Designer*, shown in Figure 1.3, that is the central component to the BRDF Design Suite. The BRDF Designer is a tool for manipulating a reflection model for car paint that is based on industry standards for measuring the appearance characteristics of the paint. These measurements include gloss for the clearcoat and three aspecular measurements for the metallic basecoat. This program interface provides a means for altering the reflectance properties of the paint.

The programs give the user a unique set of controls over a second order polynomial that defines these color families at a sequence of aspecular reflection angles. One approach, based on traditional metallic colors, allows the user to adjust the average hue, saturation, and brightness of all of the colors interpolated by the polynomial. Another method, appropriate

for the newer effect colors, permits the designer to establish face and flop colors to be reached at either end of the interpolation. In a final technique, variations produced by adjusting model parameters can be evaluated and selected.

Because the users of computer aided color design tools often have training in the arts, fashion, and other creative industries, technical CAD interfaces cannot take full advantage of the user's unique creative training. The second half of Chapter 3 proposes a set of computer graphic tools to facilitate color design in the traditional aesthetic design fields. We suggest a new reflection model that covers the widest range of color appearances encountered by designers including solid colors, metallic colors, and the glossiness of these colors. The reflection model is constructed to have the minimum number of free parameters and to select these parameters so that they correspond to color specification terms familiar to designers such as face color, flop color, travel, and gloss. The model is defined in a way that allows it to be used as a manufacturing specification for the final color. We also demonstrate how the reflection model can be used to develop effective interfaces for designers. We create a mood board that allows direct selection of the reflection model parameters from pictures. Next, we describe a novel color design interface for tweaking color and appearance directly on a 3D surface. A sketch based design interface is also developed that permits the reflection model parameters to be set from non-photorealistic illustrations.

1.2.3 Geometric color matching issues in metallic paints

Problematic color mismatches that result from geometric misalignment are studied in Chapter 4. Differences in color can result when adjacent parts of an object are coated with the

same paint but are not aligned to create a continuous geometric surface. The color difference that results due to shading can be accentuated by the use of metallic and pearlescent paints with goniochromatic properties. A metric is developed for determining when the color difference is large enough for the misalignment to become apparent. A technique is also presented in this chapter for selecting a paint that matches the adjacent part and creates the illusion of geometric continuity even though the two parts are misaligned.

1.2.4 Rapid color prototyping

CACAD has the potential to eventually generate physical samples of color and surface finish designs in the same fashion that 3D printers, stereolithography machines, computer controlled laser cutting machines, and other solid freeform fabrication devices can create physical objects from CAD specifications.

We partnered with DuPont to create the physical bridge between designing paints on the computer and fabricating physical prototypes of them. The desired aspecular measurements for paints designed in the BRDF Design Suite can be input to a paint formulation system so that the paint can be manufactured. Tests of the system repeatedly show good correspondence between designed and fabricated paints.

Chapter 5 titled *Rapid Color Prototyping* describes progress we have made in providing rapid prototyping tools to the color appearance industry. The CACAD system and paint formulation system are tested in real design situations including automotive styling and architectural design. Tools for searching color databases and other supporting CACAD software are also developed.

Chapter 2

Computer aided color appearance design using environment map based lighting

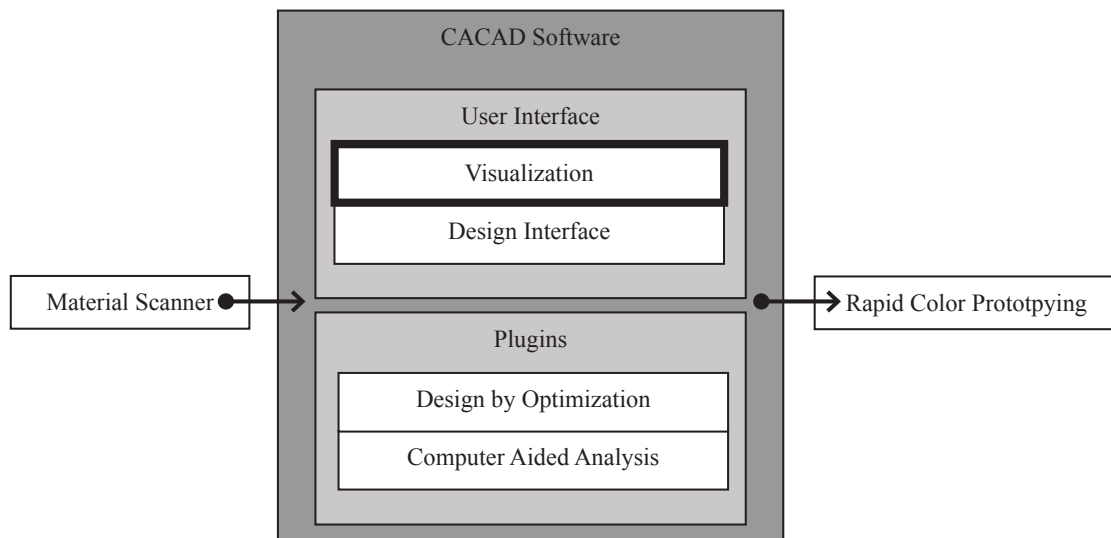


Figure 2.1: The software presented in this chapter is the main visualization component of the CACAD package.

Abstract

A BRDF approximation is developed that is suitable for interactive color appearance design in direct lighting provided by environment maps. The BRDFs are approximated as a linear combination of cosine lobes with a fixed set of specular exponents. A nonlinear optimization routine is used to fit the cosine lobes to BRDFs appropriate for a specific color appearance design application: automotive paint. Modification and rendering of the BRDF is made possible by linearly combining prefiltered environment maps for each cosine lobe in real time.

2.1 Introduction

The recent development of pixel shading hardware and software has dramatically increased the control that a user has over the color appearance of a computer graphic object. Rather than being limited to a single simple hardwired reflection model, the shading model appropriate for the desired color appearance can be programmed, and it will automatically be evaluated at each pixel on the object's surface. In addition, it is possible to change the parameters of this reflection model in real time. The ability to interactively adjust the simulation of light reflection from a surface makes it possible to design the color appearance of an object. If the reflection model accurately simulates a real paint or surface coating then a new type of CAD, computer aided color appearance design or CACAD, becomes possible [37].

Parts of this chapter have been previously published by the author in *Proceedings Computational Aesthetics '05* [52].

The evaluation of an object’s color appearance is improved by making the lighting as realistic as possible. Correctly simulating the direct illumination provided by distant area light sources, including the sky, can have a major impact on an object’s overall color appearance. This more realistic lighting can be introduced, while still maintaining interactive frame rates, by using pre-filtered environment maps [25] or spherical harmonics [26]. Although it involves a time-consuming offline computation for each set of reflection model parameters, the extra overhead is not a problem for many computer graphic applications because the reflection model doesn’t change during the simulation. However, it presents a major obstacle for the interactive CACAD program described above.

The goal of the research described in this section is to develop a CACAD program that combines the interactive control of a reflection model, implemented as a pixel shader, with the complex real-time lighting provided by an environment map. The approach begins with the assumption that the final tool is intended to solve a specific problem: the design of new automotive finishes [54]. This leads to the selection of a reflection model appropriate for automotive paint in which just a few BRDF measurements are taken and a low order polynomial is used to interpolate the data [65]. Given these important but practical restrictions, it is assumed that the space of bi-directional reflection distribution functions (BRDFs) generated by the automotive paint reflection model can be spanned by a set of basis BRDFs. If a basis BRDF can be rendered with global illumination interactively, then it is possible to render images of the combination of basis BRDFs interactively. If it is possible to rapidly compute how to combine the basis BRDFs to approximate a target BRDF, the target BRDF can be continually changed while generating images of it.

2.2 Background work

Before discussing how the metallic reflection model was implemented in the CACAD suite, some background is provided on the development of computer graphics shading hardware. Until recently, computer graphics shading hardware was quite limited in its capabilities. There was only a single simple reflection model available (the Phong model), this model could only be evaluated at the vertices of a triangular mesh, and the interior of each triangle had to be filled in by interpolation. This shading approach, called Gouraud shading, was good enough for traditional computer aided geometric design, but it is too limited for CACAD. Real-time rendering of arbitrary reflection models under complex illumination is required for CACAD.

2.2.1 Rendering the metallic reflection model under point light illumination using shaders

Many graphics engines make use of hardware accelerated programmable shaders that allow an arbitrary shading model to be evaluated, on every refresh cycle, at each pixel of the display screen. Development tools permit the shader to be written in a portable high level language similar to C and compiled into machine language. Some of the standards that have emerged for writing vertex and pixel shaders are NVIDIA CG [33], GLSL, and HLSL.

A programmable shader has two separate parts: a vertex shader and a pixel shader. The vertex shader has access to the vertex position, vertex normal, transformation matrices, and light position, as well as user definable per vertex and per object parameters. The vertex shader's input parameters are evaluated at the vertices of an object's triangle mesh. The

vertex shader's output values are interpolated across the inside of each mesh triangle, and the pixel shader takes these values as input and evaluates the rest of the reflection model. In addition, the pixel shader can access texture maps and environment maps. The final color for the pixel is rendered to the screen by the pixel shader.

A simple point light implementation of the metallic reflection model, to be discussed in Section 3.3, makes extensive use of programmable shaders. A vertex shader is used to evaluate the second degree CIE Lab polynomials and to convert the Lab values to RGB space.

As a three-dimensional object is rendered, the triangles it is composed of are sent to the vertex shader. The vertex shader takes as inputs the Lab polynomial, the vertex position, vertex normal, viewer direction, and the light direction. The aspecular angle between the viewer and the reflected direction of the light source is computed. The aspecular angle is clamped to be between zero and the clamp point of the Lab polynomials. This clamped aspecular angle is used to evaluate the Lab polynomial. Noting the reference white point, the Lab values are converted into XYZ space. Noting the monitor's white point, phosphor chromaticity, and gamma, the XYZ values are converted to RGB. The RGB color and the vertex normal is output to the pixel shader.

As vertices of the triangles are sent through the vertex shader, the vertex shader's output values are interpolated across the inside of the triangles and passed to the pixel shader. The pixel shader computes the reflected vector from the viewer and uses this to compute the specular highlight for the current gloss value. Finally this specular color is mixed with the interpolated vertex color and rendered to the screen.

Programmable shaders are a big step forward in making CACAD a reality. If a programmable shader can model a complex color appearance, it can interactively render objects that have this color appearance. Since programmable shaders can be passed variables, the interactive design of complex color appearances becomes possible. In the case of point light illumination, it is as simple as evaluating the parametric form of the reflection model in a shader. However for real appearance design work to take place, color appearance must be evaluated under complex lighting. Evaluating the appearance of an arbitrary reflection model under complex illumination is not trivial as in the case of evaluating it under point light source.

2.2.2 Background on environment map based lighting

The appearance of a surface can be thought of as a convolution between the BRDF and the distant lighting environment. This convolution is costly but can be precomputed. The convolution between the lighting environment and the BRDF can be put into a prefiltered environment map [25]. These maps can be used for fast rendering. However, the prefiltering needs to be done every time the BRDF changes. If brute force is used, the convolution can take minutes to hours or more on high resolution environment maps. However, a costly convolution in the spatial domain becomes a multiply in frequency domain. Spherical harmonics are the frequency space representation of functions on the sphere. By representing the BRDF and lighting environment as spherical harmonics, the convolution can be done in real-time [26].

Material in this section represents the state of the literature at the time that the research described in this chapter was performed.

Although the convolution is fast, every time the BRDF is changed it needs to be converted to the frequency domain before it can be used. This becomes one integral for each frequency needed to represent the BRDF. This is especially slow for glossy surfaces because hundreds to thousands of frequencies are required to properly represent these reflectances.

Precomputed radiance transfer is a technique that can render low frequency BRDFs with interreflections and shadows in real-time [56]. However, the BRDF must be “baked in” to the preprocessed transfer and cannot be changed at run-time.

The Lafortune BRDF model in [28] is used to fit a summation of generalized Phong lobes to BRDF data. The representation ends up being simple, yet very expressive. It can capture off specular, retro reflections, and anisotropic qualities in BRDFs. However, computing the fit uses a nonlinear optimization routine that does not run in real-time.

McCool and Heidrich briefly mention creating a prefiltered environment map for each lobe and using these to render images of the BRDF in global lighting environments [36]. However, since the Phong exponent is a free variable in the BRDF fitting routine, the lighting environment must be prefiltered for each Phong lobe found.

Kautz et al. presented a hardware-accelerated prefiltering of environment maps that achieves interactive rates in [27]. This may be the only existing technique that is suitable for interactive BRDF design in global lighting environments. Prefiltering performance depends on environment map resolution and the BRDF used. For example, high gloss automotive finishes need high resolution environment maps. This would push the limits of the system. Secondly, the hardware used was incompatible with high dynamic range environment maps, and it has yet to be shown that real-time rates can be achieved with them.

Combinations of linear BRDF basis have been used to synthesize new BRDFs. Matusik, et al. presented a model for isotropic BRDFs based on densely acquired reflectance measurements from a database of BRDFs in [34]. A method for defining intuitive and perceptually meaningful parametrization was demonstrated that can be used to explore BRDFs.

McAllister et al. used a set of cube maps prefiltered with varying specular exponents to approximate the appearance of a spatially varying BRDF using the Lafortune representation [35]. By approximating the varying specular exponents as MIP-maps in a MIP-mapped cube map they achieved efficient rendering. However the goal of their approach was not design work and the fitting of the Lafortune representation was done offline.

2.3 BRDF Representation

Given the objectives of CACAD, the approach taken in this research is to approximate a designed BRDF as a linear combination of cosine lobes. The cosine lobes can be rendered under global illumination using prefiltered environment maps. Figure 2.3 illustrates the range shapes of the cosine lobes. Figure 2.7 shows an environment map prefiltered by the same cosine lobe basis functions. The cosine lobes are weighted and added together to approximate more complicated BRDFs.

The BRDF is represented as a linear combination of basis BRDFs. The BRDF representation uses a set of cosine lobes [45] with various specular exponents as the basis BRDFs. The cosine lobes are weighted and added together to approximate more complicated BRDFs. The BRDF representation is described in detail in this section.

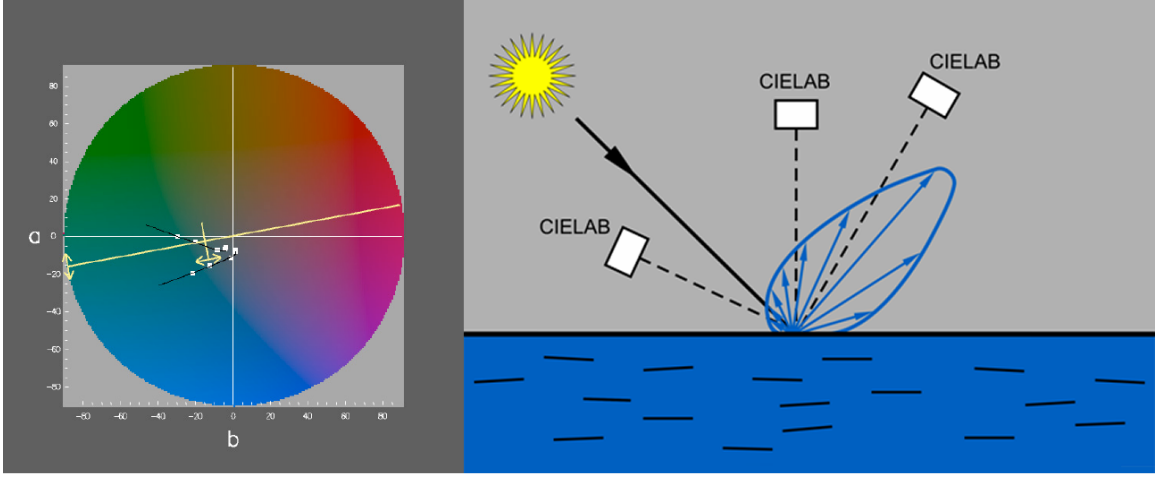


Figure 2.2: Because of the metallic nature of automotive paint, three or more tristimulus measurements are necessary to characterize its appearance. Traditional methods of picking color are extended to deal with metallic paint as a trajectory through color space instead of a single point.

The particular values for the cosine lobe specular exponents are chosen so as to best approximate the range of BRDFs that an existing CACAD system [54] can design (see Figure 2.2). The technique for deciding the optimal basis lobes uses nonlinear optimization and is described in detail in Section 2.3.2.

2.3.1 Basis BRDFs

This section describes the BRDF representation that is used in this work. The BRDF is represented as three parts: diffuse, directionally diffuse, and gloss. This is sufficient to describe the class of metallic automotive BRDFs explored in this work. These three parts are represented as a linear combination of basis BRDFs. Cosine lobes with various specular exponents are chosen to be the basis BRDFs. The diffuse color of the object is represented by K_D . The intensity of the diffuse lobe is dependent simply on the dot product between

the light \vec{L} and the surface normal \vec{N} as shown in Equation 2.3.1. The clamping of negative values to zero is not shown for simplicity.

$$Diffuse = K_D * \vec{L} \bullet \vec{N} \quad (2.3.1)$$

The directionally diffuse and glossy components are represented as the sum of a set of m cosine lobes with various specular exponents. The cosine lobes are defined to be the dot product between the direction \vec{R} of the light reflected off the surface and the view direction \vec{V} taken to a specular exponent E_i . The glossy component of the BRDF is due to the light that reflects off the first surface of the object. This is represented by a summation of the cosine lobes, scaled by K_{G_i} as shown in Equation 2.3.2.

$$Gloss = \sum_{i=1}^m K_{G_i} * (\vec{R} \bullet \vec{V})^{E_i} \quad (2.3.2)$$

The directionally diffuse color is the result of the light that penetrates through the glossy layer of the object. This is represented by a summation of the cosine lobes, scaled by K_{DD_i} . Since the directionally diffuse color is a subsurface effect, the sum is scaled by the dot product between the light \vec{L} and the surface normal \vec{N} as shown in Equation 2.3.3.

$$Directional = (\vec{L} \bullet \vec{N}) * \sum_{i=1}^m K_{DD_i} * (\vec{R} \bullet \vec{V})^{E_i} \quad (2.3.3)$$

The diffuse, directionally diffuse, and glossy components are added together to make the final color.

2.3.2 Optimal basis functions

This section describes a technique for choosing the optimal basis BRDFs. The particular values for the cosine lobe specular exponents need to be chosen so as to best approximate

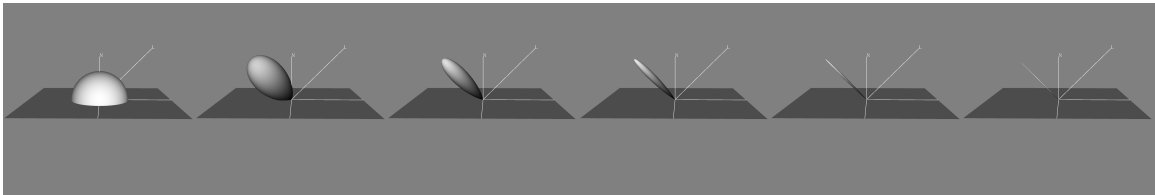


Figure 2.3: The diffuse lobe plus the five basis lobes chosen to be the optimal basis lobes in approximating the BRDF database.

the range of BRDFs that are likely to be used in a CACAD application. Although it is possible to hand pick the specular exponents of the basis functions, more accurate results can be obtained by using an optimization routine to automatically pick the optimal basis functions that best approximate a database of example BRDFs.

The specular exponents will be used in Section 2.4 as the basis functions that are weighted together to approximate a wide variety of designed BRDFs. Thus, it is necessary to have some cosine lobes with high specular exponents to represent glossy surfaces. In addition, some cosine lobes with low specular exponents are needed to represent rough surfaces with directionally diffuse reflectances. There is also the question of how many basis functions to use. There is a tradeoff between too many and not enough. A lot of basis functions can better approximate the range of BRDFs. However, too many will slow down the rendering system.

A database of example BRDFs is used to describe the range of BRDFs that are to be expected. The BRDFs in the database were created with a CACAD program for designing automotive paint. About thirty different paints were chosen to express the range of BRDFs that can be designed.

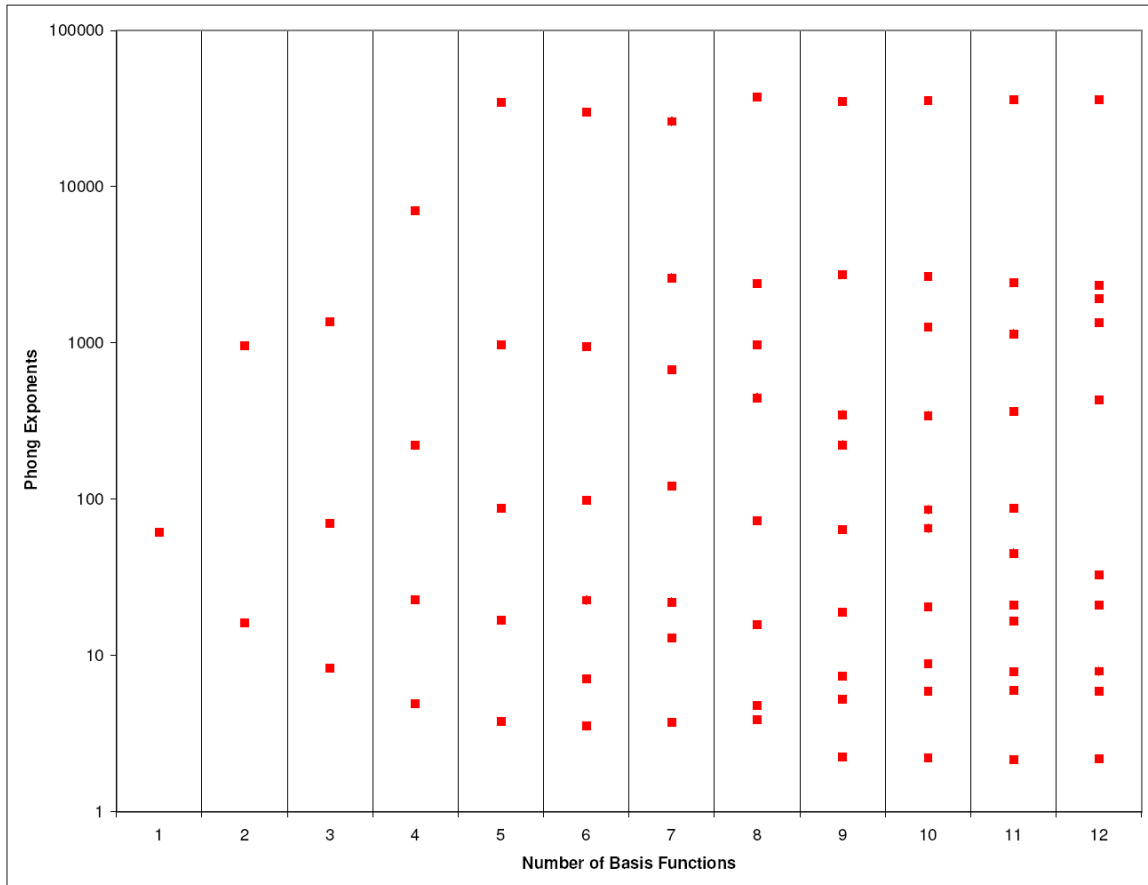


Figure 2.4: The cosine exponents chosen by the nonlinear optimization routine to be the optimal basis functions.

Principle function analysis can be used to pick the optimal basis functions that best approximate the range of BRDFs likely to be created with the BRDF Designer. This is a similar concept to principle component analysis.

To find the best specular exponents, linear optimization routines can not be used. Changing the specular exponent to a cosine lobe is a nonlinear operation, therefore linear optimization and least squares fitting can not be used.

Nonlinear optimization has been used in graphics for finding specular exponents. Eric Lafortune et al. used nonlinear optimization to fit multiple generalized cosine lobes to a measured BRDF in [28]. The technique used in this work is similar to Lensch et al.’s use of nonlinear optimization for finding the optimal basis functions to best represent spatially varying materials in [31].

Nonlinear optimization is used to find the best basis functions to approximate the BRDF database. Instead of fitting a set of cosine lobes to one BRDF, a set of cosine lobes is fit to a set of BRDFs in a BRDF database. A nonlinear optimization routine is employed to find the specular exponents of the cosine lobes in the set of basis BRDFs. Levenburg Marquart nonlinear optimization is used for the search [46].

One drawback of nonlinear optimization is that it is not guaranteed to find the optimal solution. Nonlinear optimization is very dependent on the initial guess and gets stuck on locally maximal solutions. Much supervision is required in order to successfully apply nonlinear optimization. By finding one optimal basis function for the BRDF database and adding lobes one at a time, the optimal basis lobes already found can be used as part of the initial guess when adding more lobes.

The function $f(E)$ that is minimized is a function that evaluates the error in the choice of basis functions. The set of m cosine basis lobes E_1, E_2, \dots, E_m is represented by E . Using the RMS error for the function is not enough. Although it can be used to obtain a low average error, it will leave regions of high error. This is an undesirable situation to have in a CACAD application. A slightly higher average error may be less distracting than the occasional high error. Choosing to minimize the average error plus the maximum error

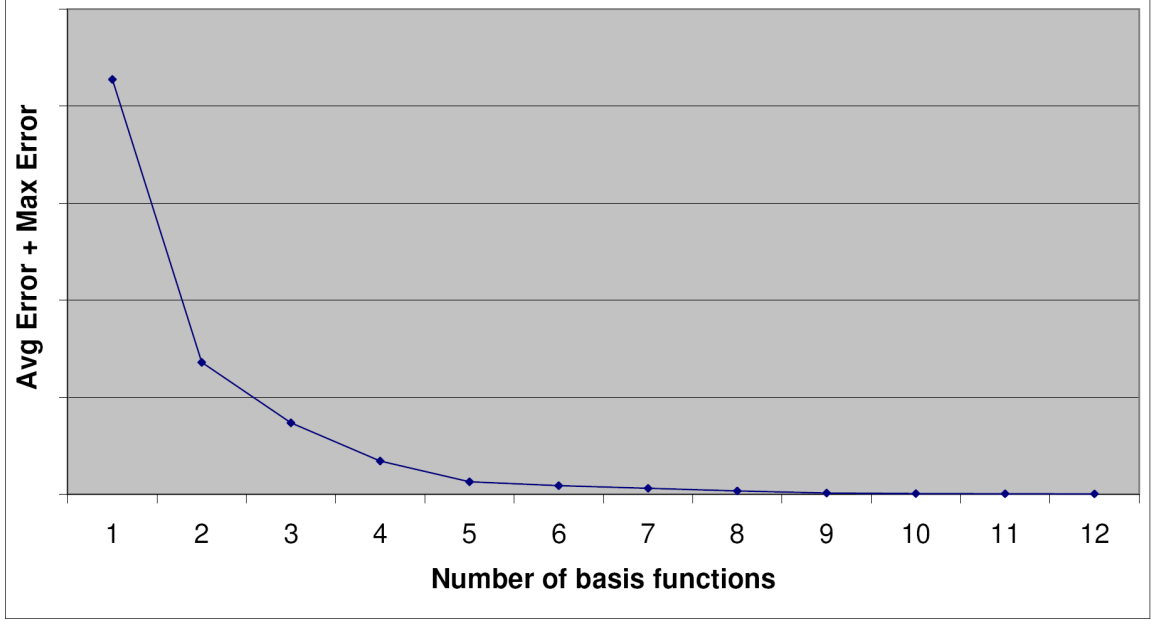


Figure 2.5: The error in the choice of basis functions used to fit the BRDFs in the database.

is shown in Equation 2.3.4. For each BRDF B_i in the database of n BRDFs, the weights of the cosine lobes are fit to the BRDF using the fast algorithm developed in the following section. Next, a function called $Error(E, B_i)$ evaluates the RMS error in using the cosine lobes E to fit B_i .

$$f(E) = \max_{i \in \{1, 2, \dots, n\}} (Error(E, B_i)) + \frac{1}{n} \sum_{i=1}^n Error(E, B_i) \quad (2.3.4)$$

This also gives an idea of how many basis functions are needed. As more basis functions are added, the max error should decrease along with the average error. Once both the average error and maximum error are within an acceptable range, there are enough lobes. Performance limitations of rendering hardware bound the number of basis functions that are useable. Figure 2.3 illustrates the range shapes of the cosine lobes chosen by the nonlinear optimization routine.

The nonlinear optimization for choosing the optimal basis functions was run for one cosine lobe up to eleven. Figure 2.4 shows the actual exponents for a given number of basis lobes. Although the results are dependent on the BRDF database used, notice how the actual exponents are distributed somewhat regularly when graphed in log space. Figure 2.5 shows the error in choosing the optimal basis functions. The actual values are omitted, since the error was measured at only a few angles and thus useable only for self comparison.

2.4 Real-time BRDF fitting

The set of basis BRDFs are combined to approximate a designed BRDF in real-time. This section describes the techniques used to fit the parameters of the reflectance model described in Section 2.3 to a BRDF. Because the application is interactive BRDF design, the fitting needs to be done at interactive frame rates using fast techniques.

First, the coefficients to the diffuse lobe are computed by lighting the BRDF at a 45 degree angle and measuring the outgoing light from an off specular angle, for example the surface normal.

Next, the glossy and directionally diffuse lobes are computed as a linear combination of the basis BRDFs found in Section 2.3.2. The basis BRDFs are cosine lobes with fixed specular exponents; therefore only the coefficients K_{DD_i} and K_{G_i} that determine their weights can be changed. K_{DD_i} is the directionally diffuse weight of basis function i and K_{G_i} is the glossy weight of basis function i . Equation 2.4.1, on the next page, shows the concept in matrix form.

$$\begin{bmatrix} BRDF \\ Basis \\ Functions \end{bmatrix} \begin{bmatrix} BRDF \\ Basis \\ Weights \end{bmatrix} = \begin{bmatrix} The \\ Target \\ BRDF \end{bmatrix} \quad (2.4.1)$$

The basis functions and target BRDF are evaluated to fill in the matrix. The cosine basis lobes are evaluated as Phong lobes. The cosine functions are sampled at angles Θ_1 to Θ_n and raised to the exponents E_1, E_2, E_3 , through E_m , where n is the number of sample angles and m is the number of basis functions. $BRDF(\Theta)$ is the target BRDF sampled at the same angles. Equation 2.4.2 shows the matrix for directionally diffuse. The matrix for glossy component is handled similarly.

$$\begin{bmatrix} \cos(\Theta_1)^{E_1} & \cos(\Theta_1)^{E_2} & \cos(\Theta_1)^{E_3} & \dots & \cos(\Theta_1)^{E_m} \\ \cos(\Theta_2)^{E_1} & \cos(\Theta_2)^{E_2} & \cos(\Theta_2)^{E_3} & \dots & \cos(\Theta_2)^{E_m} \\ \vdots & \vdots & \vdots & \ddots & \vdots \\ \cos(\Theta_n)^{E_1} & \cos(\Theta_n)^{E_2} & \cos(\Theta_n)^{E_3} & \dots & \cos(\Theta_n)^{E_m} \end{bmatrix} * \begin{bmatrix} K_{DD_1} \\ K_{DD_2} \\ \vdots \\ K_{DD_m} \end{bmatrix} = \begin{bmatrix} BRDF(\Theta_1) \\ BRDF(\Theta_2) \\ \vdots \\ BRDF(\Theta_n) \end{bmatrix} \quad (2.4.2)$$

This is in the form $Mx = b$, where the unknowns are the basis weights x . Matrix M is not necessarily square and invertible. However, x can be simply determined with least squares. The solution produced by least squares may give negative weights for some of the cosine lobes. Negative weights are physically implausible for a BRDF [32] as well as produce distracting artifacts in the rendered images. If negative weights are clamped

to zero, as in [25], error accumulates from every negative lobe and cannot be corrected. The error may increase, rather than decrease, if too many basis functions are used in the approximation.

To prevent negative weights from occurring, linear programming is used to solve for the basis weights [42]. Linear programming has the advantage over least squares in that it allows constraints to be set on each variable as the minimum error is determined. Each K_{DD} and K_G is constrained to be positive in the solver.

The absolute value of the error in approximating the BRDF is optimized to be minimal. Absolute value is nonlinear around zero and therefore incompatible with linear programming. The techniques that must be employed to convert the absolute value of error, which is nonlinear, to a linear function are beyond the scope of this document, but are described in [18].

Figure 2.6 shows the result of fitting seven basis lobes to a target BRDF's diffuse and directionally diffuse components. Gloss was omitted for clarity. Slices of the BRDF are mapped onto the unit square using the hemispherical mapping described in [55]. The mapping is responsible for the crease along the diagonal.

Since a linear programming solver computes the solution iteratively, there is no guarantee on the time it takes to find a solution. Occasionally, the solver may take a long time to settle on a solution. A time limit for finding a solution must be set to prevent pauses in interactivity. The only way the linear programming solver can compute the fit in real-time is to keep the matrix as small as possible. This is done by sampling the BRDF with as few measurements as possible.

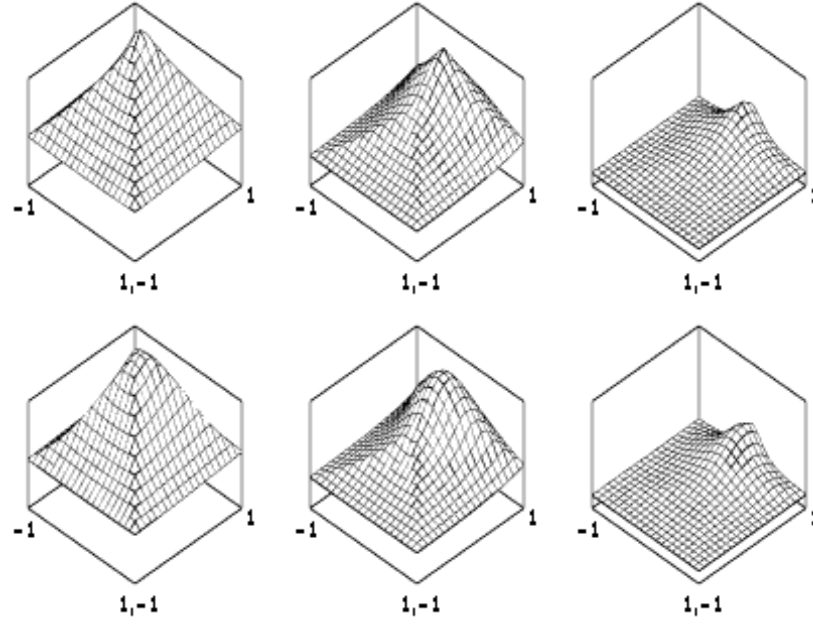


Figure 2.6: Three slices of the target BRDF (above) are compared to the approximation using seven basis lobes(below) are lit from 10, 40, and 70 degrees(left to right).

Only a few BRDF samples are needed to capture most of the interesting aspects of the BRDF. The BRDFs for the metallic automotive finishes used in this research are generally smooth and well behaved. For these BRDFs completely sampling the BRDF from every incoming and exiting light angle is overkill. The color appearance industry uses only three to six tristimulus measurements across aspecular angles plus a single gloss measurement to successfully characterize them [65]. Therefore, only a few samples are needed to approximate the BRDF. One sample is used to capture the diffuse aspect of the color, some are used to capture the directionally diffuse, and other samples in the near mirror direction are used to capture the magnitude and shape of the glossy first surface reflection. Using linear programming and a limited number of BRDF samples, the matrix in Equation 2.4.2 can be solved at real-time rates.

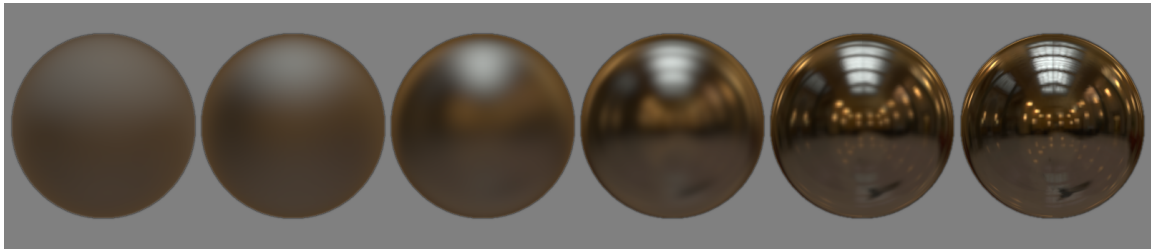


Figure 2.7: The photographically acquired HDR environment map is prefiltered by the set of cosine lobe basis functions shown in Figure 2.3.

2.5 Rendering

To render the designed BRDF in a global lighting environment, all of the basis functions can be rendered with global illumination and weighted together using the coefficients found using the method described in Section 2.4. The illumination is represented by an environment map. The Uffizi environment map comes from Debevec’s light probe gallery [12] and the Walter Library environment map pictured in Figure 2.7 was digitally photographed using a mirror ball. For each specular exponent in the set of basis functions, a prefiltered environment map is used to represent the appearance of the basis function in the lighting environment. The shader calculates the appearance of the surface, by summing the lighting environments, weighted according to their coefficient weights.

Section 2.5.1 discusses how the prefiltered environment maps representing the appearance of the basis functions in the lighting environment are computed. Section 2.5.2 describes the shader used for real-time rendering.

2.5.1 Prefiltered environment maps

A prefiltered environment map can be used to store the precomputed appearance of a BRDF in a lighting environment [25]. Normally one would compute a prefiltered environment map for the designed BRDF. However, since the BRDF is represented as a linear combination of basis BRDFs, a prefiltered environment map is computed for each basis BRDF. The prefiltered environment maps represent the appearance of the basis functions in the lighting environment. Figure 2.7 shows a photographically acquired environment map prefiltered by the set of basis functions found in Section 2.3.2.

The prefiltering of an environment map can be done offline. The prefiltering of an environment map is dependent on the specular exponent of the cosine lobe. Since the exponents are not free parameters in the fitting routine, the prefiltered environment map does not need to be computed every time the designed BRDF is changed. Software is freely available for prefiltering the lighting environment [13].

High dynamic range (HDR) cube maps are used for the lighting environment. HDR images are helpful in capturing appearance phenomena contributed from the diffuse, directionally diffuse, and glossy components of a surface finish's appearance. Although a HDR display may be available for purchase in the not too distant future [51], traditional displays can already benefit from images that are computed in HDR and then tone mapped before output.

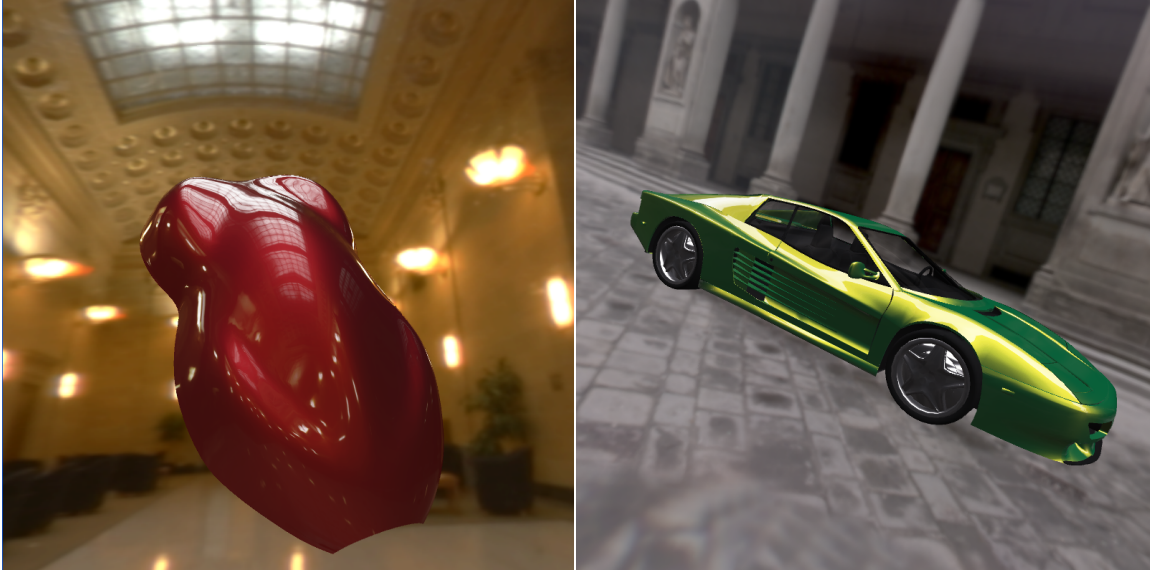


Figure 2.8: Rendering measured and designed automotive paint BRDFs.

2.5.2 Realtime shader

A shader written in nVidia's CG programming language is used for rendering [33]. As the three dimensional surface is rendered, a shader computes the surface normal \vec{N} , view direction \vec{V} , and reflected view direction \vec{R} . The diffuse term is computed in the vertex shader. Glossy and directionally diffuse components are computed in the pixel shader. Finally, the color is tone mapped for display on the output device. Figure 2.8 shows the results of rendering measured and designed BRDFs.

The directionally diffuse and gloss aspects of the BRDF are rendered as a linear combination of prefiltered environment maps. The environment maps representing the appearance of each basis function in the lighting environment are weighted by the coefficients found by the real-time fitter.

For each basis function i in the set of m basis functions the following is done. The prefiltered environment map $CubeMap_i$ representing the appearance of i th basis function is indexed in the direction of the reflected view ray \vec{R} . This is weighted by K_{DD_i} and K_{G_i} . The directionally diffuse color is a subsurface effect and therefore also weighted by $\vec{R} \bullet \vec{N}$ (\vec{R} in this case is an approximation of the light source direction.) The values are summed up in Equation 2.5.1 for directionally diffuse and in Equation 2.5.2 for glossy.

$$Directional = (\vec{R} \bullet \vec{N}) * \sum_{i=1}^m K_{DD_i} * CubeMap_i(\vec{R}) \quad (2.5.1)$$

$$Gloss = \sum_{i=1}^m K_{G_i} * CubeMap_i(\vec{R}) \quad (2.5.2)$$

One issue is that for the directional diffuse color, the Lambertian scaling factor $\vec{L} \bullet \vec{N}$ is approximated. Normally it is $\vec{R} \bullet \vec{N}$ but since environment maps are used, the light direction is replaced with the central reflected view direction. For high specular exponents, the error is small. But the wider the directionally diffuse lobe, the more this affects the results. However, the error is not visually distracting. See [25] for a more in-depth discussion of this issue.

To render the diffuse lobe, a diffuse map is used. This is done using the surface normal to index an environment map prefiltered with a Phong lobe specular exponent of 1.0.

$$Diffuse = K_D * DiffuseMap_i(\vec{N}) \quad (2.5.3)$$

The diffuse, directionally diffuse, and gloss are summed together. Finally, simple characteristic curve tone mapping and gamma correction are necessary to scale the final colors of the pixels to the range of the output device.

Increased specularity at grazing angles, also known as the Fresnel effect, can be simulated in two ways. One method is to increase the relative weights of the environment maps with high specular exponents at grazing angles. A second method is to run the BRDF fitting routine at multiple viewing lighting angles and interpolate between them in the renderer based on $\vec{L} \bullet \vec{N}$.

2.5.3 Anisotropic Gaussian model

[64] described a micro-facet Gaussian model that was used to design the parameters of anisotropic reflection. Equation 2.5.4 shows the anisotropic Gaussian model in vector form, where \vec{H} is the half angle between the viewing direction \vec{V} and the light direction \vec{L} . The diffuse term has been omitted. The parameter α_x represents the micro-facet slope distribution in the direction of principle anisotropy \vec{X} and α_y is the slope distribution tangent to the direction of principle anisotropy \vec{Y} . The reflection is isotropic if α_x and α_y are equal. α_y is assumed to be greater or equal to α_x .

$$Ward(\vec{L}, \vec{N}, \vec{V}) = P_s \frac{(\vec{L} \bullet \vec{N})}{\sqrt{(\vec{L} \bullet \vec{N})(\vec{V} \bullet \vec{N})}} \frac{1}{4\pi\alpha_x\alpha_y} \exp \left[-2 \frac{[\vec{H} \bullet \vec{X}]^2 + [\vec{H} \bullet \vec{Y}]^2}{1 + \vec{H} \bullet \vec{N}} \right] \quad (2.5.4)$$

Since the basis functions used in the fitting and rendering are all radially symmetric, the basis functions need to be combined in multiple off-specular directions to approximate the elliptical distributions found in anisotropic BRDFs. Figure 2.9 shows the elliptical distribution of an anisotropic BRDF.

The first step in approximating the anisotropic Gaussian model is to approximate the isotropic Gaussian model as a linear combination of cosine lobes. The fitting is used only to capture the width of the lobe. First, α_y is set to be equal to α_x . This produces an

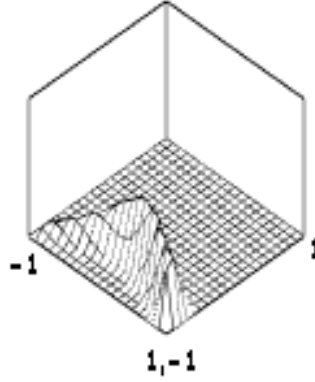


Figure 2.9: Graph of an anisotropic BRDF viewed from 45 degrees off normal.

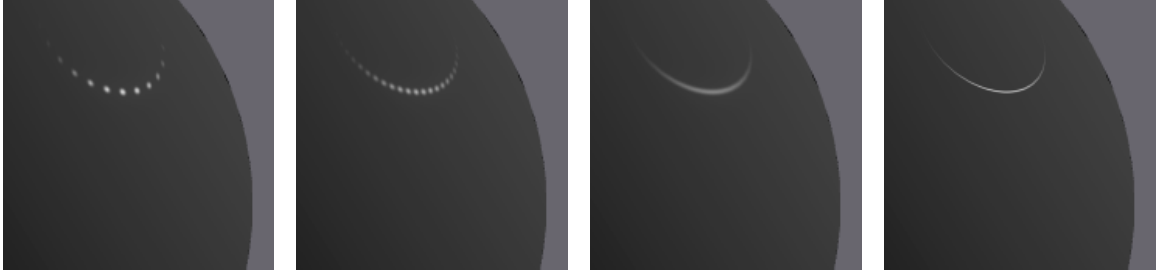


Figure 2.10: Reconstructing the reflection using multiple off specular cosine lobes: 15 lobes, 35 lobes, 81 lobes, actual(left to right).

isotropic version of the BRDF. The color P_s is set to one during fitting. Next, the fitting is done at an incoming lighting angle of 45 degrees with the same technique that is used to fit directionally diffuse lobes in Section 2.4. The result of the fitting gives K_{DD_i} , the weighting of the basis BRDFs.

Before moving on to rendering the anisotropic Gaussian, we will first describe how to render the isotropic Gaussian model using prefiltered environment maps. The following is implemented as a pixel shader. When rendering a point on the surface, the reflected view direction is computed as \vec{R} . This is the approximation of the light source direction. The

sum of the set of coefficients K_{DD_i} multiplied by the corresponding prefiltered environment maps is computed. This is scaled by the isotropic Gaussian model, replacing \vec{V} with \vec{R} . Equation 2.5.5 shows the details. The diffuse component of the BRDF can be rendered with spherical harmonics as mentioned in Section 2.5.2.

$$Color = Ward(\vec{R}, \vec{N}, \vec{V}) \frac{\sum_{i=1}^m K_{DD_i} CubeMap_i(\vec{R})}{\sum_{i=1}^m K_{DD_i}} \quad (2.5.5)$$

To render the anisotropic Gaussian model using prefiltered environment maps, the environment maps need to be sampled in multiple off-specular directions. Normally the environment maps are sampled in \vec{R} in the direction of the view vector reflected off the surface normal. To generate off-specular sample directions \vec{R}_j , the surface normal \vec{N} is rotated by an angular offset θ_j around the principle anisotropy direction \vec{X} and the view vector is reflected off the new perturbed normal to get \vec{R}_j .

The way that the number off-specular samples affects the quality of the rendering is dependent on many things. The range of the angular offset θ_j should be wide enough to cover the elliptical lobe of the anisotropic reflection. If the range is too short, the highlights will appear too short. If there are not enough samples, highlights will break apart. This will be less noticeable in reflections of larger light sources or if α_x is large, creating a wider BRDF. A systematic study was not done, but it has been noticed that on surfaces exhibiting mild anisotropy nine samples can be sufficient. On highly anisotropic surfaces with $\alpha_y \gg \alpha_x$ eighty samples or more may be necessary to avoid artifacts. Figure 2.10 shows the reconstruction of an highly anisotropic BRDF rendered in an environment with one point light source.

The shader works by generating multiple \vec{R}_j rays and sampling the environment maps with them. The prefiltered environment maps are weighted by the corresponding K_{DD_i} as before, but now each off-specular sample is weighted by the intensity of anisotropic lobe as in Equation 2.5.6. The weighted samples are summed up in Equation 2.5.7. The results of a designed reflection can be seen in Figure 2.11.

$$W_j = \text{Ward}(\vec{R}_j, \vec{N}, \vec{V}) \quad (2.5.6)$$

$$\text{Color} = \sum_j \left[W_j \frac{\sum_{i=1}^m K_{DD_i} \text{CubeMap}_i(\vec{R}_j)}{\sum_{i=1}^m K_{DD_i}} \right] \quad (2.5.7)$$

The performance of the system was tested on a workstation with dual nVidia 6800 Ultras running in SLI mode. The approximation consisted of 5 cosine lobes plus one spherical harmonic diffuse lobe. Five samples ran at 35Hz, nine samples ran at 27Hz, 31 samples ran at 7Hz, and 81 samples ran at just over 3Hz. It is interesting to note that an approximation with 81 samples corresponds to over 400 texture lookups and computations of the Ward reflection model per pixel.

2.6 Remarks

In this section, we have presented a computer graphic system for doing interactive color appearance design using environment map based lighting. The system can render BRDFs as they are being designed.

The system approximates designed BRDFs as a linear combination of a fixed set of cosine lobes in real-time. Nonlinear optimization was used to find the optimal basis functions for use with the particular domain of BRDFs being designed. The renderer combines a set of

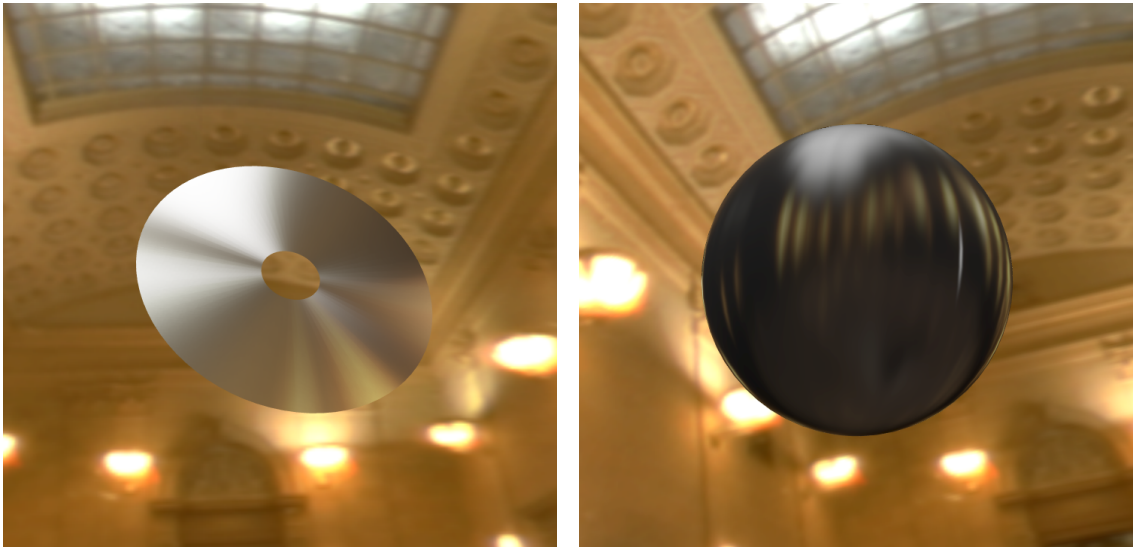


Figure 2.11: Designed anisotropic reflections.

environment maps prefiltered by each of the basis functions to render images of the BRDF in global lighting environments.

By creating a graphics pipeline that maintains interactivity during BRDF changes, this rendering system addresses the unique needs of the appearance industry in doing computer aided color appearance design work.

Since this work was originally published, there has been subsequent work on the same research problem of designing and rendering BRDFs in complex lighting environments [5].

Chapter 3

Color styling tools

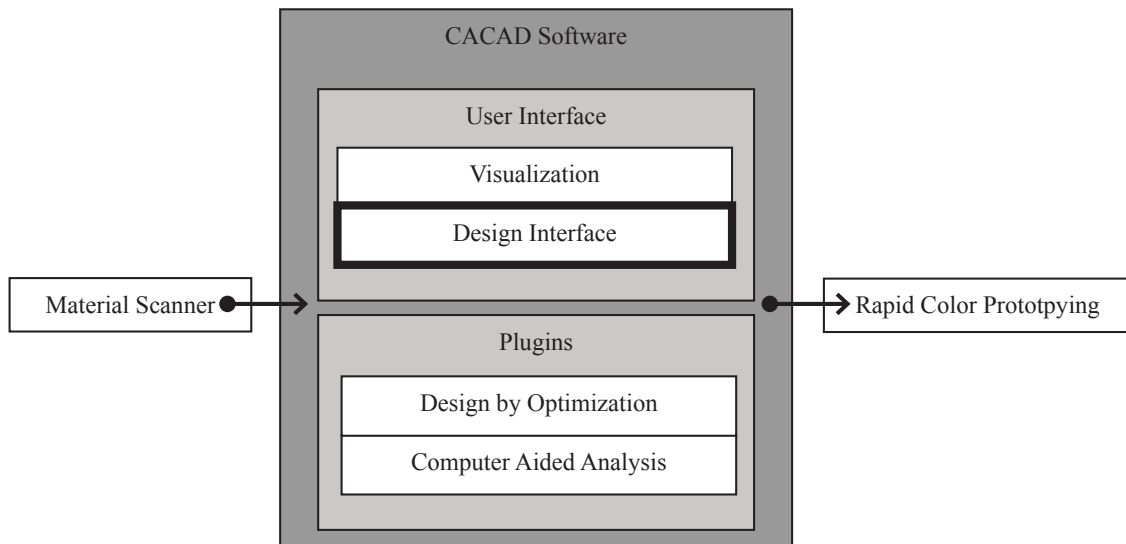


Figure 3.1: The software presented in this chapter is the design interface component of the CACAD package.

Abstract

Creative tools are proposed that allow color stylists to take advantage of their training in the fashion, art, and other design industries. A simple reflection model is employed that has the minimum number of free parameters required to design solid and metallic color finishes from conceptualization to fabrication. The parameters correspond to color specification terms familiar to designers such as face color, flop color, travel, and gloss. We demonstrate how the reflection model can also be used to develop technical CACAD interfaces appropriate for color scientists as well as effective interfaces for color stylists.

The first program is a technical design interface that gives the user a unique set of controls over a second order polynomial that defines metallic color families at a sequence of aspecular reflection angles. One approach allows the user to adjust the average hue, saturation, and brightness of all of the colors interpolated by the polynomial. Another method, appropriate for the newer effect colors, permits the designer to establish face and flop colors to be reached at either end of the interpolation. Variations produced by adjusting model parameters can also be evaluated and selected.

The next program is a virtual mood board that allows direct selection of the reflection model parameters from pictures. We also develop an image based BRDF tweaker for adjusting color appearance directly on a 3D object. Finally, a sketch based design interface that mimics the workflow of a concept artist is also introduced. The system is shown to work with hand drawn concept art.

Parts of this chapter have been previously published by the author in *Proceedings of the 11th Color Imaging Conference* [54].

3.1 Introduction

Computer graphics is on the verge of being able to provide computer aided design tools to color appearance professionals. These tools will let industrial designers and color technologists have the same interactive control over color appearance that engineers and architects have had over geometry since the beginning of computer graphics almost forty years ago. The emergence of computer aided color appearance design (CACAD) will allow color appearance designers and scientists to examine how existing paints and coatings look on new products. More importantly, CACAD will make it possible to hypothesize and visualize new surface coatings with heretofore unseen reflection properties [37].

The recent computer graphic advance which has made this possible is the development of per pixel shading hardware that permits display, in real time, of objects with arbitrarily complex surface reflection functions. While earlier graphics devices evaluated a limited shading model at polygon vertices and interpolated the result across the polygon's interior, the new hardware can compute a complex reflectance model at every pixel that composes a polygon. This makes it feasible to treat surface reflection in a very general manner, including the use of a bidirectional reflectance distribution function (BRDF) [20, 24] and wavelength based color calculations.

While the ability of computer graphics hardware to display complex surface reflection has been improving, new *effect* paints are being developed for use in a variety of different design applications. These so-called goniochromatic colors have the property that the color of the reflected light changes with the angle of reflectance. Metallic and pearlescent automotive paints are two examples that are in wide use. The appearance of these paints is difficult to

characterize because a single color measurement is not sufficient. This complicates the job of a designer who invents new goniochromatic colors, because they must specify not just one color but a whole family of colors.

Industrial designers, interior designers, and architects all make extensive use of exemplars when they choose colors for a new product. They collect material samples from suppliers, they select illustrations from fashion magazines, and they take pictures of objects with interesting surface finishes. Designers with aesthetic design backgrounds may also develop concept sketches for new merchandise. In creating these pictures they use non-photorealistic rendering techniques to convey the object's color appearance. These exemplars and sketches are organized and displayed on "mood boards" that allow the designer to compare the colors and make final selections. Traditional hue, saturation, and brightness (HSB) color organization systems are used, after the fact, to provide a name and a specification for the final color.

The existing computer graphic tools for color simulation and selection do not readily facilitate the color design process used in these traditional design fields. Computer graphic reflection models have been developed with the goal of accurately portraying subtle color appearance effects. These models have grown increasingly complex, and they include physical parameters for which aesthetic designers have no intuition. Numerous computer graphic HSB color systems have been proposed, but they are not able by themselves to convey the spatial aspects that separate one color appearance from another. In addition, in the traditional design process, exemplars and sketches are used more often than HSB color systems to ideate color.

In this chapter we propose a set of computer graphic tools to facilitate color design in the traditional aesthetic design fields. We employ a reflection model that covers the widest range of color appearances encountered by designers including solid colors, metallic colors, and the glossiness of these colors. The reflection model is constructed to have the minimum number of free parameters and to select these parameters so that they correspond to color specification terms familiar to designers such as face color, flop color, travel, and gloss. The model is defined in a way that allows it to be used as a manufacturing specification for the final color. We also demonstrate how the reflection model can be used to develop effective interfaces for designers.

We first describe a technical interface that gives the designer several unique ways to modify this reflection model. These techniques range from editing the individual data points to which a quadratic curve is fit, to adjusting the average hue and saturation of the color represented by the curve, to selecting the so-called face and flop colors that the curve must interpolate near specular and far from specular. We next improve the interface so that it is more appropriate for industrial designers. We create a virtual mood board that allows direct selection of the reflection model parameters from pictures. In addition, we describe a novel color design interface for tweaking color and appearance directly on a 3D surface. A sketch based design interface is also developed that permits the reflection model parameters to be indirectly set from a non-photorealistic illustration.

This chapter is organized into the following sections. After covering background research in the next section, Section 3.3 discusses the reflection model used for this research. Section 3.4 introduces a technical CACAD interface for designing goniochromatic surface

finishes. Section 3.5 introduces the virtual mood board interface, Section 3.6 describes the spot color styler interface for tweaking color and appearance directly on a three dimensional object, and Section 3.7 describes a sketch based interface for BRDF design. Section 3.8 summarizes and evaluates the results. The final section discusses conclusions and future work.

All of the programs use per pixel shading hardware to allow the designer to see the designed colors in real time on a three dimensional surface using the realtime rendering engine discussed in the previous chapter. Finally, the new color's variation in reflectance with aspecular angle can be written to a file for manufacturing as described in Chapter 5.

3.2 Relevant work

In recent years researchers have begun to explore new interactive interfaces that can be used to define or adjust the shape of a BRDF. The goal is to move away from sliders that modify the value of single reflection model parameter and to develop interfaces that are more intuitive to use. Initial work in this area involved the adjustment and modification of one dimensional graphs that represent the BRDF. Shimizu and Meyer provide a variety of different ways to use a curve to control the shape of a BRDF including adjusting the face, flop, and travel of a metallic color and the use of Photoshop like variations mode that facilitates adjustment by providing examples of the result (See Section 3.4) [54]. Exploration of BRDF models was explored using “variations” in [41] also. However, variations was first used as a general system for tweaking general scene parameters in [23]. The ability to perform changes to BRDFs while observing the object under complex lighting was developed in [52] and [5]. The manipulation of graphs to adjust a BRDF was taken to new level of

generality by Lawrence, et al. [30] who factored spatially varying BRDFs into shade trees with leaves that contained one dimensional functions corresponding to the specular and diffuse components of reflection.

Other new BRDF definition techniques involve drawing the expected appearance of the BRDF directly on an object or on a surrogate shape. Jaroszkiewicz and McCool [22] used homomorphic factorization to fit a BRDF to a painted example and Sloan et al. [57] examined how to map shading from works of art to geometric models. Neither of these two approaches, however, was able to operate in real time. Editing specific aspects of the BRDF has been investigated by a number of researchers. Colbert et al. [9] provided tools that allow the user to define and adjust the specular highlights produced by a BRDF. Anjyo et al. [3] permit highlights to be treated as deformable objects but the changes do not affect an underlying BRDF. Direct editing of highlight features for key light positions is provided by Pacanowski et. al [43], and their system automatically draws the highlight for other light and view configurations. Finally, Pellacini and Lawrence [44] give the user a painting interface to indicate regions on an object where the appearance is to be edited.

3.3 Hierarchy of reflection models

This section describes the reflection model that is used in much of this thesis to perform CACAD. First, the variables of the reflection model are defined, along with how they control the physical appearance of the resulting material. Since these variables cannot be directly applied to graphics rendering, they are linked to a parametric representation that has been previously tied to a realtime rendering engine [52]. Finally, we discuss how this

reflection model is connected to the physical world through measurement tools and rapid color prototyping systems.

3.3.1 Face/Flop/Travel/Gloss form

It is well known in the field of computer graphics that the reflection of light from metallic objects is primarily specular [11]. In terms of appearance, this means that metallic surfaces appear brightest when viewed in the specular or face direction and become much darker as the line of sight shifts away from specular towards, what is called, the flop direction. Metallic paints exhibit this property although it results from a directional diffuse component that comes from below the surface. The paint and coatings industries refer to how lightness changes with viewing direction as the travel of the color. On solid and metallic coatings, the appearance of the first surface specular reflection is referred to as gloss.

We propose a reflection model that has the following parameters: face, flop, travel, and gloss. Figure 3.2 gives a visualization of how the parameters of this reflection model correlate to the BRDF's shape. "Face" is the color at 15° off specular angle and is represented as a *Lab* tristimulus value. This angle establishes the directionally diffuse color while avoiding the specular highlight resulting from the first surface coatings. "Flop" is the color at far from specular and is represented as a CIE *Lab* tristimulus value. The particular angle that flop is associated with is the variable travel. "Travel" represents how color changes with viewing direction. This is intended to be the color of the diffuse portion of the material at as close to a specular angle as possible. If the face and flop colors are identical, the color is a solid color and therefore travel does not alter the appearance of the material.

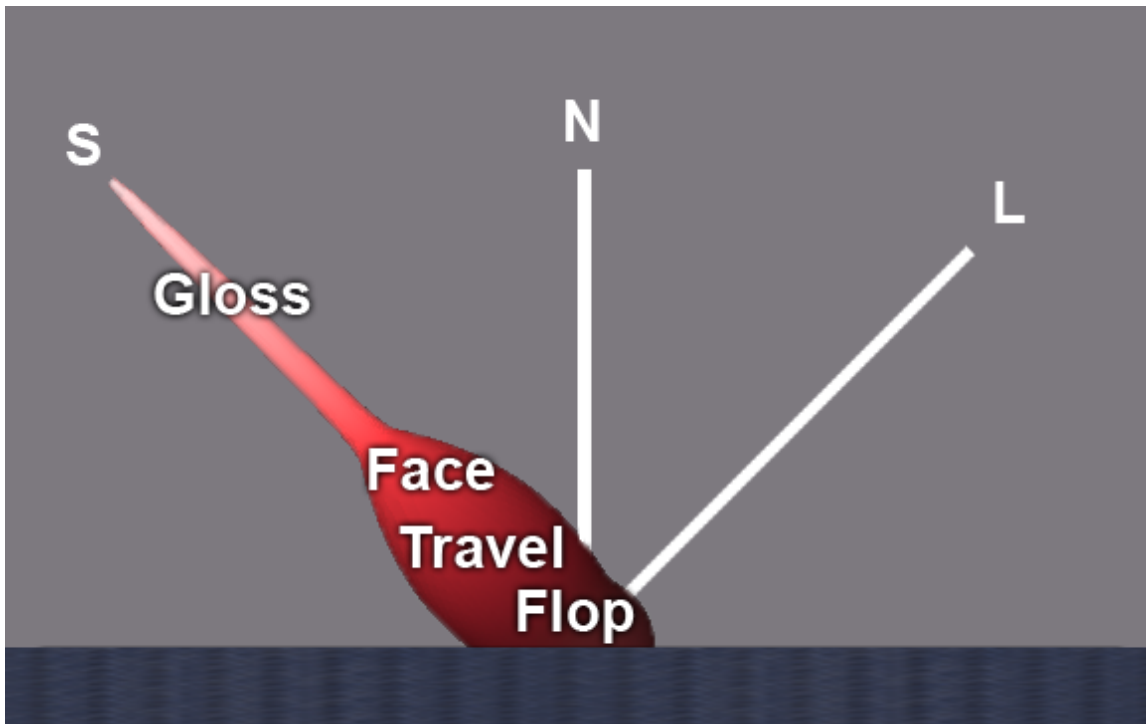


Figure 3.2: A diagram illustrating how the four components of the metallic reflection model relate to the shape of the BRDF. The light L is at 45° from normal N . The specular direction is labeled S .

In many computer graphic reflection models, gloss is represented by two parameters, one representing the color and magnitude of the specular lobe and one representing the width of the specular lobe. In the Phong model these two variables would be a color and a scalar specular exponent. In our reflection model gloss is a single scalar number represented by ASTM standard gloss. This one number controls both the size and scale of the first surface reflection's specular lobe. [65] showed a mapping between ASTM standard gloss and parameters to Phong and Ward specular lobes. This single value sacrifices some degrees of freedom for ease of use in representing first surface reflection.

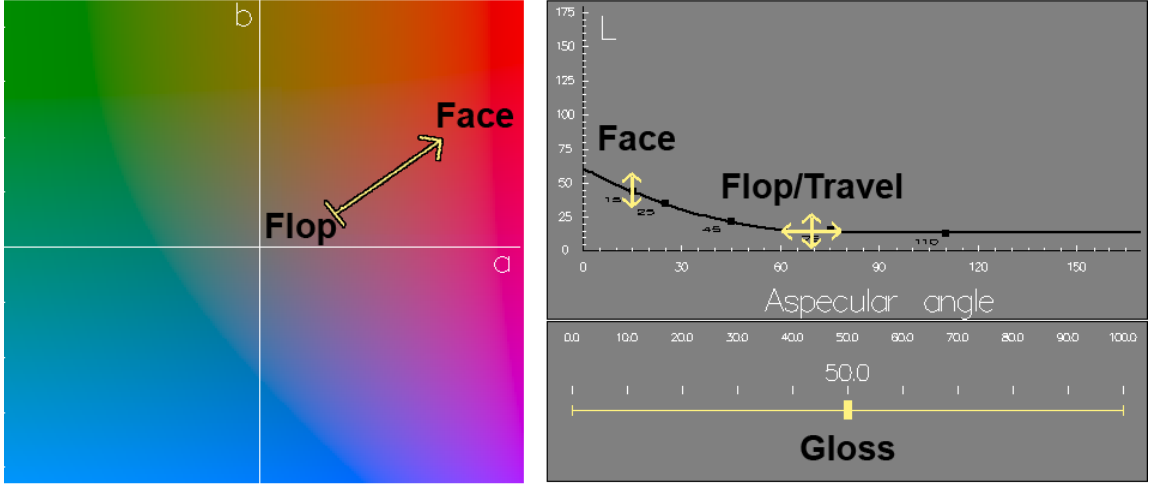


Figure 3.3: An interface for directly manipulating face, flop, travel, and gloss. The L vs. aspecular angle plot illustrates how the parametric form interpolates face at 15° and flop at θ_{clamp} .

3.3.2 Parametric form

The face/flop/travel/gloss reflection model has limited use outside of design work, and is unsuitable for direct rendering. However, it is easily converted to a parametric form for rendering purposes. Figure 3.3 shows how the face/flop/travel/gloss reflection model fits on top of the parametric form of the reflection model. This parametric form has appeared in a slightly different form in [54].

Alman in [2] performed a systematic study of metallic paint which revealed that only a few data points need to be taken in order to characterize a metallic color's travel. He found that a clamped second order polynomial could successfully interpolate CIE Lab color coordinates derived from goniospectrophotometric measurements. Therefore, we convert the face/flop/travel/gloss model's parameters into a second degree polynomial for L , a , and b .

In this section we work through the mathematical details only for the L polynomial curve. To compute the complete BRDF, the same equations are used to construct the a and b curves as well. In the equations below, L_a , L_b , and L_c refer to the three components of the quadratic polynomial representing L .

$$L(\theta) = L_a\theta^2 + L_b\theta + L_c \quad (3.3.1)$$

$$L_{clamped}(\theta) = L(\min(\theta, \theta_{clamp})) \quad (3.3.2)$$

Setting the derivative of the quadratic polynomial to be zero and solving for θ_{clamp} , we find the clamp point needed to evaluate the clamped quadratic polynomials.

$$\frac{d}{d\theta}L(\theta_{clamp}) = 0 = 2L_a\theta_{clamp} + L_b \quad (3.3.3)$$

$$\theta_{clamp} = \frac{-L_b}{2L_a} \quad (3.3.4)$$

To fit the curve, Alman suggested that three tristimulus measurements were necessary: one near specular, one near grazing, and at one angle in between. Others confirmed his results [48, 63].

To solve for the three unknowns of the quadric polynomial, three equations are needed. In general the color at three angles is necessary to define the three equations, but we can use a representation that has only two angles: face and flop. Since flop represents the quadric curve's apex and the derivative at this point must be zero, we have a third equation to find the three unknowns L_a , L_b , and L_c . The next page illustrates the initial equations and solutions.

$$L(15^\circ) = L_a * (15^\circ)^2 + L_b 15^\circ + L_c \quad (3.3.5)$$

$$L(\theta_{clamp}) = L_a \theta_{clamp}^2 + L_b \theta_{clamp} + L_c \quad (3.3.6)$$

$$\frac{d}{d\theta} L(\theta_{clamp}) = 0 = 2L_a \theta_{clamp} + L_b \quad (3.3.7)$$

$$L_a = \frac{L(15^\circ) - L(\theta_{clamp})}{(15^\circ - \theta_{clamp})^2} \quad (3.3.8)$$

$$L_b = -2L_a \theta_{clamp} \quad (3.3.9)$$

$$L_c = L(\theta_{clamp}) + L_a \theta_{clamp}^2 \quad (3.3.10)$$

To convert back is simple. First evaluate Equation 3.3.4 to find travel as θ_{clamp} in degrees. Then evaluate Equation 3.3.2 at 15° degrees and θ_{clamp} to find face and flop color as $Lab(15^\circ)$ and $Lab(\theta_{clamp})$.

3.3.3 Aspecular measurements

Current industry standards utilize three *Lab* measurements taken at 15° , 45° , and 110° from specular. The parametric form of the reflection model can be used to find the color at the three angles, and the individual colors at each angle can be fit by a curve. This industry standard provides a connection between the physical world and either measurements or prototype color.

Converting from our rendering model to industry standard values is quite simple: just evaluate the clamped quadratic polynomial at 15° , 45° , and 110° . The parametric form can be fit to the industry standard values, since three points is enough to define a second degree polynomial [54]. Combining the equations in the previous subsection yields an exact mapping from the industry standard to our model.

To measure appearance, color, and the spatial distribution of color two devices are employed. In order to measure gloss, an industry standard gloss meter is used. A three angle spectrophotometer can be used to measure the color as three aspecular *Lab* measurements. These values can be converted directly to the face/flop/travel/gloss model. Therefore, the full industry standard for the measurement of metallic paint surfaces can be easily converted to and from the face/flop/travel/gloss model.

An experiment was done in [39] that demonstrated how the three *Lab* aspecular measurements for a paint designed on the computer can be input to a paint formulation system so that the paint can be manufactured. A test of the rapid color prototyping system shows good correspondence between the designed and the fabricated paint. Additional prototyping experiments are discussed in Section 5.4.

An alternative standard for metallic paints uses 25° , 45° , and 75° as the aspecular measurements. When colors are exported from the software, we export both sets of angles to ensure compatibility with either standard.

3.3.4 Conversions between models

While each reflectance representation has strengths and weaknesses on its own, the combination is extremely useful in the context of CACAD. The combination of representations is the glue that brings color design from conceptualization to fabrication. Figure 3.4 summarizes the representations, their primary use, and how to convert between them. The strength of the face/flop/travel model's minimal representation is its utility in design applications. The parametric representation is suitable for rendering, BRDF visualization, and BRDF

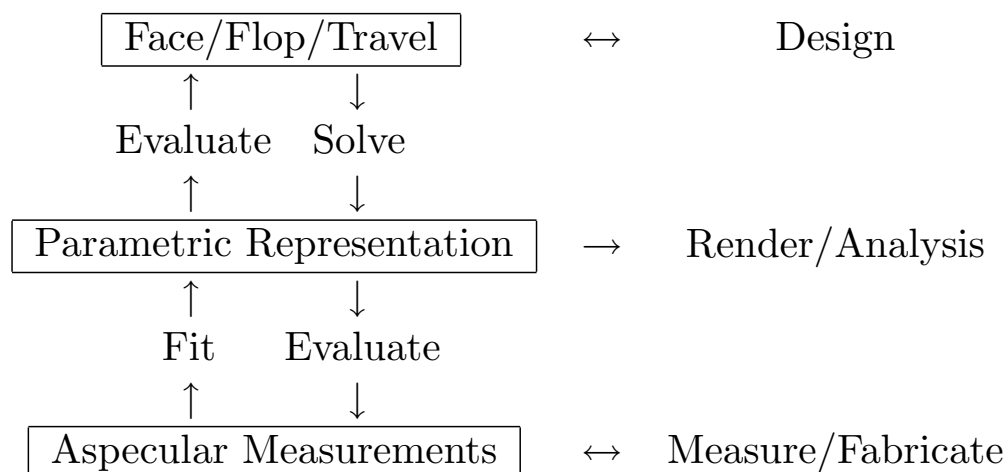


Figure 3.4: This figure summarizes the three reflectance representations, their primary uses, and conversion pathways between representations.

analysis. Finally, the aspecular measurements provide a connection to the physical world. Solid and metallic colors can be scanned into the system using simple off the shelf tools. Colors designed in the system are converted to aspecular measurements and exported as manufacturing specifications in rapid prototyping applications.

3.4 Interactive goniochromatic color design interface

This section is a description of a technical and more traditional graphical user interface (GUI) components for the design of goniochromatic colors. The interface components discussed below are the L, a, and b plots, the Hue Saturation Brightness control, the Face, Flop, and Travel Picker, the Variations mode, the Gloss slider, and the Color Palette. Before we talk about the individual components of the user interface we should mention some of our design goals. Our program must be made useable for a wide range of users, including chemists, designers, and consumers. Our main issue with designing a user interface is how to control the complicated definition of the surface appearance in a user friendly way. On

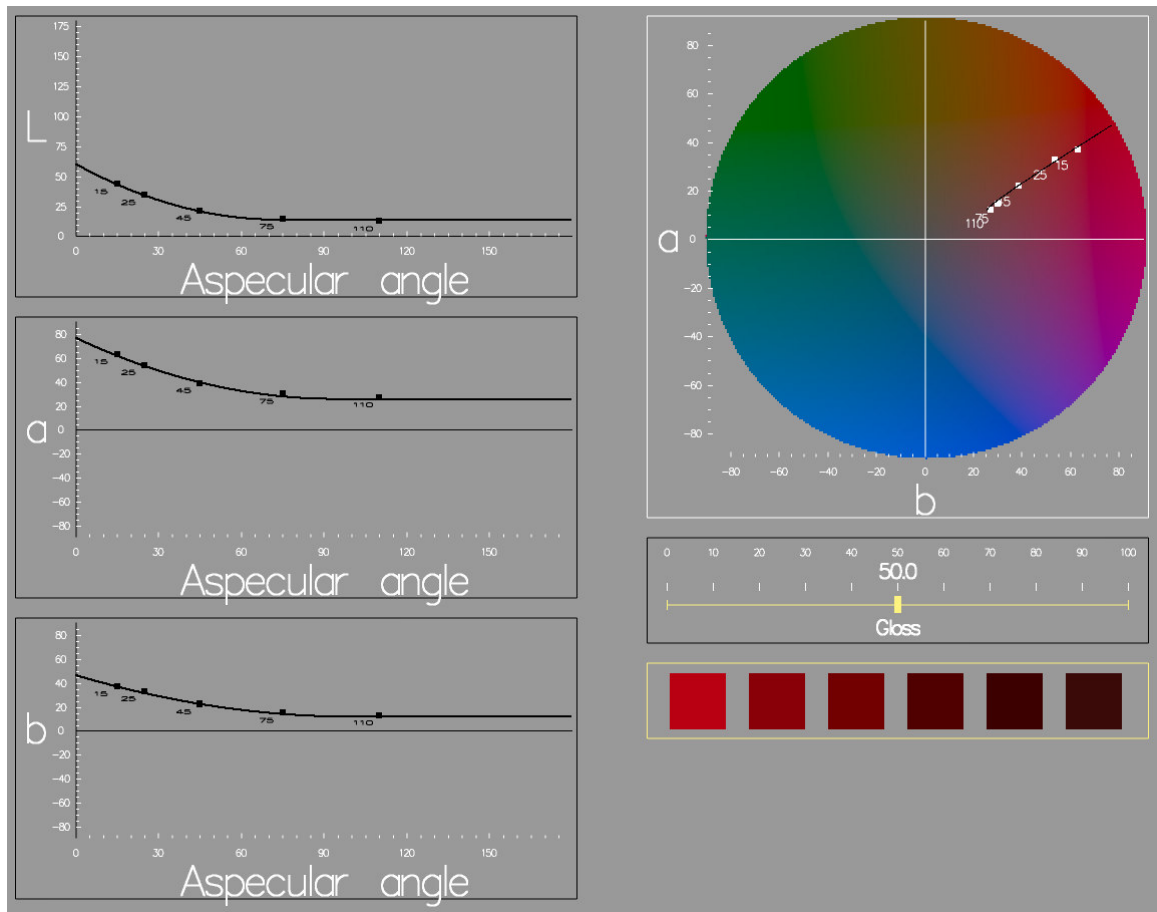


Figure 3.5: The user interface.

one hand we would like to give the user access to the complete range of colors possible, but on the other hand we should avoid overwhelming the user with a complicated interface. Our software explores a variety of options for designing goniochromatic colors, where some methods are more appropriate for certain types of users than others. Many ideas were taken from methods of dealing with traditional monochromatic colors and extended to work with the family of colors that defines a color shift.

3.4.1 Data point editor

The program's internal representation of a goniochromatic color consists of data points interpolated in Lab space as a clamped quadratic polynomial. Displaying these data points on separate L, a, and b plots, and allowing the user to move the data points up and down, provides a very rudimentary way of interacting with the color definition (see Figure 3.5). As a point is moved, the clamped quadratic polynomial that interpolates the data points is updated in real-time.

It is difficult for most users to relate the separate L, a, and b curves to the final color they represent. Combined, a and b define the hue and saturation of a color while L by itself corresponds to the color's brightness. A color wheel superimposed over an a versus b plot permits the user to edit the individual data points in the familiar space of hue and saturation. The one dimensional a and b components are combined to become a two dimensional set of data points on the a versus b plot. This locus of data points forms a slightly curved line through a versus b space. The colors that the locus passes through represent the goniochromatic color shift across aspecular angles.

Editing the data points directly is tedious since the goniochromatic color can be sampled at several different viewing angles in Lab space. Defining a completely new color requires the user to move many data points. As a result, the main use of this control would be to enter color data sampled from a goniospectrophotometer.

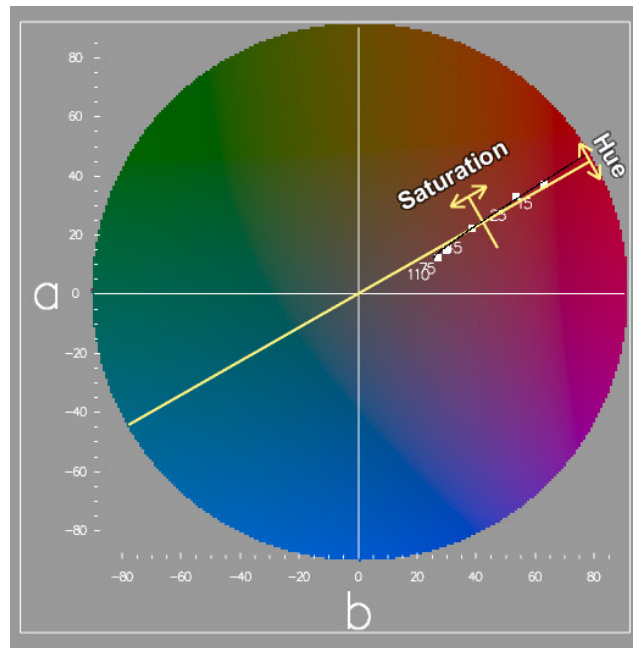


Figure 3.6: Hue and saturation control.

3.4.2 Hue, saturation, and brightness control

The color shift of a traditional metallic automotive color consists primarily of a change in saturation and brightness while hue remains constant. This can be seen in Figure 3.6 where the locus of points for a metallic red can be approximated by a straight line that extends radially outward from the center of the a versus b plot. This is a line of constant hue on the a versus b diagram.

The hue, saturation, and brightness control allows the user to edit, as a group, the family of colors that defines a goniochromatic color shift. Moving the saturation control in and out from the center of the a versus b plot changes the average saturation. Adjusting the angle of the hue control rotates the color to a new average hue. This is implemented using rotate and scale linear transformations upon the original data points. The resulting

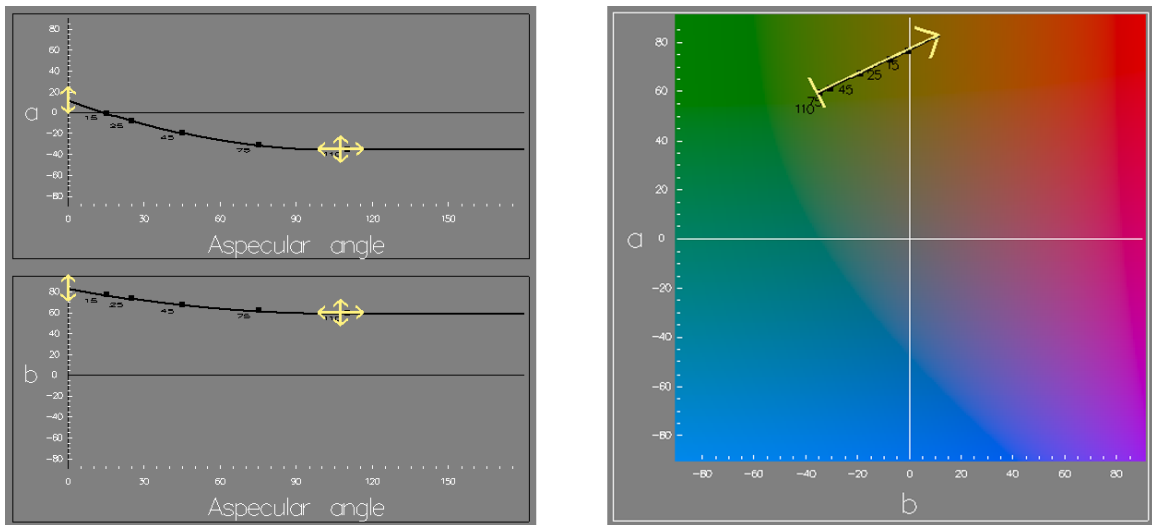


Figure 3.7: Modifying a color by its control points.

color appearance will have a different color, but it will retain the relative spacing between the color control points. The user manipulates brightness by moving a line drawn through the average value of the L plot.

The hue, saturation, and brightness method is useful for adjusting a traditional metallic paint to see what it would look like in a different hue. This approach has the disadvantage of only permitting the user to change the average hue and saturation; it does not allow the user to independently adjust the color appearance across different viewing angles.

3.4.3 Face, flop, and travel color picker

The locus of data points on the a versus b plot forms a straight line segment through ab space. The face, flop, and travel color picker allows the user to control the endpoints of the locus individually as well as move the entire locus around as a unit. Face, flop, and travel colors correspond directly to the control points of the clamped quadratic polynomials used to represent a goniochromatic color.

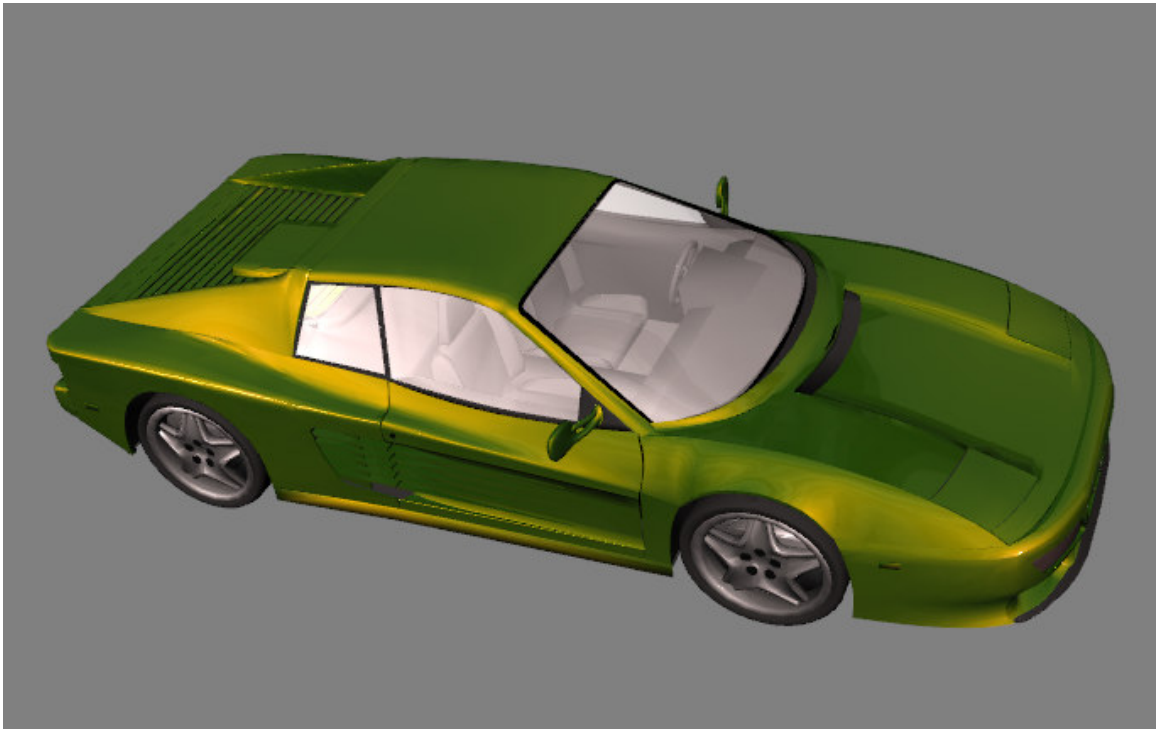


Figure 3.8: The color corresponding to Figure 3.7.

The user interface displays an arrow on the a versus b plot (see Figure 3.3a) that corresponds to the control points of the a and b clamped quadratic polynomials as seen in Figure 3.7. The arrowhead is positioned on the face color and can be moved to define the color that occurs in the specular direction. The base of the arrow is situated on the flop color and can be adjusted to establish the color that is produced far away from specular. The arrow can also be dragged as a complete unit. Controls for the face and flop colors are also displayed on the L , a , and b plots. The travel can be modified through the L , a , and b plots by dragging the flop/travel control horizontally.

This method is the best way to design a metallic color with dramatic changes between the face and flop colors. These “effect” colors are becoming more commonplace as paint

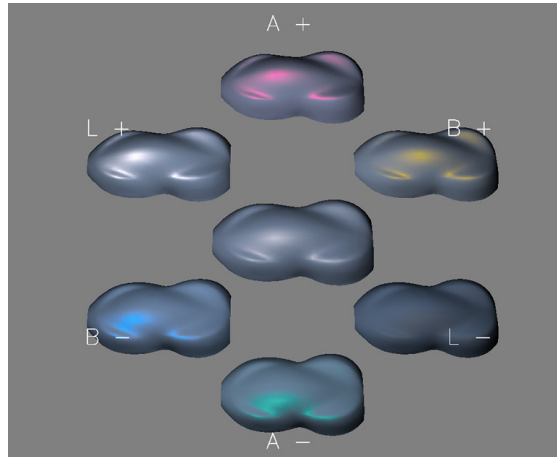


Figure 3.9: Variations on the face color.

technology continues to improve. Since this method of dragging the ends of the arrowhead and adjusting the control points on the L, a, and b plots are complex tasks, the face, flop, and travel color picker may be difficult for people without training.

3.4.4 Variations control

We would like to have a method for designing a color that allows a novice computer user full control over all aspects of the color in a straightforward manner. The Variations mode is simple yet powerful goal-oriented approach for designing color. Starting with any color definition, that color is rendered on an object surrounded by variations on that color (see Figures 3.9 and 3.10). The user clicks on any variation that is a closer match to the desired appearance. The colors are then updated. This cycle is continued until the user reaches a color with which they are satisfied. Since there are so many variations on a color, the variations are arranged into the categories face color, flop color, and travel and gloss. The degree of variation can also be modified by the user.

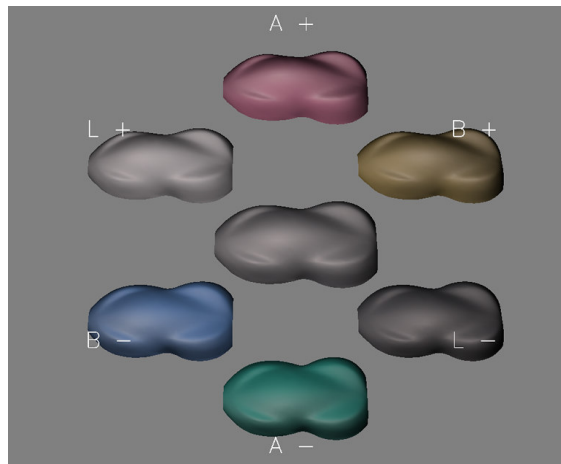


Figure 3.10: Variations on the flop color.

There are strengths and weakness to the Variations method. This method is good for novice computer users, since pointing to the variation they prefer and clicking is all that is required. Since variations on all aspects of the color definition are displayed, the variation mode is powerful enough that a user can achieve any color that our system can render. The main drawback is that it takes many clicks to design a completely new color, so a person familiar with the program's other modes of operation may find variations too tedious. Adobe Photoshop also has a variations mode. It is worth noting that an artist suggested the use of this method.

3.4.5 Gloss control

To design gloss, the user moves a gloss slider from 0 to 100. The values are based on industry standards designed to be perceptually uniform. From the single gloss value, the program then chooses both the specular exponent and weight parameters to the Phong model using a method that was introduced by Westlund and Meyer [65]. The specular exponent and weight are constrained so as to be energy conserving.



Figure 3.11: A three dimensional color pallet.

3.4.6 Color pallet

Since a normal color palette does not convey the information needed to fully describe the color shift and gloss of a metallic paint, we must extend the idea of a color palette to work with color shifting and gloss. We have chosen to make a gradient bar that shows the color shift across viewing angles. The gloss value is displayed by the brightness of the border surrounding the color bar. This allows the entire color description to be displayed in compact form for display in a color palette. Alternatively, the color pallet can also be displayed as a shaded three dimensional booklet as shown in Figure 3.11.

3.5 Virtual mood board

Designers frequently seek inspiration from images and other visual artifacts. In Figure 3.12, the automotive speed shape's color appearance was inspired by fashion trends. Their creative work flow often starts with something called a mood board [4]. Mood boards can also be called collages, story boards or inspiration boards. A mood board typically consists of a large piece of foam core or cardboard. A designer uses thumbtacks to arrange images cut from magazines, concept art, and other visual artifacts on the mood board.

In the aesthetic design fields, mood boards are used extensively for material selection. The process might start out with a stylist collecting images from a stock art web site or from a fashion magazine. Materials such as a piece of leather from a glove, a belt buckle, or a seashell might also be placed on the mood board. Figures 3.13 and 3.14 were created as examples of mood boards for proposing color concepts.

This section presents a virtual mood board for supporting the design process from conceptualization to fabrication. While others have created systems that allow designers to collect and arrange digital images [7], our goal is to help designers turn these images into new color appearances that they can evaluate on 3D shapes. A stylist uses our virtual mood board to organize digital images that provide material inspiration, but they also use the pictures on the board to seed the parameters of the metallic reflection model.

Typical work flow starts with the stylist laying out a mood board with various digital images as shown on the left of Figure 3.15. This mood board was created to select color appearances for a hydrogen concept vehicle. Next, they select the face, flop, and gloss of



Figure 3.12: The automotive speed shape's color and travel were directly selected from a Dior fashion advertisement.

the reflection model from the mood board using eyedroppers and visualize the results on an object as shown on the right. Once satisfied with the design, they export the color as standard aspecular measurements to be rapidly prototyped using a paint formulation system.

The digital images can be obtained from variety of sources such as a digital camera, a scanner, or the web. Images of color pallets can be imported into a mood board and work as a specialized color picker for a particular industry. An image of a collection of Pantone colors can provide a color stylist who has a print background with a familiar pallet. A stylist with an artistic background may prefer pages of the Munsell color system or photos of other color wheels.

Figure 3.13: In the aesthetic design fields, mood boards are used extensively for material and color selection. The process might start out with a stylist collecting images from fashion magazines and other visually appealing artifacts. The art director of a style and fashion magazine was invited to participate in the user study. She proposed “Orange Ball of Paris” that appeals to a young and fashionable audience.



Figure 3.14: Inspired by the sporty fashion trends of California’s Orange County, another mood board was created for a color called “Hydrogen Blue in the OC” for a hydrogen powered concept car.

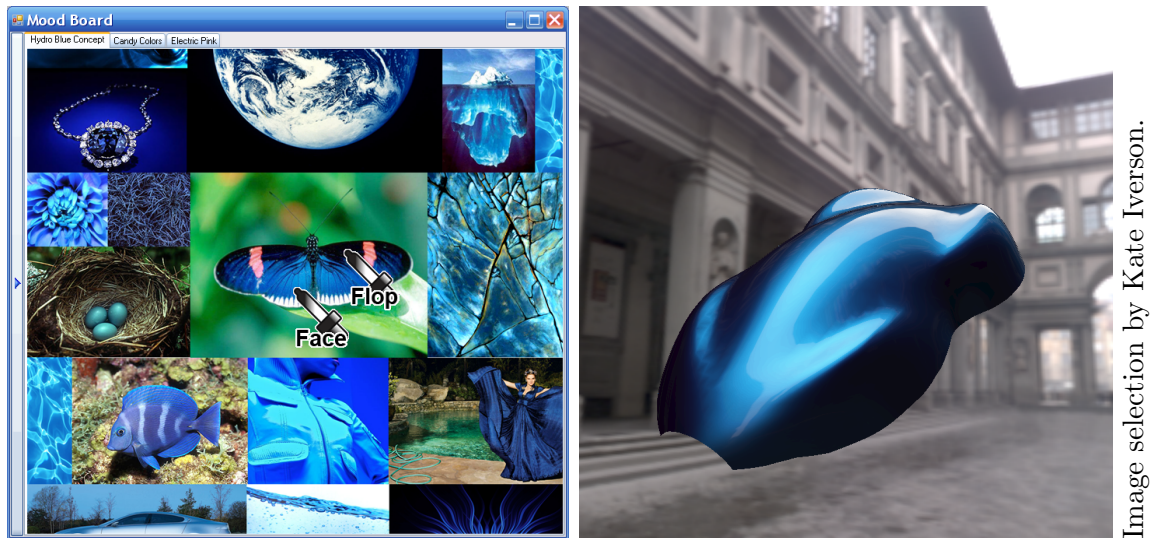


Figure 3.15: A designer was instructed to create a virtual mood board relevant to a hydrogen concept vehicle (left). Designers arrange inspirational images for material concepts on the mood board. They select the 15° face color and θ_{clamp} flop color using eyedroppers. The rendering on the right is of a material seeded by the colors in the butterfly’s wings.

3.5.1 Interface

The virtual mood board’s user interface is designed to mimic the work flow of a real mood board. The user creates separate boards for different projects using the virtual mood board’s tabbed interface. In the same way a stylist arranges images cut from magazines on a real mood board using thumb tacks, the stylist arranges digital images on the virtual mood board using the mouse to drag them around. The scroll function of the mouse is mapped to zooming in and out of the image under the cursor. Once the stylist has some images arranged on the mood board, they can now use the system to select and visualize materials.

Although it would be ideal to be able to sample full BRDF measurements from the images found on the mood board, this is not yet possible. Obtaining BRDFs from materials in photographs is an inverse rendering problem. A reflected light field is a convolution of the

incident lighting and the BRDF [47]. Therefore, to reconstruct a BRDF from a photograph, the incident lighting and scene geometry are needed. There are a variety of techniques for photographic acquisition of BRDFs. These techniques need scene geometry, controlled or known lighting, and/or multiple photographs [68, 31, 67]. Because the images found on a mood board do not have information about scene geometry and incident lighting, inverse rendering techniques cannot be used for obtaining BRDF information.

Human observers are able to estimate material properties easily from photographs, and there has been a variety of research in perception looking at how human observers are able to estimate material properties of objects [8]. Even though multiple combinations of lighting and materials can be consistent with a given image, humans can discern material properties from images without lighting cues because of the regularity of typical illumination [17]. By computing statistics on luminance distribution of multi-scale band-pass filtered version on a HDR image, [14] was able to classify reflectance from photographs with unknown lighting and known geometry.

Accurately estimating a BRDF from a single image with no lighting information and no scene geometry is still an open topic for computer graphics. Although this thesis does not claim to have solved it, the mood board interface provides a useful compromise.

The reflection model presented in Section 3.3 allows the virtual mood board to use a simple but effective interface for selecting material properties from images. Remember, the parameters of the reflection model that need to be set are face, flop, travel, and gloss. The parameters are set using eyedroppers to directly sample color from the mood board. One eyedropper is labeled face and is used for picking $Lab(15^\circ)$. One eyedropper is labeled flop

and is used for choosing $Lab(\theta_{clamp})$. A special gloss eyedropper selects gloss. A slider provides control of travel (θ_{clamp}).

3.5.2 Face/flop eyedropper

The metaphor of using an eyedropper to select a color from an image is best known from Adobe Photoshop, although other commercial products also use the eyedropper paradigm for color selection. Although the use of eyedroppers is not new, a dramatic improvement in usability is achieved because the eyedroppers are paired with the virtual mood board and the face/flop reflection model.

The user drags each eyedropper over images in the mood board using the mouse cursor. As the user drags the eyedropper over the images the program samples over a small range of pixels under the mouse cursor to provide a steady color selection. When the user releases the mouse cursor the eyedropper rests over the drop point.

The mood board software converts the face and flop color sampled from the eyedroppers (as well as the travel from the sliders) to the parametric form of the reflection model. The system uses the rendering engine described in [52] to display a preview of the color as the user drags the eyedropper around the mood board. The parametric form of the reflection model is used (along with pre-captured environment maps to this rendering engine) to display the new colors as they are designed in real time.

One interesting use of eyedroppers is to pull color inspiration from one type of material to seed another type of material. These material types can be widely differing. For instance, Figure 3.16 shows a designed metallic automotive paint that is the color of a velvet sport



Figure 3.16: Although the spatial distribution of velvet is not captured from this image, the system still duplicates the color appearance.

coat. While the metallic reflection model cannot represent the spatial reflectance of velvet, the eyedroppers can still capture the particular shades of that color.

There are some improvements to the system that make it more useable. Since retroreflective colors are uncommon and not well represented by the face/flop/travel reflection model our software assumes that the face component of the reflection model is never darker than the flop component. The system defaults to automatically swap the eyedroppers if the user is selecting a face color that is darker than the flop color or vice versa. This option can be disabled to style retroreflective colors. Another interface improvement is to allow the eyedropper to sample parts of the screen outside the mood board. This allows the designer to sample from not only images inside the mood board, but also directly from websites, videos, 2D and 3D color collections, Quicktime VRs, and any interactive 3D application.

3.5.3 Gloss eyedropper

The gloss dropper uses a simple image processing approximation to make a rough guess for contrast gloss. We use a simpler method that is a rougher approximation compared to inverse rendering techniques, but can be used with low dynamic range images with unknown lighting and unknown geometry. By ignoring complicated gloss appearance attributes like standard gloss, sheen, haze and distinctness of image we use the idea of an appearance attribute called contrast gloss [21]. This is defined as the contrast between the specularly reflecting areas and other areas. Although this metric is normally used for low gloss surfaces, the concept is reasonable in the context of our virtual mood board. When we take advantage of the fact that a human is guiding the gloss eyedropper to interesting parts of the image that are representative of the object's gloss, we can use this technique on an image without any lighting or geometry information.

The shape, size, and scale of a specular highlight is dependent on material properties as well as incident lighting and object shape. However, the gloss portion of a BRDF is imaged onto a picture as the brightest peak of a specular reflection. The non-gloss components of the BRDF appear in darker regions around the specular reflection.

The user is instructed to guide the gloss eyedropper to areas representative of the objects gloss level like specular highlights, boundaries of specular reflections, or dull areas of matt objects. As the user moves the gloss eyedropper over an image, it samples a small region of pixels under the cursor. A histogram is created from these pixels. Since we are working with low dynamic range digital images, brightness is measured on a scale of 0 to 1. The

software computes average brightness of the top 10% of pixels and the bottom 10% of pixels. The difference between these two numbers is the contrast and is linearly mapped from 0 to .5 difference in brightness to 0 to 100 gloss. Differences greater than .5 are assigned a gloss value of 100. We blend gloss samples over consecutive frames to improve the stability of user interaction. The radius of the region of pixels sampled is adjusted in an options menu.

Limitations of this technique are that it is only an approximation and it will only work on images with locally smooth geometry around the eyedropper’s sampling area. It will incorrectly classify surface texture, geometric topology, and shadow boundaries as gloss. Second order image statistics using gray level co-occurrence matrices (GLCM) were used to attempt to classify regions of surface texture and try to prevent the user from sampling gloss from these regions. However, this method did not disambiguate between surface texture and specular reflections. Since the user will know that textured and shadow regions are not representative of the appearance of gloss, we do not expect this to be an issue. See [61] for more information on using GLCM for texture analysis and classification. The mapping from the brightness differences to gloss levels was selected by trial and error. Future research will explore the use of multidimensional scaling for mapping local contrast to gloss values.

3.6 Image based BRDF tweaker

Color stylists often want to make minor modifications to automotive color designs. They may realize that the color needs tweaking only after seeing the color on a three dimensional surface like a car mockup. They may want the color on the hood to be a little brighter or the color on the doors to be a little less saturated. Since the car is painted a uniform

color, their request must be interpreted as modifications to the face and/or flop of a color that will affect the entire surface. A stylist with a deeper understanding of the behavior of automotive finishes would be able to make adjustments to the face, flop, and travel to indirectly get the desired appearance of the automobile. A tool that would allow stylists to specify color adjustments directly at particular positions on the body of a car would provide them more precise control over the genesis of the color's appearance.

The image based BRDF tweaker is a color design interface for tweaking the color and appearance of the reflection model directly on a 3D object. With the BRDF tweaker, we are extending the ideas originally proposed in [9] for use on any shape to provide rich, complete control over the parameters of the face/flop/travel/gloss reflection model.

We first describe the mode of operation and then describe the how the software achieves it using an off-screen buffer to map image space screen coordinates to the parameters of the BRDF.

3.6.1 Tools and mode of operation

The BRDF tweaker is integrated into a simple point light rendering engine. The BRDF tweaker is context sensitive and changes the display and mode of operation depending on a number of factors. The tool consists of a draggable *crosshair* widget for tweaking color at specific areas on the object and a heads up display(HUD) for visualizing and adjusting spatial aspects of the BRDF.

When the draggable crosshair widget is positioned on top of the 3D object, the crosshair widget expands to show color manipulation tools and the HUD is disabled. The color

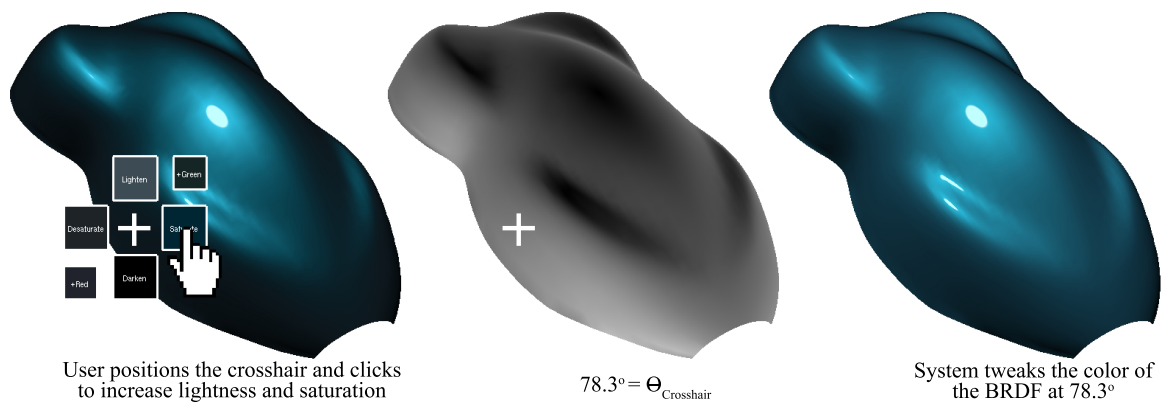


Figure 3.17: The original color looks a little too dull on the bottom left edge of the object. The stylist positions the crosshair over this area and increases saturation and brightness (left). A shader renders aspecular angle to an off screen buffer to assist mapping adjustments from image-space to BRDF space (center). By indexing into the buffer with the crosshair coordinates, the system calculates that the color should be adjusted at 78.3° (right).

manipulation tools let the user drag a crosshair to positions on the object and directly adjust the lightness, saturation, and hue at that particular area of the object. As the crosshair is moved across the surface of the object, the widget samples the aspecular angle under the crosshair. The color of the BRDF at the particular aspecular angle is computed. Surrounding the crosshair are buttons that show variations of the color of the BRDF under the crosshair. Above and below the crosshair are buttons that show lighter and darker versions of the color. To the left and right are increased and decreased saturation (also called chroma), and diagonally are hue rotations. When a button is pressed, the color is adjusted at that position, it updates the reflection model using the technique described in Section 3.6.2, and the change is reflected in the entire image. For example, if the crosshair is over the *face* region (as shown on the bottom left of Figure 3.17) of the 3D object, then adjustments only change the *face* of the BRDF while leaving the *flop* color untouched. If

the crosshair is in between the face and the flop and the saturate button is clicked, it will adjust the saturation color at both face and flop to varying degrees.

When the draggable crosshair widget is dragged off of the object, the crosshair widget contracts and hides the color manipulation tools and the HUD is enabled. The HUD shows a visualization of the aspecular lighting angles as a topology map. This is very useful for understanding exactly how the color plays or travels across the object. The heads up display is driven by a hardware shader that computes the angle between the reflected light and view vector (the aspecular angle). The left side of Figure 3.18 shows the heads up display over a three dimensional shape designed by the automotive industry to help evaluate color appearance. Pixels being rendered by the shader are highlighted if their aspecular angle is within a few degrees of 15° , 45° , or θ_{clamp} . The topology of the ring representing θ_{clamp} changes depending on the rate of travel of the BRDF. Additionally, the gloss region is displayed with a checkerboard. In this mode, the stylist can drag the ring representing θ_{clamp} to end at a particular position on the 3D object. Also, if the user clicks on the edge of the specular highlight they can drag it to adjust the width of the specular highlight to affect the gloss. Finally, if they click in the center of the specular highlight then they can drag the specular reflection to a new point on the surface of the object. This is an easy goal driven way of adjusting the light position.

3.6.2 Making adjustments

The BRDF tweaker is powered by a series of shaders that render extra information about the scene's reflectance in image space into off screen buffers. Point lighting allows us to compute

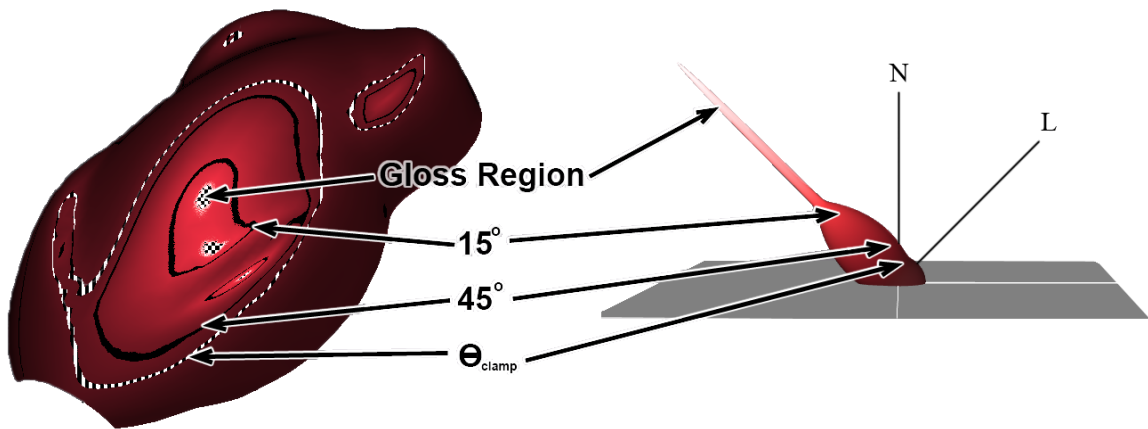


Figure 3.18: The left shows the heads up display over an auto speed shape. Specific aspecular angles in image space are correlated to positions on a graph of the BRDF for this illustration (right).

an exact mapping between pixels on the screen and lighting angles or viewing angles of the BRDF. The principle parameter of the reflection model presented in Section 3.3.2 is aspecular angle. A shader computes this and stores it in an off screen buffer. This needs to be computed when the scene, view, or lighting changes. It does not need to be recomputed if the only modification is to the BRDF.

Adjust color

If the crosshair is on top of the object on any spot other than a specular highlight, adjustments are made to specific angles of the metallic portion of the reflection model depending on exactly where the crosshair is positioned. If the user has clicked a color adjustment button, the face and flop of the reflection model is adjusted by a delta in lightness (ΔL), saturation/chroma (ΔC), or hue (ΔH) as shown in equations 3.6.1, 3.6.2, and 3.6.3 respectively depending on which button they picked. These equations are applied to *both*

face and flop to create temporary colors, marked by a single prime symbol, $Lab'(15^\circ)$ and $Lab'(\theta_{clamped})$.

$$Lab' = (L + \Delta L, a, b) \quad (3.6.1)$$

$$Lab' = (L, a * (1 + \Delta C), b * (1 + \Delta C)) \quad (3.6.2)$$

$$Lab' = (L, a * \cos(\Delta H) - b * \sin(\Delta H), \\ a * \sin(\Delta H) + b * \cos(\Delta H)) \quad (3.6.3)$$

To make the color adjustments happen at specific angles, the aspecular angle, $\theta_{crosshair}$, of the position under the crosshair is used to compute the ratio, R , of how the face and flop color will be adjusted. Equation 3.6.4 maps $\theta_{crosshair}$ from between 15° and the θ_{clamp} angle to 0 to 1. If the angle is less than 15° it treats it as the face and assigns the value of 1.0 to R . If it is greater than the color's θ_{clamp} it treats it as the flop and sets R to 0.0.

$$R = \begin{cases} 0 & 15^\circ > \theta_{crosshair} \\ \frac{\theta_{crosshair} - 15^\circ}{\theta_{clamp} - 15^\circ} & 15^\circ \geq \theta_{crosshair} \geq \theta_{clamp} \\ 1 & \theta_{crosshair} > \theta_{clamp} \end{cases} \quad (3.6.4)$$

The temporary colors are blended with the original color by the ratio, R , to get the final colors, marked by a double prime symbol, for face and flop:

$$Lab''(15^\circ) = (1 - R) * Lab(15^\circ) + R * Lab'(15^\circ) \quad (3.6.5)$$

$$Lab''(\theta_{clamp}) = R * Lab(\theta_{clamp}) + (1 - R) * Lab'(\theta_{clamp}) \quad (3.6.6)$$

Adjust travel

When the mouse is depressed, the system samples the off screen buffer to retrieve the aspecular angle at the coordinates under the cursor, θ_{cursor} . In the first scenario the user

clicked on the ring visualizing travel. This is detected by comparing θ_{cursor} to θ_{clamp} to determine if it is within a few degrees. If the user wants to adjust travel to coincide with the curvature of the object, they can click and drag the ring representing θ_{clamp} . They set the position where the color travel visually stops by using the mouse to move the spot directly on the object. As the user drags the mouse, the θ_{clamp} (the travel parameter of the face flop model) is set based on the aspecular angle under the new position of the cursor.

Adjust gloss

Adjusting the size of the gloss lobe works in a manner similar to adjusting travel. When the user clicks and drags the edge of the gloss, the gloss level is adjusted based on the new aspecular angle under the cursor as it repositioned. A mapping between gloss and aspecular angles needs to be made to detect when the edge of gloss is being clicked on. The implementation is relatively straightforward.

Move light

Finally, we describe a simple but useful tool for positioning the light by dragging the specular highlight. To determine if the user is trying to click on the highlight, the system samples the aspecular angle of the mouse cursor position from the off screen buffer, θ_{cursor} . The gloss parameter determines the shape and size of the specular lobe of the BRDF. By sampling the gloss lobe with the aspecular angle of the cursor position one can determine if the user clicked on the center of the highlight (to reposition the light), the edge of the highlight (to adjust the gloss level), or clicking the object to rotate it.

When the user clicks near the center of a specular highlight and begins to drag it, a different shader is used for the off screen buffer. Instead of computing the aspecular angle, this shader computes at every pixel on the object the direction that the light would need to be in if the specular highlight was centered on that particular pixel. The required light vector is simply the view vector reflected off the surface normal. This vector is stored in the off screen buffer encoded as RGB values. As the user drags the cursor across the object, the system sets the new position of the light to be the light vector that is encoded in the off screen buffer at the coordinates of the cursor. The light is updated and specular highlight tracks the mouse cursor.

3.7 Sketch based color styling

Artists and designers often communicate initial vision for a final product through the use of “concept art”. Concept art may take many forms - from hand-drawn renderings to modifying existing images that provide visual insight into the designer’s ideas on form, color, texture, mood and so on. The software described in this section provides a sketch based BRDF design interface that effectively utilizes the contributions of the concept artist in the final design. Color appearance is designed by directly painting it onto an image of an object. Again, the parameters of the reflection model that need to be modeled by the sketch based interface are face, flop, travel and gloss. These are modeled by using standard fitting routines to find the parameters of the reflection model that match the concept artist’s design.



Illustrations by Nick Golfis.

Figure 3.19: The concept artist traced the outlines of a rendering onto a new sheet of paper. Next, he used colored markers to fill in the outlines with his concept color. This artwork was scanned back into the system using a flatbed scanner, and Photoshop was used to align the scanned artwork with the existing scene. The algorithm matched a pink pearlescent color to his concept art.

Although it would be ideal to produce complete BRDF measurements directly from concept art, this is impossible. Obtaining BRDFs from images is an inverse rendering problem. Since concept art is a 2D image and thus does not have geometry and lighting information, full BRDF information cannot be obtained from pictures using inverse rendering techniques. However, if concept art has shape and lighting information, a full BRDF representation can be extracted. Rather than attempting to back out shape and lighting from the concept art, the artist simply draws over a rendering of an existing scene of known geometry and

lighting. With this information we can use inverse rendering to find BRDF information. Therefore, the system presented in this section allows a user to make alterations to an image of a previously modeled object, but not create a completely new image from scratch.

More research needs to be done to be able to fully characterize the many types of artistic techniques that concept artists use and this work is beyond the scope of this thesis. We do however show that our sketch based system works with a selection of artistic techniques. Work has been done in registering artistic drawings with computer renderings. Artists were asked to create line drawings of a variety of 3d shapes with diffuse reflectance in [10]. Among other things, they studied how the lines the artists drew correlated with lines predicted by computer graphic techniques as well as the topology of the figure’s surface. They showed that while there is overlap in the lines that artists drew, there were some lines that were unique to individual artists and many lines that current graphics algorithms do not predict.

We now present the sketch based BRDF modeling interface. There are three main steps to the system. First, a setup step prepares the initial image upon which the designer will base their concept art. Next, the artist creates concept art over the initial image using an image editing program such as Adobe Photoshop. Alternatively, they can use pen and paper illustration techniques by printing it out and tracing or painting their design over the hardcopy, and scanning their concept art back in. Finally, a BRDF fitting system finds the parameters to the reflection model that best approximates the concept art. We start by walking through the workflow in point lighting environments. We extend this technique to environment mapped based lighting in Sections 3.7.5.

3.7.1 Setup

The artist starts by positioning a 3D object and a simple point light in a scene. A preprocessing step saves a rendering as the initial image that the designer will use as a basis for their concept art. The system's default is silver, but the user is free to use any color as a starting point. In addition to the screenshot, it renders the scene using a special shader that encodes lighting and viewing geometry on a per pixel basis. The shader computes the aspecular angle between the reflected light and view vectors (θ) as well as the cosine between the light and surface normal (ϕ). This is the minimum information needed to completely index the metallic reflection model. Aspecular angle, θ , is encoded in the red channel, ϕ is encoded in the green channel, and the blue channel is simply used for foreground background segmentation by encoding a value of 100% for material to be designed and 0% for the background and nonmetallic trim.

3.7.2 Artist interaction

The initial image is loaded into Photoshop. The user may then view and modify the image using all of the tools that Photoshop has to offer. Because of the choice of the fitting routine used in the next step, it is important that they paint the color in a manner that is consistent with the scene and lighting geometry. The user may use Photoshop's magic wand to mask the automobile and adjust the color of the car using Photoshop's rich set of color correction tools. They may also use Photoshop's burn and dodge tool to adjust the brightness of the face and flop color or the rate of travel. The artist may also repaint the object completely from scratch, using the gradient paint bucket, airbrush, and other

painting tools. Once the user is satisfied with the changes that have been made, the image is saved and the modifications are sent to the fitting routine.

Alternatively, the stylist can use traditional pen and paper illustration techniques. They start by printing out the initial image to a hardcopy form. Next, they either trace over the image or paint their design over the hardcopy. Finally, they scan their concept art back into the system and superimpose the scan over the initial Photoshop image. Care must be taken to align the images exactly and mask out the background.

3.7.3 Fitting

The final step uses least squares to fit the parametric form of the metallic reflection model to the artist's drawing. The parametric form of the metallic reflection model is written for the R or red component in Equation 3.7.1.

$$\theta_i^2 \varphi_i a_R + \theta_i \varphi_i b_R + \varphi_i c_R = R_i \quad (3.7.1)$$

The subscript i is the index of the i th of n changed foreground pixels. θ_i and ϕ_i are the aspecular angle and lambertian term of the i th changed pixel. This term is never needed for design, but is present here because the parametric form is used in an inverse rendering context. a , b , and c are the three parameters for each of the red, green, and blue quadratic equations.

A matrix is constructed that represents the mapping between the BRDF and the image of the artists design. Every pixel in the foreground of the image that was modified by the artist is inserted into the matrix. Since we are not solving for gloss white pixels, near white pixels, and pixels with low aspecular angles are removed to discount for gloss. An inverse

gamma correction function is applied to take the colors from the nonlinear RGB values for display to linear RGB for calculation. The matrix is shown below.

$$\begin{bmatrix} \theta_1^2\phi_1 & \theta_1\phi_1 & \phi_1 \\ \theta_2^2\phi_2 & \theta_2\phi_2 & \phi_2 \\ \vdots & \vdots & \vdots \\ \theta_n^2\phi_n & \theta_n\phi_n & \phi_n \end{bmatrix} \begin{bmatrix} a_R & a_G & a_B \\ b_R & b_G & b_B \\ c_R & c_G & c_B \end{bmatrix} = \begin{bmatrix} R_1 & G_1 & B_1 \\ R_2 & G_2 & B_2 \\ \vdots & \vdots & \vdots \\ R_n & G_n & B_n \end{bmatrix} \quad (3.7.2)$$

Because the parametric form of the BRDF is a clamped quadratic polynomial rather than a U shaped parabola, θ_i needs to be clamped to be less than θ_{clamp} when constructing the matrix. Since θ_{clamp} is unknown at the time the matrix is constructed, multiple values of θ_{clamp} are tested and the solution with the least error is used.

Although this matrix equality is over constrained, a , b , and c for the red green and blue channels can be solved for using least squares fitting. We are guaranteed to find the parameters of the metallic reflection model. Least squares minimizes the error of approximating the artistically designed BRDF in the concept art as the coefficients to quadratic equations for red, green and blue. The least squares fitting is robust enough to find a solution even if the artist did not perfectly draw the material, although an image that was not drawn accurately will have poor correspondence with the BRDF found by least squares.

The solution needs to be converted from RGB to *Lab* color in order to load the color back into the design system. The RGB parametric form is simply evaluated at 15° , 45° , and 110° and the RGB values are converted to *Lab* values.

Gloss is not solved for using the matrix. Gloss can be ignored and given a default value of 50. Alternatively, it can be approximated using the simple contrast gloss technique

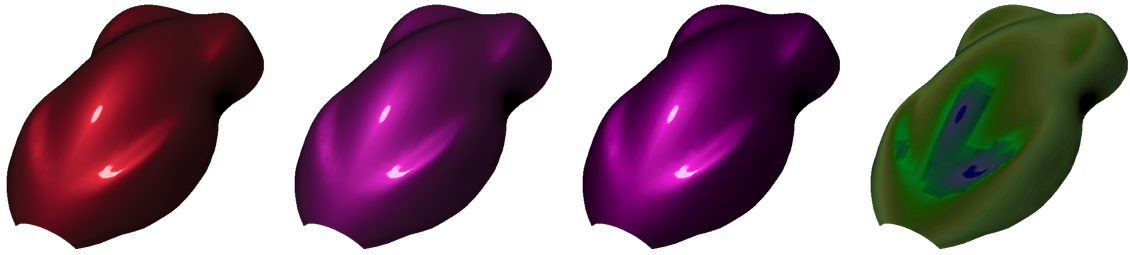


Figure 3.20: The initial image (left) was manipulated in Photoshop by rotating the hue to create the goal image (middle left). The least squares fitting routine found a close match (middle right). A contrast enhanced difference image visualizes the error (right).

described in Section 3.5.3. Instead of using the gloss eyedropper, the histogram is created using a set of pixels at and around highlights by using all pixels in the foreground that have an aspecular angle less than 15° .

3.7.4 Results

In Figure 3.20, the original image (not shown) was manipulated in Photoshop by rotating the hue to create the goal image (left). Compared to the goal, the rendering of the found material (middle) has a RMS error of $2 \Delta Es$. The image on the right visualizes the difference between the goal and found image.

In Figure 3.21, the initial image was printed to a physical copy. The artist created his concept art by tracing the shape of the car onto a new sheet of paper and filling in the outlines with markers as shown on the top of Figure 3.21. The art was scanned back into the computer, and aligned over the initial image using Photoshop. At first the least squares routine gave very poor matches, because of the geometric misalignment of the image, fine details, and specular highlight. After manually masking out the problematic areas and redoing the fit, a rendering of the final match is shown (bottom). The final match has a relatively high RMS error of $14 \Delta Es$. This is because the artistic marker techniques used

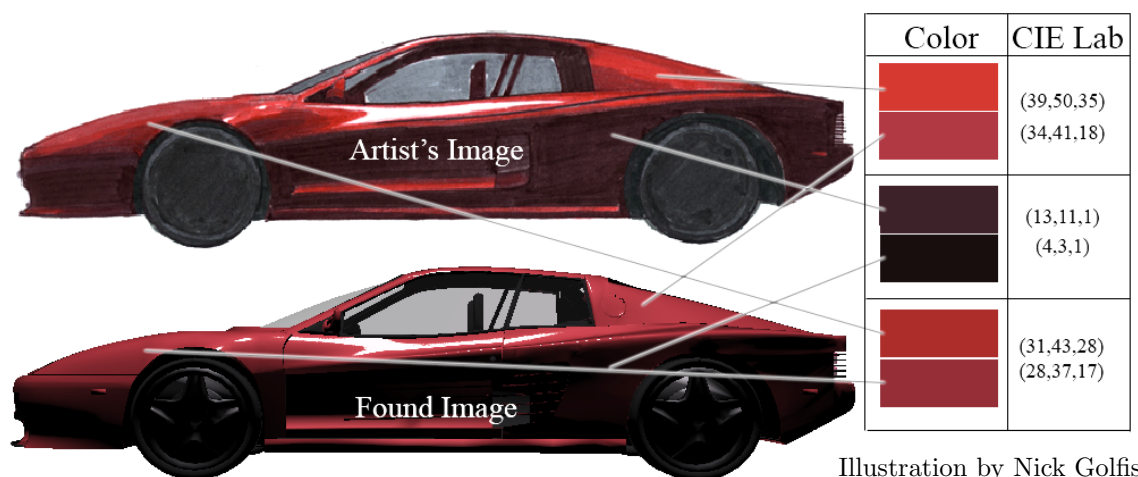


Figure 3.21: The initial image (not shown) was printed to a hardcopy. The artist created his concept art by tracing the image and filling in with markers onto a new sheet of paper (top). A rendering of the final match is shown (bottom). Color samples in Lab space show that the computer's fit to the hand drawn image is not perfect, however it is a good match visually.

are not photorealistic. A low error is possible only if the artist is photorealistic and manages to create an image that precisely matches the lighting and behavior of the BRDF.

Finally, if the linear approximation fails to find a good fit, the system simply returns a diffuse color that is the average of the changed pixels. The linear approximation can fail if the color gradations on the artistically designed image do not match the lighting close enough. Changes using Photoshop's color manipulation tools almost never fail. Completely repainting the color using Photoshop's airbrush tool has moderate chance of failing on the first try(in our experience about 20%), but usually will succeed after minor adjustments are made to the art image to create a more consistent color gradation. Tracing and scanning back in a concept art image has the highest chance of failure(in our experience about 35%), but again will usually succeed after adjustments are made to the art image to create a more consistent color gradation.

3.7.5 Extension to environment mapped based lighting

We extended the sketch based BRDF design system to work with environment mapped based lighting. After generating an initial image of an object in an environment map based lighting environment and creating concept art based on this image, we proceed with the fitting step. Because we have the scene's geometry and original lighting environment, we use nonlinear approximation to find the parameters of the reflection model [28]. Nonlinear optimization needs a set of variables to search space (X), a starting condition (x_0), and a search heuristic ($f(x)$). The parameters of the search space, (X), are the tristimulus face and flop colors, travel, and gloss. A neutral silver with a mid gloss level is chosen as the starting condition, (x_0).

The search heuristic is in the form of an objective function, ($f(x)$), that compares the concept art to a rendering of the scene with the current guess of the material. The objective function code starts by rendering an image of the scene with the current guess of reflection model parameters. It computes the root-mean-squared error of the artistically designed goal image to the rendering of the current guess. The error is computed only for pixels in the foreground. Once the search starts, the optimization routine iteratively tries new guesses of reflection model parameters to minimize the objective function as shown in Equation 3.7.3. The search iterates until no further improvement can be made. The search takes several minutes to converge on an answer, (x').

$$x' = \min_{x \in X} (f(x)) \quad (3.7.3)$$

Figure 3.19 shows advanced use of the sketch based BRDF design interface. Using the environment mapped tool, a screenshot is rendered and printed to a hardcopy using a color printer. The concept artist then traced the outlines onto a new sheet of paper. Next, he used colored markers to fill in the outlines with his concept color. This artwork was scanned back into the system using a flatbed scanner, and Photoshop was used to align the scanned artwork with the existing scene. This seeds the BRDF fitting routine. The algorithm matched a pink pearlescent color to his concept art. Although the optimization routine found a reasonable match, as expected the RMS error was a relatively high 15 ΔE_s .

3.8 Evaluation

We evaluated the image based BRDF design interface by asking several designers familiar with automotive metallic paints to use our software to create several new colors. We began our informal tests by using real paint samples to make sure that each designer understood what was meant by the terms face color, flop color, travel, and gloss. The participants were then requested to perform three different color styling tasks using both the interfaces described in 3.5, 3.6, and 3.7 and the goniochromatic color design interface shown in Fig. 3.3. The designers were asked for their reactions to using the new and the old interfaces.

Select the face color, flop color, travel, and gloss for a new metallic color:

In our new interface this is accomplished by using the virtual mood board to choose the face color, the flop color, and the gloss for the color. The image based BRDF tweaker is employed to determine the travel and adjust the color. In the existing goniochromatic color design interface this task is accomplished by designating the face and flop colors on a

hue/saturation diagram, adjusting the L curve for the color, and setting the position of a gloss slider (see Figure 3.3).

The participants remarked that the pictures on the mood board interface suggested better starting points for their color design and allowed them to use their own reference material to seed the design process. They found it difficult to find a particular color using the single color wheel available in the existing goniochromatic color design interface. Using the BRDF tweaker to point at the surface and adjust the color travel was considered to be more straightforward than using the old goniochromatic color design interface to manipulate the endpoints of a second order curve.

Adjust the hue, saturation, and brightness of an existing metallic color: This is done with the new image based BRDF design interface by transferring a snapshot from the BRDF tweaker into Photoshop, altering the color in Photoshop, and letting the computer find the parameters for the face/flop/travel color model that correspond to the image. In the old goniochromatic color design interface (see Figure 3.3) there is a built in hue, saturation, and brightness interface.

The participants said that using Photoshop provides many additional ways to adjust the color besides hue, saturation, and brightness. Some of the other Photoshop color alteration methods employed by the participants included Color Balance, Brightness/Contrast, Selective Color, and Match Color. Using Photoshop turned the task into an image manipulation problem and allowed the designers to apply their knowledge of this powerful application. However, several participants noticed that using the image to determine the parameters of the reflection model introduced small errors into the color.

Sketch the color appearance of a new metallic color: In the image based BRDF design interface this is accomplished by transferring a screen shot into Photoshop, sketching over the top of the image, and then fitting the face/flop/travel reflectance model to the new picture. The free-form equivalent in the old interface (see Figure 3.3) is a feature which allows the reflectance curve to be “sketched” by interactively adjusting the CIE Lab value for individual aspecular angles.

In addition to using the Photoshop drawing tools, without coercion the participants also employed the gradient tool and the burn & dodge tools to produce interesting shading effects. Practice was required in order to match the shading and get consistent results using the sketch based approach. Participants said that sketching the reflectance curve is appropriate for engineers and scientists but not for designers.

3.9 Conclusions

We have proposed a simple but powerful reflection model that can accurately represent the solid and metallic colors that are of practical importance in most traditional design applications. The model includes a straightforward curve drawing interface that can be used to directly set the model’s limited number of parameters, and, because of its simplicity, the model allows indirect selection of its variables via design oriented interfaces. The parametric form of the face, flop, travel, and gloss reflection model also makes it easy to use in rendering applications. Finally, because this reflection model can readily generate target measurements for industry standard color measurement instruments, it can be used without difficulty to seed existing computer based paint formulation systems.

To deal with the fact that goniochromatic colors are not a single color but an entire family of colors, this chapter has suggested four novel CACAD interfaces: one technical design interface and three color styling interfaces that take advantage of the underlying simplicity of the proposed face, flop, travel, and gloss reflection model.

In the technical interface, one approach to the design problem treats the group of colors as having an average hue, saturation, and brightness. This is most successful for traditional solid metallic colors and some simple pearlescent paints. Another method provides the designer with interactive control over the color found near the specular direction and the color found far from it. This works best for the newer *effect* paints that are becoming more commonplace. Finally, the user of the program is given an interface that allows them to easily see and select variations of the color that are the result of small changes in the parameters of the model.

The creative design interfaces attempt to mimic the typical work flows that are found in the fashion, interior, and industrial design fields. The virtual mood board allows designers to use exemplars to directly inspire new color appearances. Pictures of collected color artifacts can be organized and displayed, and values for the parameters of the reflection model can be selected by making direct reference to these illustrations. The spot color styler allows changes to color and appearances to be made directly on a 3D object. This approach allows the shape of the object and the lighting to be considered as the color is manipulated. The sketch based color styling interface permits new color appearances to be suggested from concept art created by designers. Least squares and optimization techniques are used to find reflection model parameters to match the color appearance illustrated in designer's sketches.

Chapter 4

Predicting and fixing geometric color mismatches

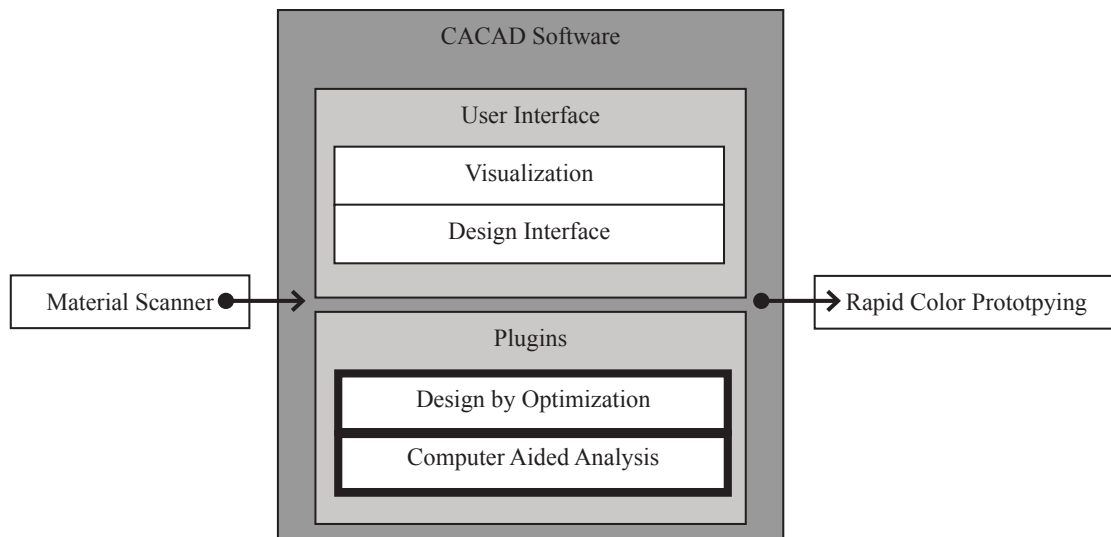


Figure 4.1: The software presented in this chapter are the design by optimization and computer aided analysis components of the CACAD package.

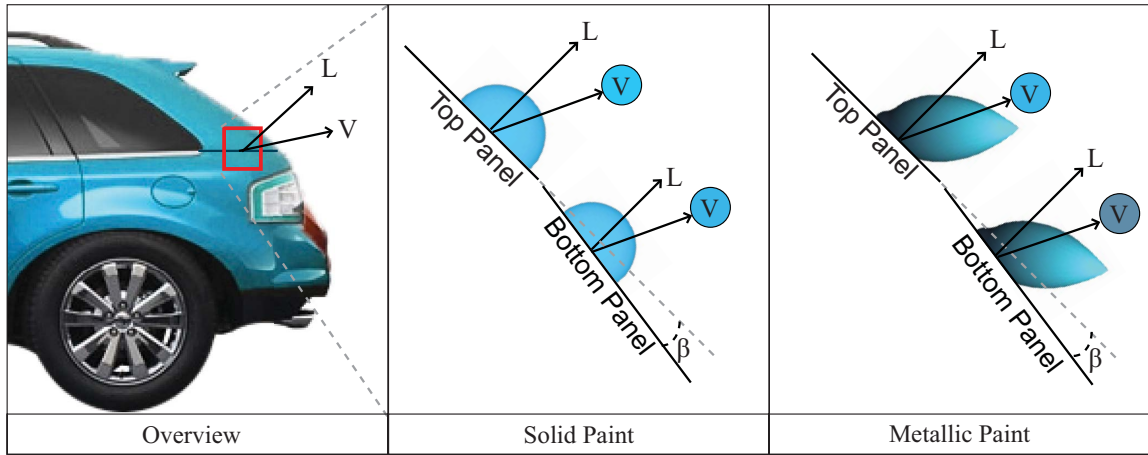


Figure 4.2: Color difference occurs between misaligned body panels. Because color and intensity vary with reflection angle for metallic and pearlescent paints, the effect is stronger for these goniochromatic colors (right) than for solid colors (center).

Abstract

Color mismatches that result from geometric misalignment are studied. Differences in color can result when adjacent parts of an object are coated with the same paint but are not aligned to create a continuous geometric surface. The color difference that results due to shading can be accentuated by the use of metallic and pearlescent paints with goniochromatic properties. A metric is developed for determining when the color difference is large enough for the misalignment to become apparent. A technique is also presented for selecting a paint that matches the adjacent part and creates the illusion of geometric continuity even though the two parts are misaligned.

Parts of this chapter have been previously published by the author in *Proceedings of AIC Colour 09* [53].

4.1 Introduction

Industrial designers often use metallic paints to enhance the appearance of curvature in products. Most notably in the automobile industry [49], but also other consumer markets including personal electronics, household appliances, and architectural finishes [6]. However, a metallic paint’s exaggeration of curvature can induce unexpected color matching problems. Since the color of the reflected light changes with the angle of reflectance, an objectionable color mismatch is sometimes noticed at a joint where two panels meet at a slight angle. Even though the two panels are painted identical colors, a mismatch is still seen (see Figure 4.2). The color mismatch comes from a difference in lighting and viewing geometry. This problem is more noticeable on certain colors and on certain cars. Solid colored paints exhibit the issue, but to a much lesser degree, because light reflects uniformly across viewing angles. Metallic paints are called goniochromatic because the appearance varies with lighting and viewing angle. This document refers to the color difference due to geometric misalignment as a *goniogeometric color mismatch*.

This chapter proposes a new metric, the goniogeometric index, for ranking and predicting the magnitude of goniogeometric color mismatches on particular paints or particular geometric designs. It also introduces a new technique, inverse trompe l’oeil, for fixing goniogeometric color mismatches.

4.2 Background

A variety of color difference metrics and color indices have been proposed and are used by industry to objectively determine when material pairs will exhibit noticeable mismatches in

color appearance. However, most of these color difference metrics and indices have ignored the spatial aspects of color appearance and thus have been limited to the analysis of solid color.

Many materials are unlike solid colors and have the property, called goniochromism, where the appearance changes with viewing angle. To fully characterize these gonioapparent materials, a specialized instrument called a goniospectrophotometer takes multiple color measurements at various lighting and observation angles.

In computer graphics, material reflectance is represented by a Bidirectional Reflectance Distribution Function (BRDF). A BRDF is a function which describes the ratio of the incoming light to the outgoing light for every possible incoming and outgoing light direction. This is the most general way of specifying surface reflection. Pictures of objects illuminated by a point light can be generated by using a shader to evaluate a parametric form of the BRDF.

4.3 Goniogeometric index

As described in the introduction, a goniogeometric color mismatch is a color mismatch between two objects, with identical reflectance, that are geometrically misaligned. Although the color and reflectance of the objects are identical, the color difference comes from the objects being lit and viewed from slightly different angles thereby causing the viewer to see dissimilar portions of the material's reflectance lobes. The issue of goniogeometric mismatch is a subtle problem facing designers today. When a manufactured product exhibits goniogeometric mismatches, people may notice a problem but incorrectly diagnose it.

We will illustrate the issue using a car bumper that exhibits a goniogeometric mismatch relative to the adjacent front-end panels of the car. A quality assurance technician may assume that the color mismatch problem is from the paints not being formulated correctly and order the car to be repainted – especially if the bumper and front end were manufactured on separate days or in separate factories. A customer evaluating the car for purchase may be suspicious that the car was in an accident and repainted incorrectly. A color scientist may hypothesize that the two parts exhibit goniometamarism [50], but measurements with a multi-angle spectrophotometer could miss the problem altogether.

4.3.1 Formulation

In order to characterize goniogeometric color mismatches, this chapter proposes a simple metric, titled the *goniogeometric index*, for ranking and approximately predicting the magnitude of this issue for a particular paint or a specific geometric design. Instead of a difference in ΔE that the CIE Lab color difference metric measures, the goniogeometric index measures, in degrees, the minimal angle of geometric misalignment needed to create a certain level of ΔE difference. That level would typically be a just noticeable difference or one JND.

Imagine two panels of the material in question joined at an adjustable angle β degrees. Given the specific material, with reflectance function f , illuminated under a particular lighting Ω and viewing geometry Ψ , the goniogeometric index is the minimal angle of geometric misalignment β_{min} needed to create a certain amount of color difference.

To assist with the evaluation of the reflectance functions we reframe how the BRDF is calculated. Geometrically rotating an object by β degrees is equivalent to keeping the object fixed and rotating the lighting and viewing geometry by β , denoted by Ω_β and Ψ_β .

In order to keep this metric as useful as possible, we propose the metric in a generic way that can be applied in a number of specific situations. Note that lighting Ω could either be a specific lighting angle or a global lighting environment. The viewing geometry Ψ could be any viewing angle or angles. The reflectance function of the material, f , can be any BRDF. The variable denoting the color difference threshold, ε , is measured in CIE ΔE s, but can be more or less than one JND depending on the application of the metric.

The color difference between color of the object at the original and rotated geometries is a ΔE difference and is computed with a ΔE function. The equation below shows the generic formula for the goniogeometric index. The large vertical bar denotes a mathematical constraint on the minimum value of β , namely the goniogeometric index is computed by minimizing β subject to the constraint on the right hand side of the equation.

$$\beta_{\min} = \min \beta \quad \Big| \quad \Delta E \left(c(f, \Omega, \vec{\Psi}); c(f, \Omega_\beta, \vec{\Psi}_\beta) \right) \geq \varepsilon \quad (4.3.1)$$

In this expression, $c(f, \Omega, \vec{\Psi})$ is a function that determines the color for each panel given the BRDF, the lighting, and the viewing circumstances. For the simple case where there is a single viewing direction \vec{V} and a single light source in direction \vec{L} with intensity I the value of c is determined as follows:

$$c(f, \vec{L}, \vec{V}) = I * f(\vec{L}, \vec{V}) * \vec{L} \bullet \vec{V} \quad (4.3.2)$$

where $\vec{L} \bullet \vec{V}$ is Lambert's cosine law.

4.3.2 Application to solid paints

Before we move on to complex materials, we first apply the goniogeometric index to solid paints. In the case of solid paints, the assumption is that light reflects uniformly in all directions. The only change in color is the shading due to the lighting angle. This change in reflectance is very gradual and is approximated by Lambert’s cosine law. It does not matter what angle you look at the material from – you observe the same color. For a simple lighting and viewing circumstance

$$I * f(\vec{L}, \vec{V}) = \bar{C}_{\text{diffuse}} \quad (4.3.3)$$

in the above expression for c . Because there are no inter-reflections, the product of the light source intensity and the BRDF yields a constant CIE Lab value after tristimulus integration is performed.

(Note that this research discounts the color of the specular highlight because the highlights do not need to line up across a seam in order for the color of the material to match. We think that this is a reasonable assumption and doing so simplifies the calculations.)

To apply the goniogeometric index on a solid paint, assume an industrial designer is creating a product that is painted a solid color. The manufacturing specification dictates that the exterior shell is manufactured as two panels that meet together at a seam. Because of the manufacturing process, the seam is not exactly flush, but has a minor angle, and we want to set a manufacturing tolerance for the design. The ideal would be that the panels meet perfectly flush, but we want to know how misaligned they can be before a difference is noticeable – we want to compute the goniogeometric index.

4.3.3 Application to metallic paints

In this section, we apply the goniogeometric index to metallic automotive paints. In the case of materials that have non-trivial reflectance, computing the goniogeometric index is more complex than for solids. The appearance of a metallic varies with both lighting *and* viewing angle. To compute the goniogeometric index we need the formula for reflectance, and we need to specify lighting and viewing geometries as well a color difference threshold.

Ignoring gloss, the product of the intensity I and the reflectance f of a metallic automotive paint is approximated using the parametric form of the metallic reflection model found in our previous work [65, 54, 39], which is based on the work of Alman [2] and Rodrigues [48]. The color of the metallic is represented by a few variables that correspond to the face($\overline{C}_{\text{face}}$), flop($\overline{C}_{\text{flop}}$), and travel(θ_{flop}) of the color. In terms of the previous expression for c :

$$I * f(\vec{L}, \vec{V}) = g(\vec{L}, \vec{V}, \overline{C}_{\text{face}}, \overline{C}_{\text{flop}}, \theta_{\text{flop}}) \quad (4.3.4)$$

g evaluates a second order polynomial that goes from $\overline{C}_{\text{face}}$ at 0 aspecular angle to $\overline{C}_{\text{flop}}$ at θ_{flop} aspecular angle. g returns $\overline{C}_{\text{flop}}$ for aspecular angles greater than θ_{flop} . Just like the diffuse calculation, because there are no inter-reflections, the function g yields a CIE Lab value.

(Note that this research currently only considers in-plane reflections from metallic paints.)

The situation that this formula is emulating is as follows. The point light illuminates two panels that are painted identically but geometrically misaligned. We want to know how far the panels can be out of alignment before a color difference of one JND ($2.3\Delta Es$) is observed.

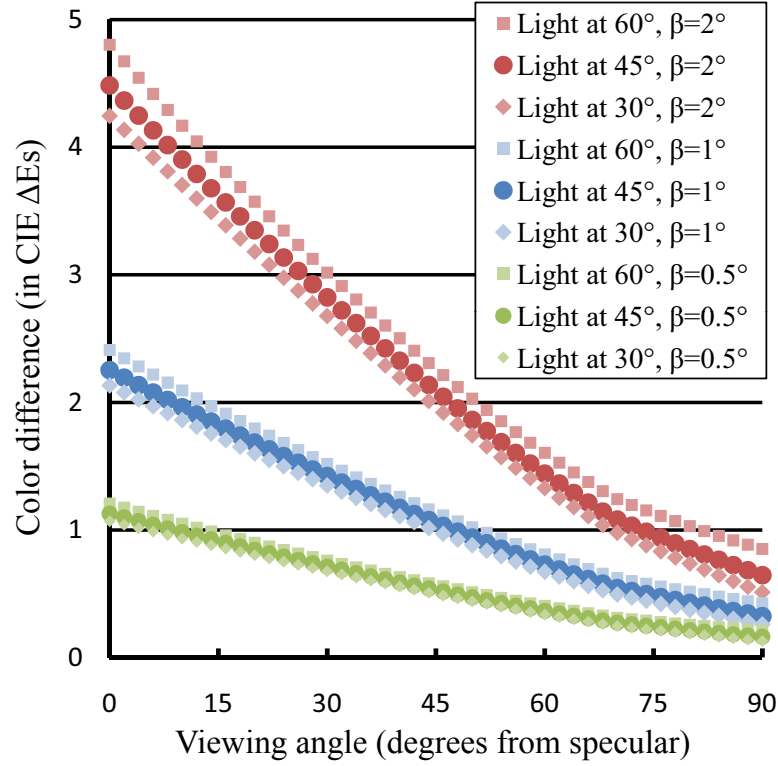


Figure 4.3: Variation of color difference between panels as a function of viewing position, light source position, and geometric misalignment.

Figure 4.3 illustrates how the goniogeometric index can be determined graphically for a metallic paint. Each curve shows how the color difference between two painted panels varies as a function of the viewing direction, \vec{L} , from which the panels are observed, the lighting direction, \vec{V} , from which the panels are illuminated, and the amount of misalignment, β , between the panels. In this case, to find β graphically, one selects the curve which is below the acceptable color difference threshold for some range of possible viewing and lighting directions. The misalignment angle β associated with this curve is the goniogeometric index.

4.4 Inverse trompe l’oeil

Trompe l’oeil designs make flat architectural interior elements look like complex three dimensional shapes. French for “to trick the eye”, trompe l’oeil designs [58, 59] actually go back to the Romans who decorated walls with simulated columns and open windows. Although some designs create striking three dimensional deceptions intended to capture viewer’s attention, other trompe l’oeil designs are so good that they may be overlooked as the real thing.

In the same way that traditional trompe l’oeil creates the illusion of curvature on a geometrically flat object, this section proposes *inverse trompe l’oeil* to suggest flatness across a geometrically creased object. This idea is offered as a potential solution to certain cases of the geometric color matching problem in which two panels are joined together at an angle and create an apparent color difference. Two panels that come together at an angle can be painted slightly different colors to account for the change in reflectance due to lighting or viewing geometry. How exactly should the color be tweaked to reduce the color difference across the seam?

We seek to minimize the difference in color reflected from the surface by posing this question as a mathematical minimization problem. Although it is impossible to completely eliminate color difference from all lighting and viewing angles, we can minimize color differences over a limited set of lighting angles and a limited range of viewing angles.

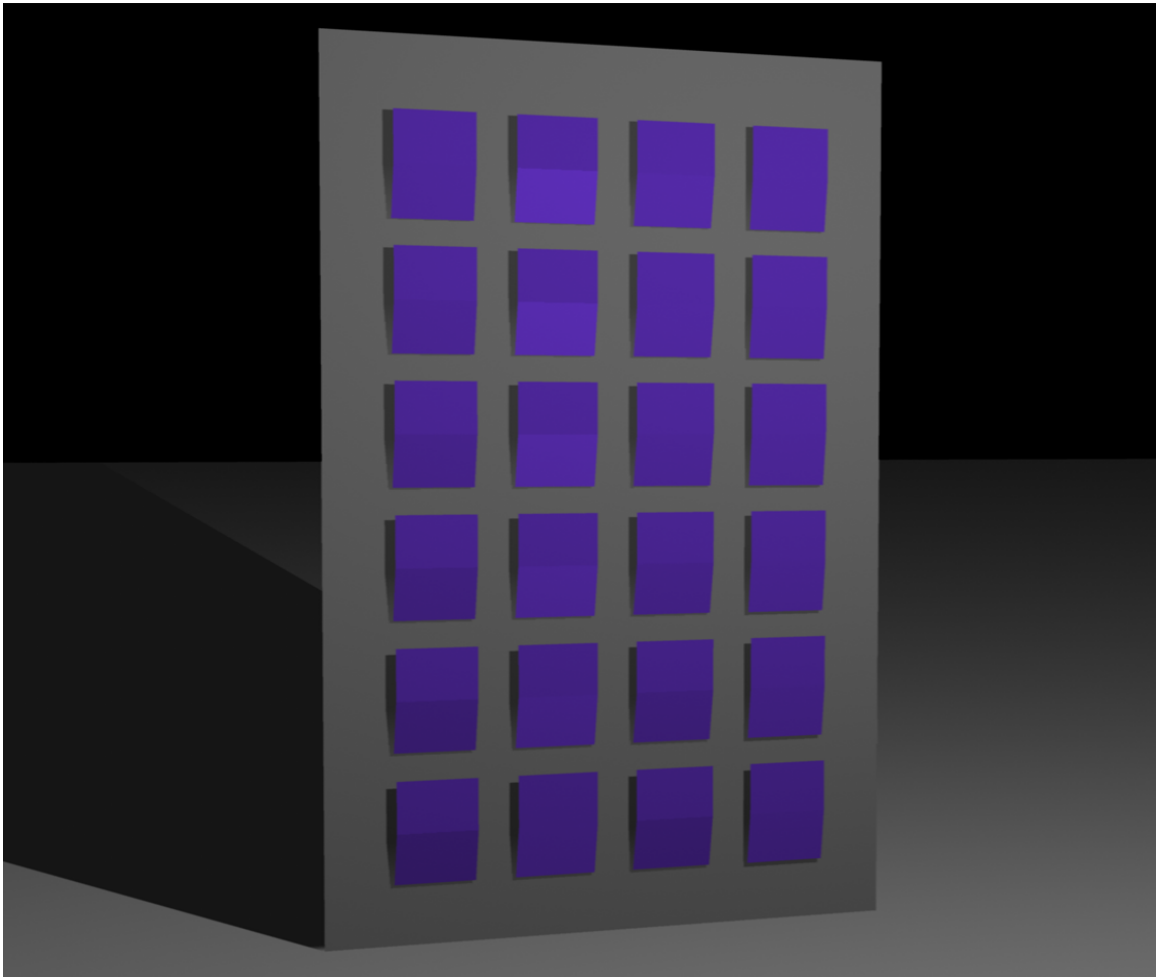


Figure 4.4: Determining a solid color for the bottom half of each panel that matches the top half of the panel even though the two halves are misaligned by 3 degrees. Each row represents a different light source direction and each column a different solution technique. See text for details.

4.4.1 Diffuse paints

In Figure 4.4, a scene is constructed as a test bed for illustrating different optimization heuristics for applying inverse trompe l’oeil to solid colors. The figure shows a grid of colored panels. The top and bottom halves of each panel are geometrically misaligned by 3

degrees. A simple point source lights the panels at 0° , 15.5° , 29.1° , 39.8° , 45.0° , 52.0° from normal (top to bottom rows).

The leftmost column shows the control case where the top and bottom sections of each panel are painted the same color. The color difference across the seam of each panel is a result of shading differences due to misalignment of the panel halves.

The remaining columns are painted using the idea of inverse tromp l’oeil. In the second column, we compute a new color for the bottom half of the panels, using an optimization routine that minimizes the ΔE_s color difference across the seam at a 45° lighting angle. Employing parametric forms of the BRDF to calculate the ΔE_s color difference, we use the solver functionality in Microsoft Excel [29] to determine the parameters of the reflection model. In the case of a solid color, the reflectance is uniform across viewing angles and only changes with lighting angle. Therefore, the system is able to find a perfect match at 45.0° , but the quality of the match fades off as the lighting angle moves away from 45.0° . The match is quite poor at 0° , about $2\Delta E_s$.

In the third column, the optimization heuristic solves for the RMS error of the color difference across all of the seams in the column combined. In effect this reduces the color differences across the seams while avoiding any excessively poor matches. In this case the worst error is about $1\Delta E_s$.

In the final column, we create a separate paint for the bottom half of each panel by solving for each row independently. The solver found six inverse tromp l’oeil colors that effectively eliminate the appearance of the geometric misalignment.

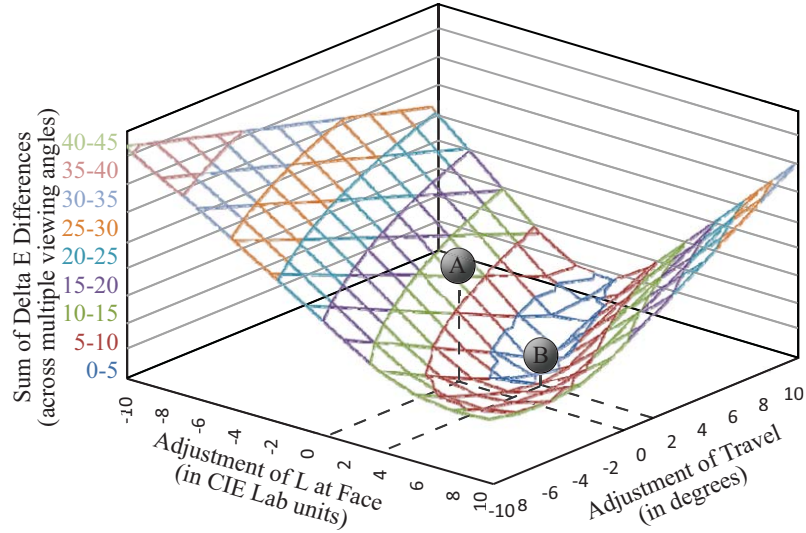


Figure 4.5: Finding a silver color that matches another silver color even though the two paints are on panels that are misaligned by 3 degrees. Color difference A results when the paints are identical, and the decreased color difference B occurs when there are dissimilarities between the face color and the travel for the two paints.

4.4.2 Metallic paints

In this section we apply the idea of inverse trompe l'oeil to a metallic paint reflection model. Because the reflectance of metallic paints varies with lighting and viewing angle, there are more constraints on the solution. However, because the metallic reflection model has more parameters, it can be fit at more angles.

Consider the simple example of a silver paint with a black flop color (basic metallic reflection). In this case, because there is no chromatic travel, the face color CIE Lab L value and the amount of L travel are the only free parameters available to solve the inverse trompe l'oeil problem. Figure 4.5 shows how color difference varies with face L and L travel for a 2 degree geometric misalignment problem. The minimum delta E is easily found to occur when face L increases by 3.4 units and travel increases by 2.0 degrees.



Figure 4.6: Bumper and fender misaligned by 8 degrees. Identical metallic paints cause a color mismatch (left) while painting the bumper a different color, determined using the inverse trompe l'oeil technique, eliminates the problem (right).

A more complicated goniogeometric color mismatch problem is shown in Figure 4.6. Although the car on the left of the figure is painted with a single metallic paint, a goniogeometric color mismatch is visible across the seam between the bumper and fender. The car's bumper is not flush to the fender and exhibits a goniogeometric color mismatch. (In order to clearly illustrate goniogeometric color matching issues, this example uses an exaggerated misalignment of 8° to create a color difference that will be more visible.)

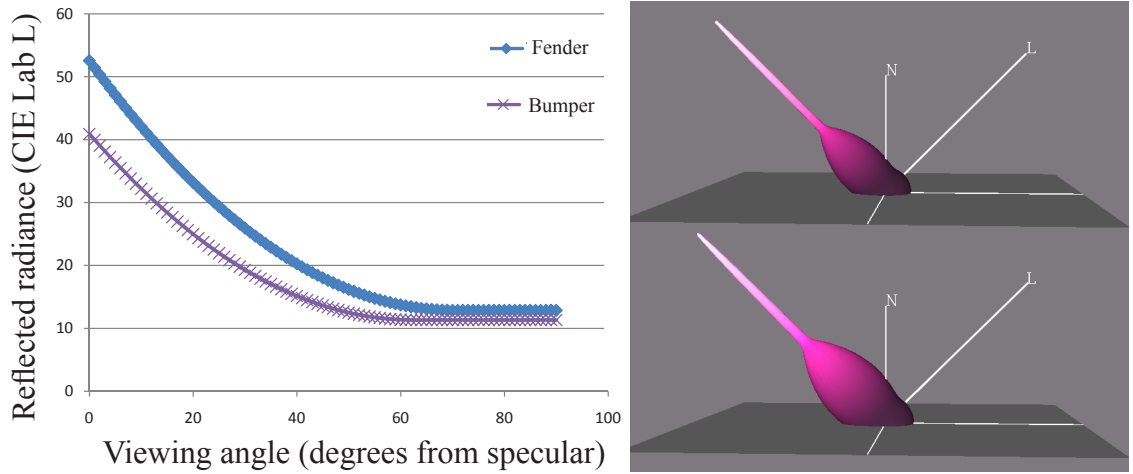


Figure 4.7: (left) Goniogeometric mismatch between the misaligned fender and the bumper in Figure 5 when they are both painted the same color. (right) Comparison between the BRDF for the original paint (top) and the BRDF for paint found using the inverse trompe l’oeil technique (bottom).

The image on the right is geometrically the same as the left image, but the bumper is painted a separate color from the fender. The color of the bumper was chosen using inverse trompe l’oeil to create a visual match across a seam that would normally have a goniogeometric color mismatch. An optimization algorithm was used to find values that produced the minimum color difference.

A comparison of the original BRDF on the fender to the BRDF computed for the bumper is shown in Figure 4.7. The computed BRDF is brighter (to account for the difference in lighting angle). The difference is far more substantial in the “face” region than the “flop” region to account for the difference in aspecular viewing angle across the seam. The face color is brighter and more chromatic while the travel occurs over a slightly larger range of aspecular angles. The system calculated the optimal tangent point of the computed BRDF θ_{flop} to be approximately 8° more than the original BRDF in this example.

4.5 Conclusion

We conclude this chapter with a list of styling guidelines that, if followed, will help designers reduce the effect of color mismatches stemming from geometric misalignment of surfaces. 1) Choose high travel paints only when you can ensure that seams in flush panels come together precisely parallel. 2) Choose solids or low travel paints when seams are not flush. 3) Avoid placing seams in orientations that will be commonly viewed at low aspecular angles. 4) Set geometric manufacturing tolerances based on the types of paint being used and select paint based on the precision of the seams on the object. 5) Choose seams that limit the range of viewing angles, this reduces artifacts and opens the door for inverse trompe l'oeil type corrections.

Chapter 5

CACAD for rapid color prototyping

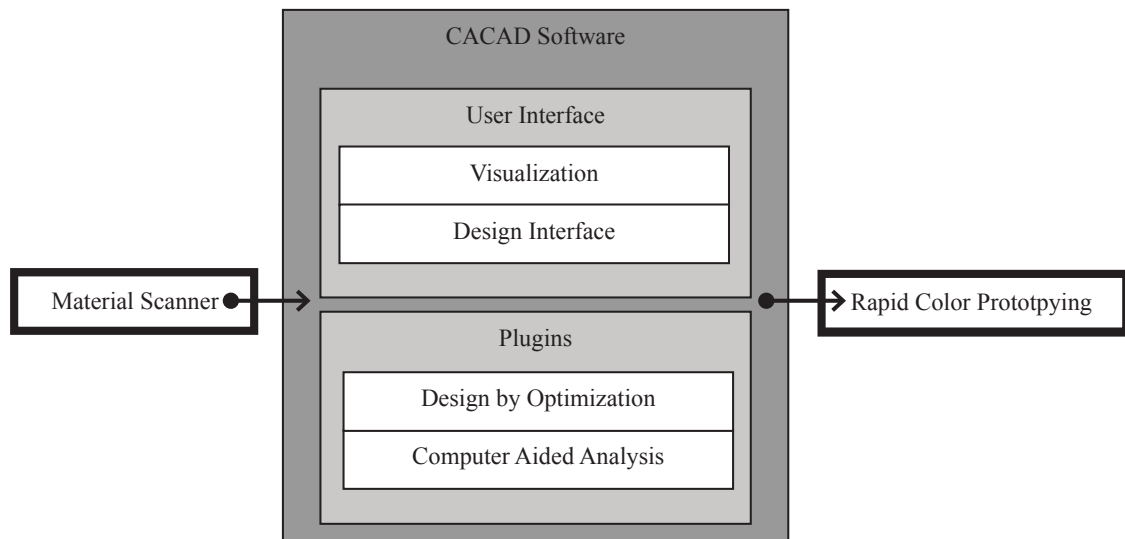


Figure 5.1: The research presented in this chapter connects the CACAD software package to and from the physical world.

Abstract

This chapter demonstrates how the digital color design tools described in previous chapters were connected with paint formulation systems to create a complete computer aided color appearance design system. Colors can be input into the system via measurement or selected from a database of existing colors. The CACAD software is used to tweak existing colors or design entirely new colors from scratch. These new colors are formulated and mixed using DuPont's ColorNet color system. Additional tools were created to browse and search through the paint database. Finally, a series of experiments demonstrate that the CACAD system is effective at designing and formulating paints in a wide variety of real world situations.

5.1 Introduction

Rapid prototyping is one of the most exciting aspects of Computer Aided Design(CAD). 3D printers, stereolithography machines, computer controlled laser cutting machines, and other solid freeform fabrication devices can create physical objects from CAD specifications. The automatic generation of a physical prototype gives designers a tangible object to evaluate. Rapid prototyping is the bridge that brings electronic designs into the physical world.

The creative workflow loop in CAD was complete when these three types of tools were made available:

Parts of this chapter have been previously published by the author in *Proceedings of AIC Colour 05* [39], *Proceedings of ACADIA 08* [6], and *Proceedings of Computational Aesthetics 05* [38].

- Tools for scanning physical objects into digital form
- Geometric design software
- Rapid prototyping tools for creating real prototypes of digital designs

While CAD has been traditionally employed to do geometric design work, color appearance design is an emerging application of CAD. Computer Aided Color Appearance Design, or CACAD for short [37], has been made possible largely by advances in computer graphics hardware and software. Now that three dimensional surfaces can be rendered realistically and the color appearance of these surfaces can be manipulated in real time, color stylists are using computers to do color appearance design work.

A complete creative work flow loop for CACAD needs a set of tools that are similar to the CAD tools. In our efforts to apply CAD to color design we have partnered with the appearance industry to create and composite the first complete set of CACAD tools:

- Tools for scanning color appearance into digital form
- Color appearance design software
- Rapid color prototyping tools for creating physical prototypes of digital color designs

The existing computer graphic representations for color simulation and selection do not readily facilitate the color design process used in industry. This is particularly true if there is a need for a physical prototype. Computer graphic reflection models have been developed with the goal of accurately portraying subtle color appearance effects. These models have grown increasingly complex, and they include physical parameters for which aesthetic

designers have no intuition. Numerous computer graphic hue, saturation, and brightness color systems have been proposed, but they are not able by themselves to convey the spatial distribution of the light reflected from a surface that separates one color appearance from another.

In the first section of this chapter, we discuss background work. This includes the advances in computer graphics hardware, computer graphics software, automotive color appearance, and CACAD that make this research possible.

The next section of the chapter presents some of the tools that were created to assist with the selection and fabrication of metallic automotive colors. We first present an XML file format that is used for importing colors from measurement tools, exporting colors to paint formulation systems, and the interprocess communication of automotive color within the system. Then we describe a virtual SpectraMaster color book and some of the information we found from an analysis of it. Finally we describe ColorSnap, a visualization, search, and color matching tool for the extensive collection of SpectraMaster colors.

The final section presents a set of four rapid color prototyping experiments. These experiments demonstrate the maturity and utility of CACAD and were possibly the first examples of rapid prototyping applied to complex surface finish design. Experiments were performed in collaboration with DuPont, The Center for Creative Studies (CCS), Ford, HouMinn Practice, and the University of Minnesota's school of architecture. The designers involved had varying levels of experience with automotive color design from very experienced to naive.

5.2 Background

The design of new automotive color is done using cutting edge chemistry and nanotechnology, but with very outdated creative tools. Traditional design tools, such as mood boards and concept art, have been accepted as the best tools available for communicating color design intent to paint suppliers. However, advances in computer graphics hardware and software are leading to the development of computer aided design tools for color appearance professionals. In this section we will discuss the advances in computer graphics, automotive color appearance, computer aided color appearance design, and rapid prototyping that make this research possible.

5.2.1 Shading hardware/software

Computer graphics technology has been evolving at a dazzling rate. While computer graphics software is continually simulating the visual world to finer and finer levels of detail, each generation of graphics hardware accelerators allows more and more complex optical phenomena to be simulated in real-time. While the multibillion dollar video game industry is the tenacious force that drives the hardware evolution, the movie industry's demand for fresh special effects continues to provoke advances in software simulation.

The color appearance industry will benefit from these advances in the form of computer aided color appearance design tools. Programmable graphics hardware makes color appearance design possible. Before programmable graphics hardware became generally available, real-time graphics was only able to represent very simple surface finishes. A single reflectance model, the Phong model, was available and was not versatile enough to represent

the range of surface finishes that are of interest to industrial designers. Programmable graphics hardware replaces the hard-wired reflection model with arbitrary reflection models in the form of a *shader* [33].

A shader is a small computer program that represents appearance and is evaluated by the graphics hardware at every pixel as a three dimensional object is rendered on the screen. The shader and its parameters can represent the appearance of various surface finishes. Real-time appearance design is made possible by coupling a design interface to the parameters of the shader [54].

5.2.2 BRDF/Envmap

In computer graphics, reflection models are represented by something called a Bidirectional Reflectance Distribution Function (BRDF). A BRDF is a function which describes the ratio of incoming light to outgoing light for every possible incoming and outgoing light direction. This is the most general way of specifying surface reflection. Renderings of the BRDF under a point light can be generated using a shader to evaluate a parametric form of the BRDF. Environment mapping is used for creating images of objects under complex illumination. Environment maps can be synthetically generated or photographically acquired using high dynamic range images. Basic environment mapping only simulates perfect mirror BRDFs, while other techniques are used to generate renderings of non-trivial BRDFs under photographically acquired lighting [25, 26, 40, 1]. A technique for interactive BRDF design in environment map based lighting is presented in Chapter 2 [52].

5.2.3 CACAD/automotive rendering

Computer graphics has traditionally been about modeling the visual world to finer and finer levels of detail. However, modeling with higher subtlety comes at the expense of ease of design. A layered shader model based on the microscopic structure and optical properties of the constituent pigments, metallic flakes, binders, and substrates was proposed in [16]. This bottom up approach does not facilitate color styling because of its highly technical nature. In Section 3.3, we present a simple reflection model for doing computer aided color appearance design for automotive paints. Although our model has connections to and from the physical world, because it is an appearance model, it stands in contrast to physically based reflection models.

A BRDF acquisition system for automotive paints and a shader for realtime raytracing were presented in [19]. Susumu Umemura of Toyota Motor Corporation briefly outlined a procedure that uses computer graphic renderings to communicate automotive color appearance design ideas from color designers to paint suppliers [62]. However, important details of the system were not described in the publication.

5.2.4 Color styling tools

All of the colors that are created in this chapter were designed with the color styling tools presented in Chapter 3. This part of the BRDF Design Suite has both technical design interfaces as well as creative design interfaces for the specification and manipulation of metallic automotive paints.

The software package uses a simple reflection model that has the parameters required to design solid and metallic surface finishes. This reflection model is described in Section 3.3. The reflection model has three separate representations. One form of the reflection model is constructed to have the minimum number of free parameters and these parameters are chosen so that they correspond to color specification terms familiar to designers such as face color, flop color, travel, and gloss. Another form has a parametric representation for rendering and analysis. Finally, the hierarchy has an industry standard measurement driven representation. This representation allows colors to be scanned from physical samples using commercial measurement tools. It also allows new color designs to be used as a manufacturing specification for rapid color prototyping. While each representation has strengths and weaknesses on its own, the combination is extremely useful in the context of CACAD. This combination is the glue that brings color design from conceptualization to rapid fabrication.

5.3 Tools

We partnered with DuPont Performance Coatings to create the physical bridge between designing paints on the computer and fabricating physical prototypes of these surface coatings. SpectraMaster® is a color system created by DuPont™. It is designed both as a matching system for their automotive refinish business and as a design system for color specifications of paints [15]. Our research uses two of the components of their system: a book of colors and a paint formulation system called ColorNet. We created two additional tools based on a database that they provided to complement the rest of the BRDF suite

covered in the previous chapters. An XML file used for interprocess communication ties all of the tools together.

5.3.1 XML file format

We define an XML file that specifies all solid and metallic colors inside of the BRDF design system. It is used for importing colors from measurement tools, exporting colors to paint formulation systems, and the interprocess communication of automotive color within the BRDF Design Suite. The rendering engine, presented in Section 2, reads the color definition file for visualization. The color styling tools, presented in Section 3, are able to read and write the color definition files.

The XML file ties all of the software tools together by providing a common format that all tools can read and/or write. Color appearance is specified with standard D65 illumination at 45° from normal. The color sample is defined in the XML file using the automotive industry's standard of 3 or 5 CIE Lab tristimulus values as well as the aspecular angles of each value. The XML file also contains a single number for standard gloss.

Since the XML file format uses the automotive industry's standard method of specifying solid and metallic colors. Paints can be quickly and accurately measured using commercially available multi-angle spectrophotometer and imported into the BRDF Design suite. We also use this XML file format to specify electronically designed colors to be formulated.

5.3.2 SpectraMaster book

The physical book includes about three thousand solid colors and about three thousand metallic and pearlescent colors. This collection of colors is enormous because it needs

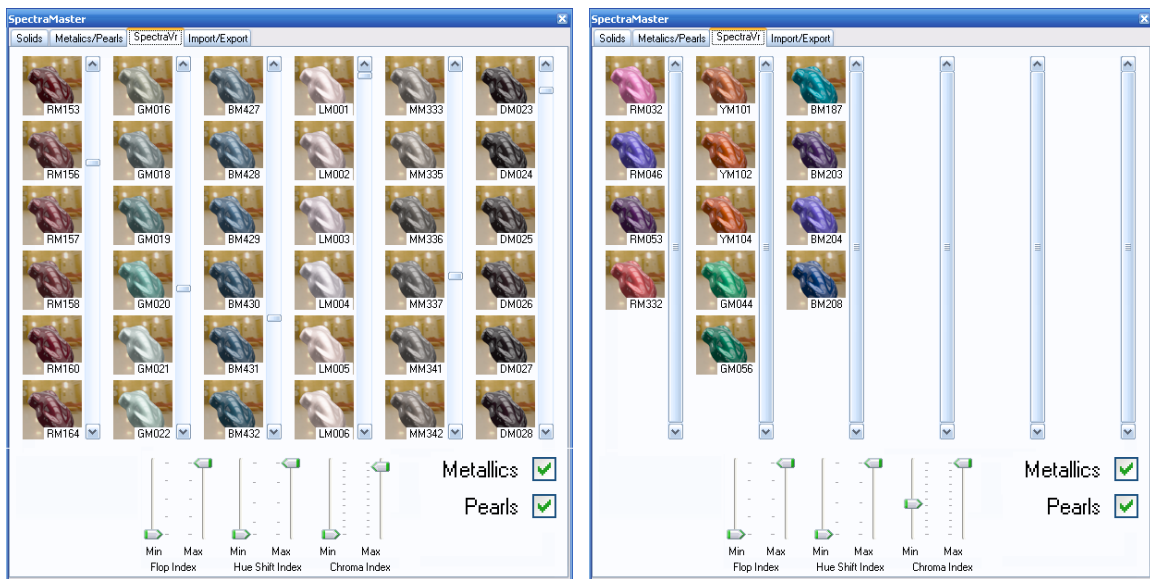


Figure 5.2: The Virtual SpectraMaster Color Library shown as a thumbnail preview, rendered with environment map based lighting, along with the paint code. The entire collection of over 3,000 metallic and pearlescent paints is shown on the left. Sliders allow the user to filter the selection of colors to, for example, colors with high chroma travel(right).

to match the vast majority of the automotive colors that are on the road today. If an automobile gets scratched and needs a paint touch up, the refinish catalog needs to have a color that will be a close match regardless of make, model, or year. The book is a companion to DuPont's ColorNet paint formulation system and is used by body shop technicians as a visual reference for refinish colors.

5.3.3 Virtual SpectraMaster color library

The Virtual SpectraMaster Color Library is an application that is driven from the database of SpectraMaster colors. Every color in the collection has a name and CIE *Lab* tristimulus values (obtained by DuPont using a three angle spectrophotometer). The application allows you to browse colors by name or by thumbnail preview. The preview is a computer graphic

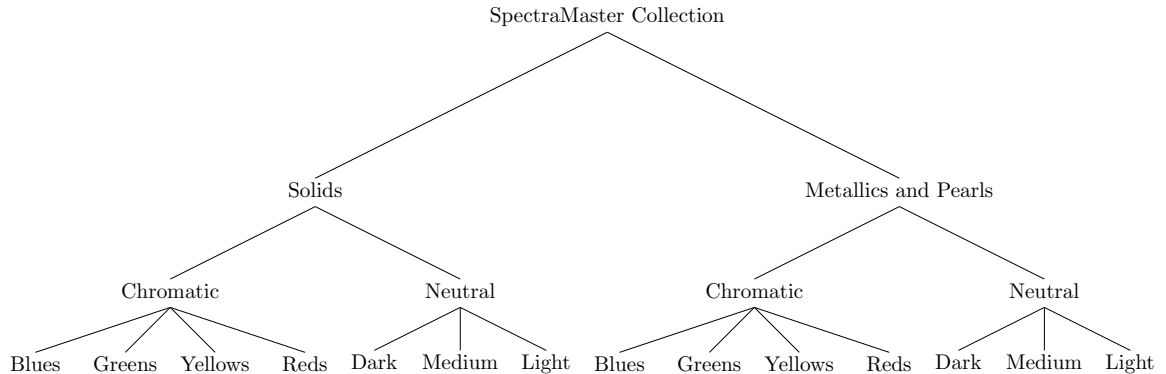


Figure 5.3: The Virtual SpectraMaster Color Library follows the intuitive hierarchical organization the physical book uses to categorize six thousand solids, metallics, and pearls.

rendering of the paint on a three dimensional surface for quick evaluation as shown in Figure 5.2. When a color is selected, it is loaded into the software suite for analysis, modification, and visualization.

The Virtual SpectraMaster Color Library follows the intuitive hierarchical organization the physical book uses. The colors are divided into two main sets: solids and metallics/pearls. Metallics and pearls are grouped together because it is not apparent if a paint is a metallic or a pearl just by looking at it. Each set is further divided into chromatic colors and neutral colors. The chromatic colors are divided by hue into blue, green, yellow, and red sets. The neutral colors are divided by value into light, medium, and dark sets. See Figure 5.3. This scheme facilitates finding and matching colors.

Search interface

The software includes three check boxes to limit the selection of colors to solids, metallics, and/or pearls. The software also provides sliders to set upper and lower bounds on three metrics specific to metallic colors: Flop Index, Hue Shift Index, and Chroma Index. The

three metrics can be used individually or together to narrow the selection of colors in the database. Each metric corresponds to the change in appearance along separate dimensions of the color space of metallic(brightness, hue, and chroma).

Flop Index gives a measurement of the magnitude of travel for a metallic color [2, 66]. It is a metric computed from the L dimension(luminance) of the three standard aspecular Lab measurements of a paint. The equation for Flop Index is given as

$$\text{Flop Index} = \frac{2.69(L_{15^\circ} - L_{110^\circ})^{1.11}}{(L_{45^\circ})^{.86}} . \quad (5.3.1)$$

Solid colors have a Flop Index of 0 because L_{15° and L_{110° for solids are identical. All metallics have a Flop Index above zero. The average Flop Index in the database is 11.38. Over 96% of colors have a Flop Index between 0 and 20. The graph in Figure 5.4 illustrates the distribution of flop indices for the solids, metallics, and pearls in the database. Most colors with Flop Index beyond 25 are the result of numerical instability of the formula for very dark colors.

Taking this into account, Flop Index can be used to limit the colors by magnitude of travel in luminance. For example, bounds on the Flop Index sliders could be set to be between three and ten to get colors with moderate luminance travel. If the bounds are set to be between seventeen and twenty-five, the colors selection will only include colors with more extreme travel.

Since Flop Index is computed exclusively on the luminance dimension of the BRDF, it cannot distinguish colors that have high or low travel in chroma or hue. In this document we present two new metrics to rank colors by color travel and hue travel. Ignoring the

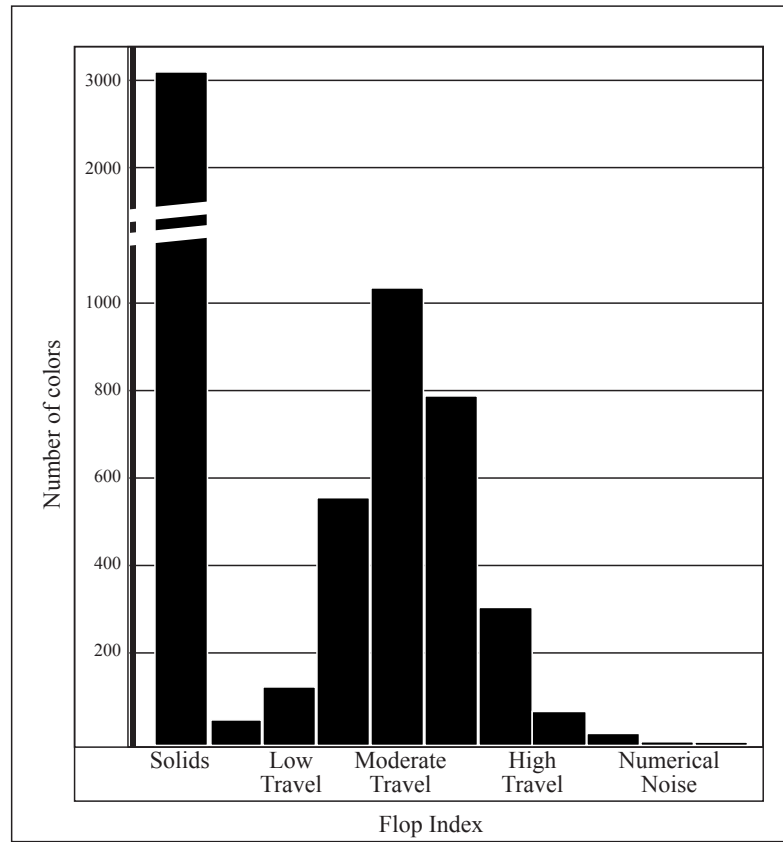


Figure 5.4: The distribution of flop indices for the solids, metallics, and pearls in the SpectraMaster database. Solid colors have a Flop Index of 0. Ignoring solids, the average Flop Index in the database is 11.38. Over 96% of colors have a Flop Index between 0 and 20.

brightness (L component) of the Lab aspecular measurements, only the a and b values of the color at Face and Flop are considered in the calculating the Chroma Index and the Hue Shift Index. Both of these formulas compute in units of $Lab \Delta E$.

If a paint has color travel, the Chroma Index provides a measurement of the paint's change in saturation across viewing angles. To compute it, the Chroma Index is simply the absolute difference of the chroma of the color measured at 15 degrees and the chroma of the color measured at 110 degrees. This is an index of the change in saturation that is not

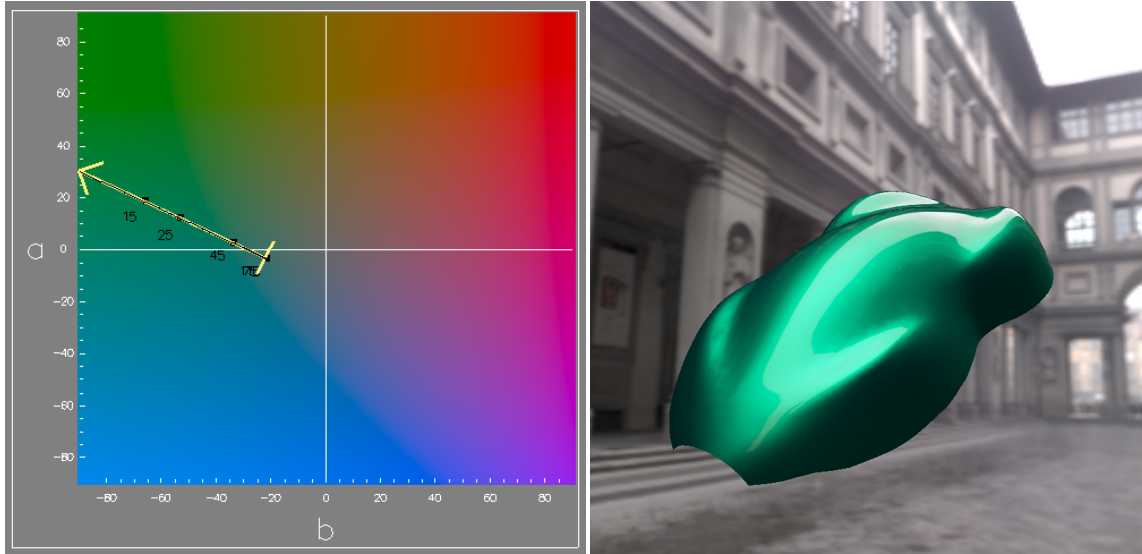


Figure 5.5: This shows GM044 that has a Chroma Index of 46 ΔE s.

affected by the change in brightness or hue with respect to reflection angle. The equation is shown as

$$\text{Chroma Index} = \left| \sqrt{a_{15^\circ}^2 + b_{15^\circ}^2} - \sqrt{a_{110^\circ}^2 + b_{110^\circ}^2} \right|. \quad (5.3.2)$$

Another dimension that a metallic paint can travel in is hue. The Hue Shift Index provides search control over hue shifting colors. If a paint has a color shifting effect pigment, the hue at Face will be different than the hue at Flop. The formula for the geometric distance from a point to a line is used to compute the Hue Shift Index as shown in Equation 5.3.3 To compute the Hue Shift Index, measure the distance between the ab_{110} color to the nearest point on a line projected from the origin through the ab_{15} color. Although this works well for many hue shifting pigments, this metric will fail on extreme colors that rotate nearly 180° around the hue circuit such as interference based paints and situations where the face color is achromatic.

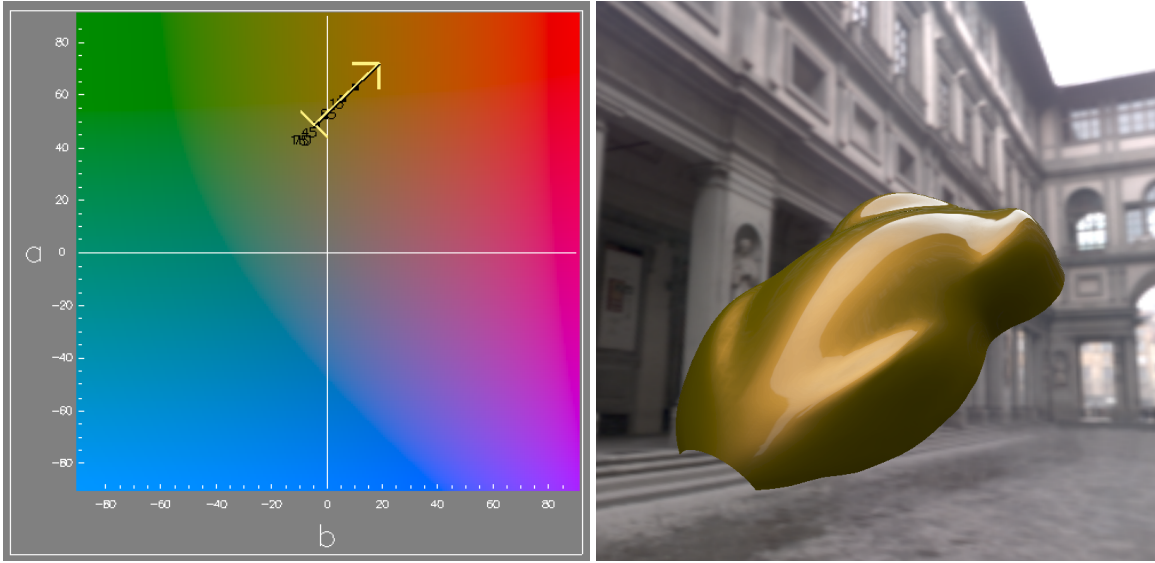


Figure 5.6: This shows YM144 that has a fairly high Hue Shift Index of 12.6 ΔE s.

$$\text{Hue Shift Index} = \frac{|a_{110} * b_{15} - a_{15} * b_{110}|}{\sqrt{a_{15}^2 + b_{15}^2}} \quad (5.3.3)$$

The upper and lower bounds on the metrics can be used to explore the SpectraMaster library. To find hue shifting colors we limit the search to colors with a high Hue Shift Index. Figure 5.6 shows a color coded YM144 that was found to have a fairly high Hue Shift Index of 12.6 ΔE . Figure 5.8 shows the color coded GM027 that has an extreme Hue Shift Index of 19.8 ΔE . To find colors with a lot of color travel we limit the search to have a high Chroma Index. Figure 5.5 shows a color that is coded GM044 that has a Chroma Index of 46. The search metrics can be combined. When searching for colors with high Flop Index but a low color travel we found BM304 that has a moderately high Flop Index of 16.6 but a low Chroma Index of 5.6 ΔE as shown in Figure 5.7.

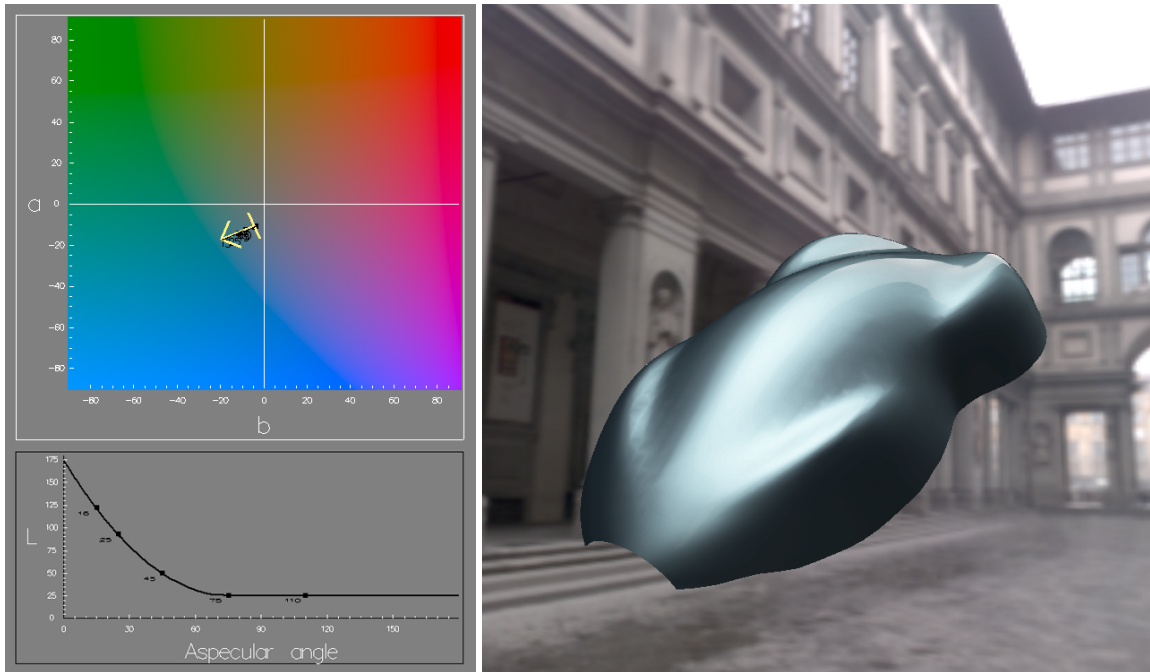


Figure 5.7: This shows BM304 that has a higher Flop Index of 16.6 but a low Chroma Index of 5.6 ΔE_s .

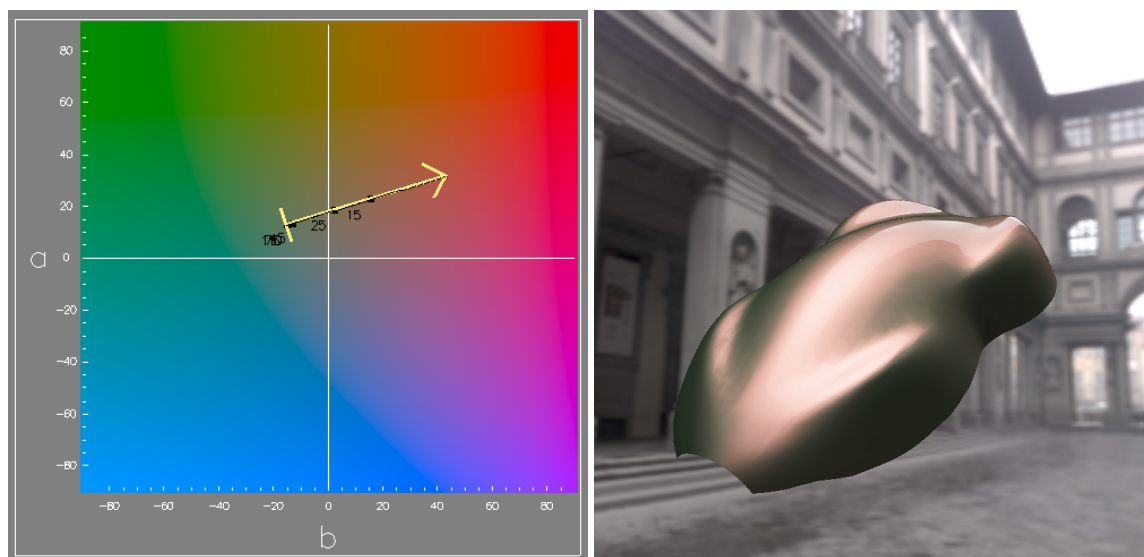


Figure 5.8: This shows GM027 that has an extreme Hue Shift Index of 19.8 ΔE_s .

5.3.4 ColorNet

ColorNet® is DuPont’s software for formulating automotive paint in their refinish business. Typically this program is used to find formulas for paints that do not exist in the SpectraMaster database. For example, if the original color of a car has faded, the paint code specified by the vehicle’s make and model would not be a good match. In this case, the paint technician will supply ColorNet with measured aspecular *Lab* values of the paint as well as the paint code for a near match of the color as a starting point for the reformulation. ColorNet will tweak the formulation of the start color until it finds a paint formula that will be a close match to the scanned aspecular *Lab* measurements.

We utilize ColorNet to create formulas for paints designed in the CACAD software. The aspecular *Lab* values (the parameters from the reflection model) are required as well as a paint code to be used as a formulation starting point. The BRDF Design Suite outputs the aspecular *Lab* values as an XML file to be imported into ColorNet. Since the color may be designed from scratch we need to find the paint code for a close match. ColorSnap, described in Section 5.3.5, finds the paint code of the closest color.

5.3.5 ColorSnap

In order for ColorNet to formulate a paint designed from scratch, it needs the paint code of a similar paint to use as a starting point. We designed ColorSnap to solve this problem. ColorSnap finds the closest color in the SpectraMaster database to a designed color. It visualizes the designed color relative to the entire SpectraMaster database in a three dimensional graph.

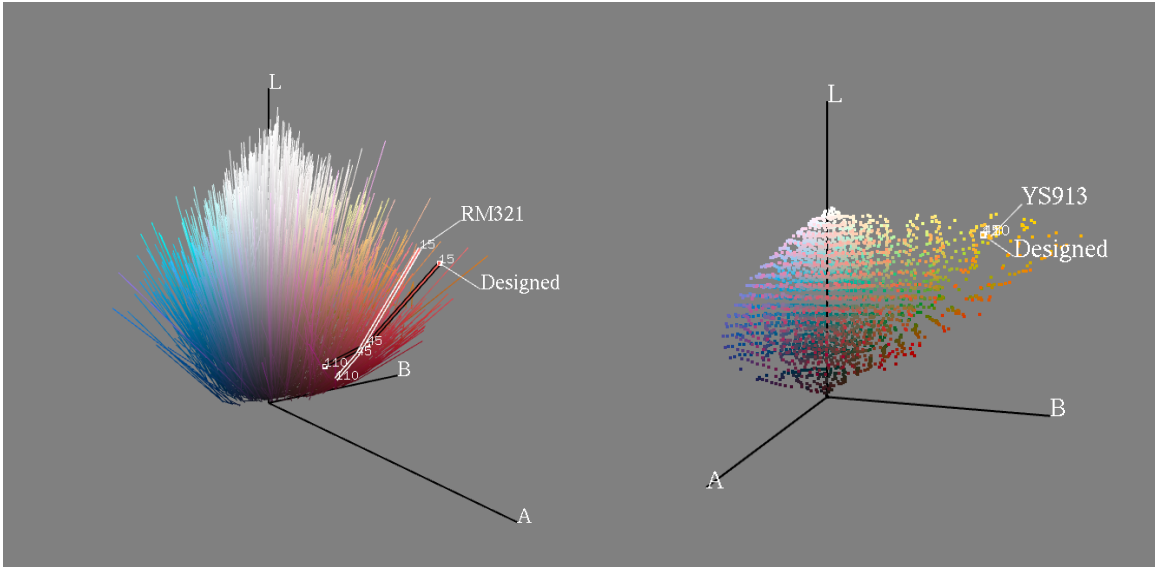


Figure 5.9: Screen shots of ColorSnap: A designed metallic red is shown relative to the nearest metallic color in the SpectraMaster database (left). A bright diffuse yellow color design is shown relative to the nearest solid color in the SpectraMaster database (right).

Colors are plotted in *Lab* space. The nearest color is determined by finding the color in the database with the smallest total ΔE color difference at the three standard aspecular angles. Even though 6,000 colors are searched, the result is found in real time. This is because of the simplicity of the reflectance model representation. Figure 5.9 shows screen shots of ColorSnap in action. A designed metallic red is shown relative to the nearest metallic color in the SpectraMaster database (left). A bright yellow diffuse color's design is shown relative to the nearest solid color in the SpectraMaster database (right).

In Figure 5.10, ColorSnap's visualization exposes two problematic color designs. The designed color on the left is too deep in saturation and shows up plotting far outside the range of colors in the collection. The nearest match, RM209, is the correct hue, but is not chromatic enough. The designed color on the right of Figure 5.10 has a unusual off-radial

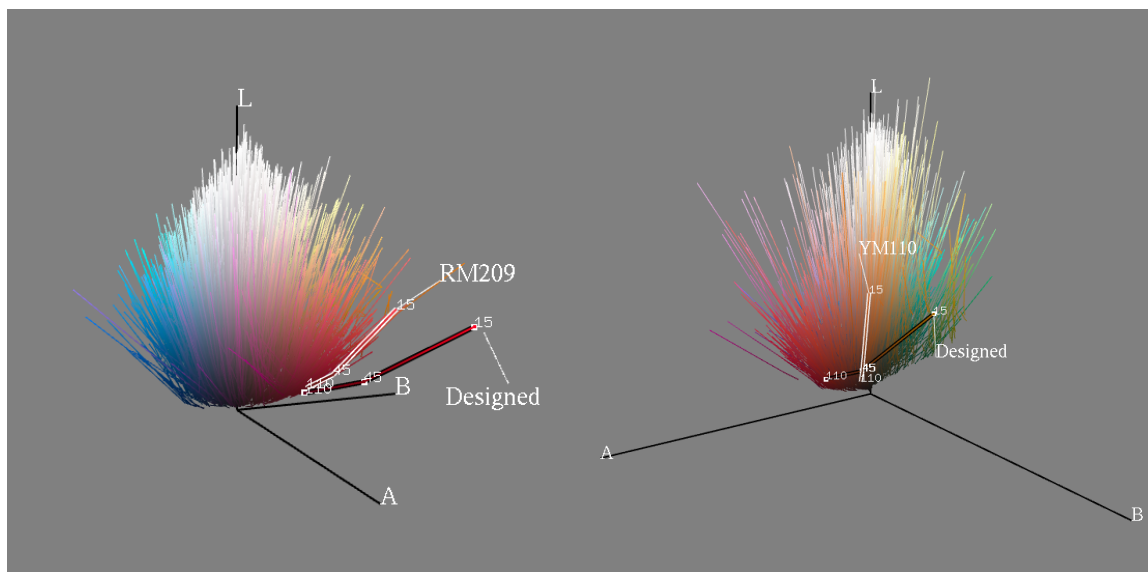


Figure 5.10: ColorSnap’s visualization exposes two problematic color designs. The designed color on the left is too deep in saturation and shows up hanging far outside range of colors in the collection. The nearest match, RM209, is the correct hue, but not chromatic enough. The designed color on the right has a unusual off-radial travel. The closest match does not capture the hue-shifting nature of the design.

travel. The closest match does not capture the hue-shifting nature of the design. A paint chemist needs to be consulted to determine if this color can be manufactured with available technology.

The BRDF Viewer can render multiple colors on a single object. This is useful for comparing a designed color to the closest match in the database or a predicted match from ColorNet. ColorSnap’s visualization reveals that a designed color has a brighter face and a darker flop than the nearest match (Figure 5.11 left). A rendering is used to evaluate the difference between the designed color compared to the closest match, RM331 (right image). Given RM331 as a starting point, ColorNet will attempt to formulate a better match for the designed color.

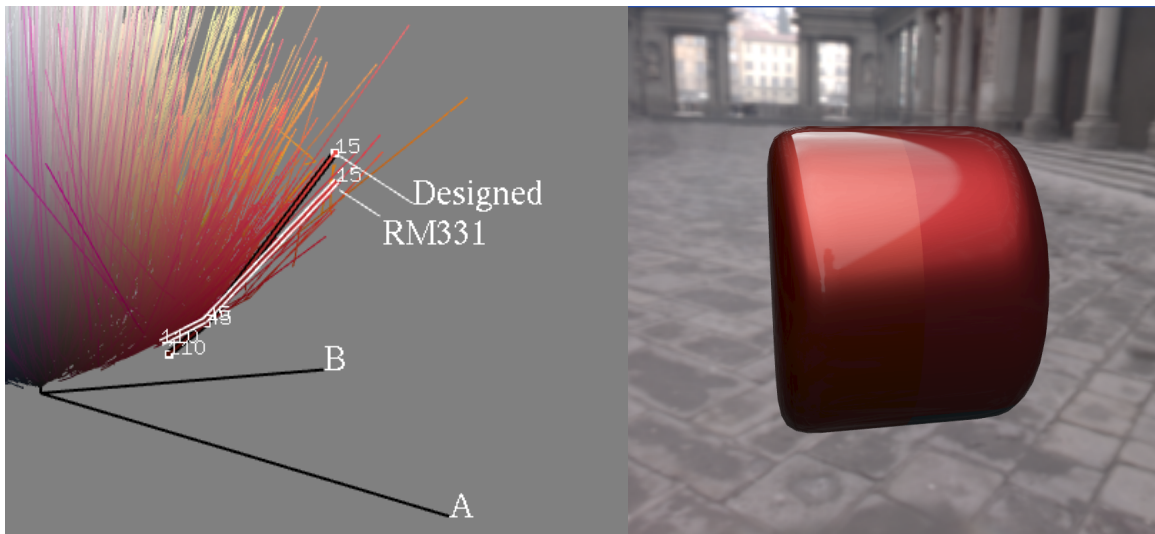


Figure 5.11: ColorSnap’s visualization reveals that the designed color has a brighter face and a darker flop than the nearest match (left image). The rendering shows the designed color on the left side of the cylinder and the closest match, RM331, on the right side of the cylinder (right image).

5.4 Results

We have made several attempts at testing the rapid color prototyping system. The first experiment was with DuPont. The authors participated in a successful one day rapid prototyping experiment using a CACAD system [38, 39]. An automotive stylist used a CACAD tool to create a new paint based on an existing paint [54]. With the help of a paint formulation system, the paint was mixed and sprayed on a surface. Under controlled lighting and using calibrated monitors, a cross comparison was made between the designed paint and the actual paint samples. The chemists, designers, and computer scientists involved in the experiment thought that the accuracy of the comparison of color and reflection was satisfactory for use in an actual automotive production environment. The details of the experiment were first published in [39].

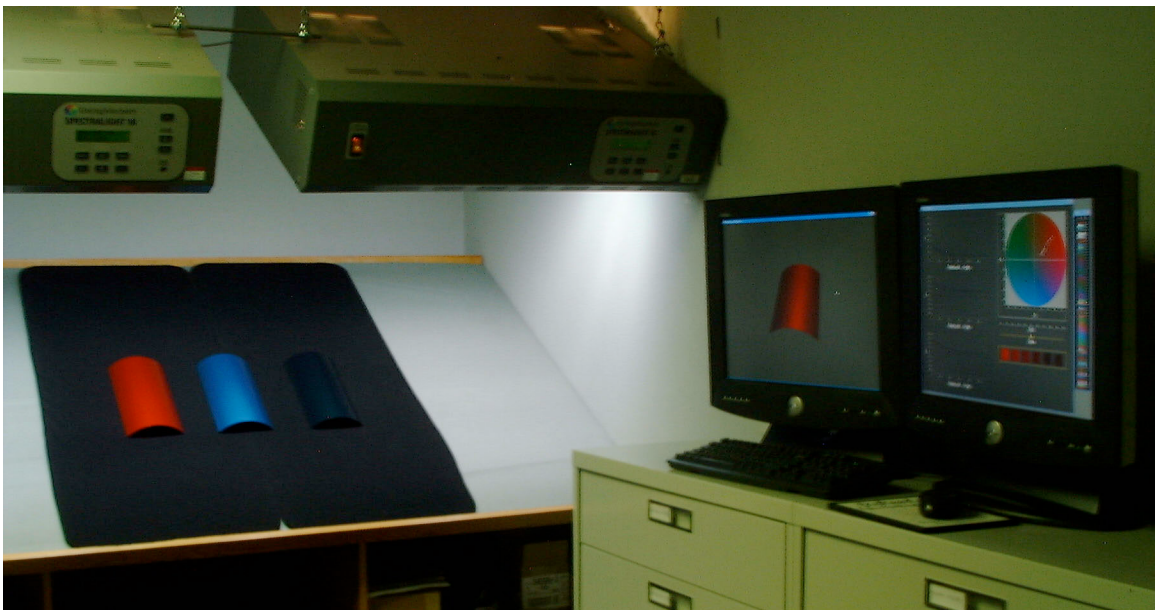


Figure 5.12: Experimental setup for the rapid color prototyping experiment at DuPont.

The rest of the experiments were variations of the first and will be discussed in turn in this section. The experiment with CCS involved creating colors for an entire classroom of students studying automotive design. The experiment at Ford's automotive design center was done using only the paint systems found on their site. The experiment with University of Minnesota's School of Architecture used colors selected from a photograph and interpolated to create a metallic color gradient for a building facade.

5.4.1 Ford Design

Two tests were performed using members of the professional automotive design staff at the Ford Motor Company in Dearborn, Michigan. An initial experiment, done at the headquarters of DuPont Performance Coatings in Troy, Michigan, involved the creation of three new paint colors. The hue of an existing blue metallic paint was shifted towards green,



Figure 5.13: Ford Design Center color test.

the lightness of another blue metallic paint was increased, and gold highlights were added to the travel of a red metallic paint. These paints were formulated, mixed, sprayed, and evaluated at DuPont's labs (Figure 5.12). The satisfactory results of this experiment have been previously documented in [39].

In a more recent test, a new paint color was designed right on Ford's premises. The travel of an existing blue metallic paint (Figure 5.13) was decreased. DuPont used their software to determine the paint formula necessary to achieve the design intent, but the paint was mixed and sprayed at Ford. The whole process, performed during a meeting of Ford's color and trim group, took less than an hour. The outcome was judged to be adequate by the design professionals who participated.



Figure 5.14: Ryan Abellera's gold truck.

5.4.2 College for Creative Studies

The software was used by the students in a one term junior level transportation design class at the College for Creative Studies (CCS) in Detroit, Michigan. CCS is one of the premier automotive design schools in the world, and the design project undertaken in each course is sponsored by a major automotive manufacturer. In this particular class, Toyota asked the students to create a next generation vehicle for their Scion brand. The students were responsible for the complete development of their design, from concept artwork that defines the initial shape and form of the vehicle, through tape drawings that are used to refine the



Figure 5.15: Sarah Montgomery's mood board.

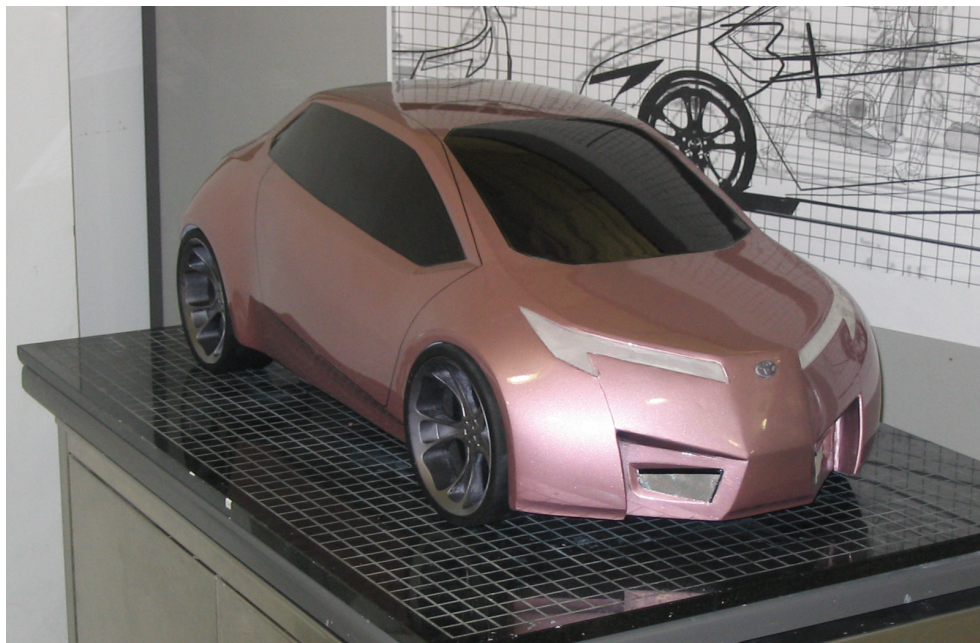


Figure 5.16: Sarah Montgomery's car with color selected to match fashion stockings.

lines of the car, to a final one quarter scale clay model that is finished using automotive paint. The students in the class were given the option of selecting their paint color using our software tools or by working with traditional paint chips.

The students primarily employed our software to visualize the small physical color samples in the SpectraMaster Book (see Section 5.3.2) on a three dimensional form. Many of the students who started the color selection process from scratch found it useful to first browse

through the real SpectraMaster Book to identify a range of interesting colors. They were then able to refine their selection by working with the Virtual SpectraMaster Color Library (see Section 5.3.3) to pick specific colors and by using the BRDF Viewer (see Section 2) to observe the color on a three dimensional form. Figure 5.14 shows a color that was selected by using this process.

Some of the students had very specific ideas about the colors that they wanted to use for their designs, and a few of them had artwork or pictures that illustrated the desired color appearance. The software did not contain the artistic color styling tools described in Chapter 3 at the time that the experiments were performed at CCS. This made it necessary to visually match the colors in the student's pictures with the available colors in the Virtual SpectraMaster Color Library. A "mood board" for one of the students is shown in Figure 5.15, and the color that was chosen to match a clothing item on the board is illustrated in Figure 5.16.

A few students attempted to create custom colors by using the BRDF Designer (see Section 3.4). In most cases this was accomplished by making a small adjustment to an existing color in the SpectraMaster Color Library. The desired CIE Lab values at specific reflectance angles were output by the BRDF Designer program and were passed to the DuPont ColorNet software (see Section 5.3.4). It was not possible to determine a paint formula for each of the designed colors. The concept art which inspired one color design is shown in Figure 5.17, the student used the BRDF Designer to recreate the car paint from his concept art, and the final paint applied to the model is illustrated in Figure 5.18.

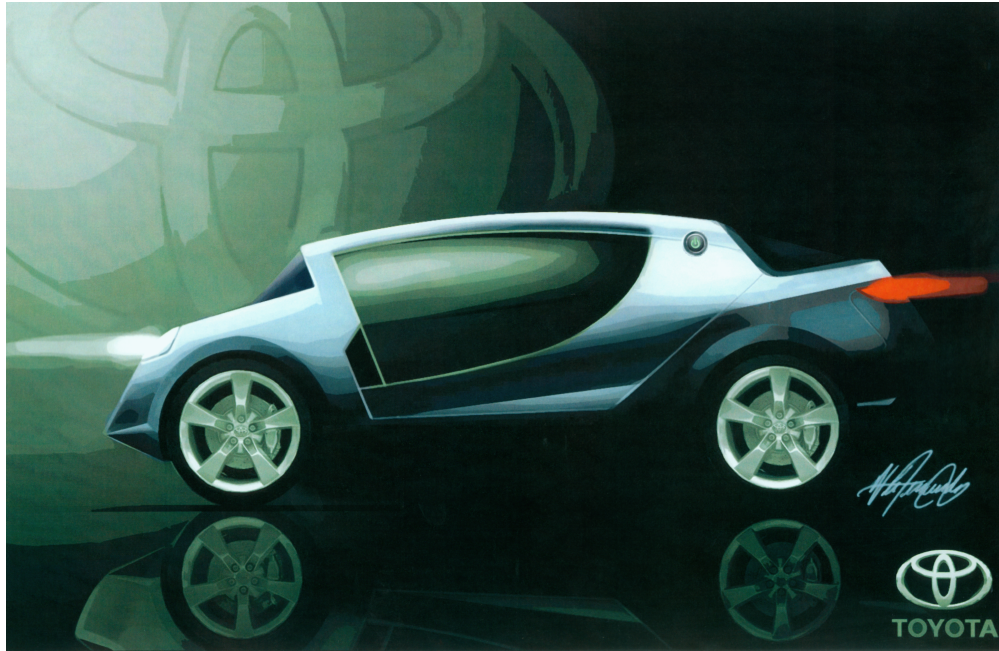


Figure 5.17: Victor Fernandez's concept art



Figure 5.18: Victor Fernandez's car with custom paint.



Figure 5.19: The BRDF Design Suite was employed by a paint engineering group at a major automotive manufacturer to redesign an old silver paint (left) to a new silver paint (right) to better compete with their competitor’s selection.

5.4.3 Automotive Engineering

At the request of the paint engineering group for a major automotive manufacturer, the BRDF Viewer was employed to compare the travel of the company’s silver paint with the travel of two competitor’s silver paints. Measurements were provided for all three paints and were input into the BRDF Designer. The resulting pictures generated by the BRDF Viewer are shown in Figure 5.19. Engineers present at a meeting were able to see qualitative differences between the paints, could discuss the significance of the variation, and were able to formulate a strategy to improve their competitive position.

5.4.4 UM Architecture/HouMinn Practice

The BRDF Design Suite was employed to select metallic colors for an architectural façade. This prototype wall was constructed from large metal “bricks” that were each painted a different metallic color. The goal was to create metallic color sequences for the wall that blended into the surrounding environment but were also harmonious. A small amount of additional software was developed to interpolate between the principle metallic colors that were selected by the project’s architect [6]. The final prototype is shown in Figure 5.20.



Figure 5.20: UM architecture façade.

5.5 Conclusions

A recent cross-pollination of ideas and technologies has enabled the creation of a complete CAD suite for the design of metallic automotive surface finishes. Computer graphics provides the tools for interactive realistic rendering and computer aided design of color appearance. Color science and the appearance industry provide measurement, formulation, and manufacturing technologies. This partnership has culminated with the creation of a rapid color prototyping system.

This chapter describes how digital color design tools were connected with paint formulation systems to create a rapid color prototyping system for metallic automotive paints. The Virtual SpectraMaster Color Library provides both a traditional interface for browsing the colors as well as advanced filtering capabilities. Another tool, called ColorSnap, visualizes designed colors relative to the rest of the SpectraMaster database and finds starting points for the paint formulation system. Finally, a series of experiments showed the rapid color prototyping in action in a variety of environments.

Rapid color prototyping enables us to create new solutions to problems faced by the color appearance industry. One issue confronted by color stylists is that the current breed of CACAD tools are too technical. These tools are unable to leverage the unique creative skills of many color stylists who have been trained in the traditional creative fields such as fashion design, industrial design, or the traditional arts. Chapter 3 describes new creative electronic design tools inspired by traditional creative processes employed by color stylists in the industry today. The surface finishes designed with these creative tools can be rapidly prototyped using the system described in this chapter.

In Chapter 4, we have looked at another common problem facing color stylists in the automotive industry: color mismatches stemming from geometric misalignment of body panels. Even though the color is consistent across the two parts, a visual difference in color is seen because they are viewed at slightly different angles. We are using computer graphics to understand this problem, and we are employing mathematical optimization techniques to help the color stylist to avoid and/or correct these geometric color mismatches. Rapid prototyping of color allows the color of both or just one of the two body panels to be adjusted to account for the observed color differences.

The future may include CACAD systems for all types of material design including plastics, glass, textiles, wood stains, and other nanotech surface finishes. In order to be truly useful, these CACAD systems will have measurement, visualization, analysis, design, and rapid color prototyping tools. Color, texture, and appearance will be manipulated at macro, meso, and microscopic detail levels. Finally, rapid color prototyping will be integrated into 3D printers to create a physical objects, complete with surface finish, from electronic designs. The future of industrial design is very bright.

Chapter 6

Conclusions

The main research contribution of this thesis is the first complete working computer aided color appearance design system. All of the major components and ideas of CAD are applied to color appearance. This dissertation used the real-world task of styling metallic automotive finishes as the problem domain. The fundamental components of CAD are applied to this undertaking including visualization, design, analysis/optimization, and scanning/prototyping tools.

The ability of computer graphics to visualize parametric and polygonal surfaces in real time made CAD possible. Seeing how a shape changes in real time is a fundamental component of the iterative design loop. The design component of the system is the interface between the computer model and the user. CAD software often provides many techniques for creating and modifying surfaces and shapes. Low level interface modes allow for manipulation of individual vertices or control points.

Higher level interface modes, like genetic variations or procedural generation, represent new ways to create surfaces. Analysis and optimization of the virtual model represent the

highest echelon of the design interface. For example, finite element analysis allows the virtual testing of a design before it is manufactured. When coupled with an optimization algorithm, a numerically quantifiable heuristic like cost or efficiency can be minimized or maximized. Scanning and prototyping is the connection between the physical world and the CAD environment using 3D laser scanners, CNC milling machines, and solid freeform fabrication devices.

One of the most important aspects of the computer aided design workflow is the ability to continually visualize changes as the design is created. Simple point lighting does not allow accurate depiction of complex surface reflection effects. In Chapter 2, a computer graphic rendering system is created to do computer aided color appearance design using photographically acquired lighting. This represents the visualization component of the CACAD package.

In Chapter 3, a number of color styling tools are developed. This is the main design interface of the CACAD package. The first tools created were very technical in nature, but they were still adopted by industry as tools that the color scientists and chemists could use for working with metallic paints. The rest of the tools in Chapter 3 are creative tools for designers. A virtual mood-board replicates the important brainstorming that many color stylists use to conceptualize and refine color and material ideas. A spot color styler allows a designer to refine a surface finish as it plays across a 3D object in a direct way. Finally, a sketch based design interface that utilizes the workflow of a concept artist is also introduced. The system is shown to work with hand drawn concept art and concept art created in Photoshop.

In Chapter 4, color mismatches that resulted from geometric misalignment were studied. Differences in color can result when adjacent parts of an object are coated with the same paint but are not aligned to create a continuous geometric surface. The color difference that results due to shading can be accentuated by the use of metallic and pearlescent paints with goniochromatic properties. By using computer graphics and computer science we were able to approach this problem from an entirely new perspective compared to a traditional color science approach. We were able to create a metric for determining when the color difference is large enough for the misalignment to become apparent. We were also able to create a technique for selecting a paint that matches the adjacent part and creates the illusion of geometric continuity even though the two parts are misaligned.

In Chapter 5, a rapid color prototyping system is created to bring color concepts from conceptualization to fabrication. This system was the first rapid prototyping system for color appearance. This chapter was made possible by a partnership with the color scientists at DuPont Performance Coatings. A virtual SpectraMaster book guides the user to browse color collections in a targeted manner. A search tool takes the user's new designs for paints and rapidly obtains the color chip code for the closest existing paint for review. This paint code can be employed as a starting point for use of the color styling tools.

By creating the first complete and fully operational CACAD system, this research brings the concept of computer aided color appearance design to realization. Because of its utility, commercial CACAD systems will emerge for all fields of design where color and appearance are important. These color design systems will have all of the components of CAD specialized for color appearance.

CACAD's success depends on the software creators having a cross disciplinary approach accounting for the engineering requirements to manipulate color appearance as well as the tasks and mindset of the people using the software. In the case of designers, their creative discipline [60] creates a completely different mindset than that of an engineer. These differences should be celebrated when producing a CAD interface for these talented individuals.

The CACAD system created for this research was shown to work successfully in a variety of environments from automotive design to prototyping architecture color schemes. The first experiment was done at DuPont Performance Coatings' headquarters with an experienced color stylist from the Ford Motor Company. The task was to design a few new metallic colors using the design software. These colors were formulated and painted onto color proposal cylinders for evaluation. The experiment took less than a day and was considered a success by everyone involved.

Many people doing material design in the automotive industry have backgrounds such as fashion design, interior design, or the traditional arts but are forced to work with technical design tools. Currently the existing computer tools for color simulation and selection do not readily facilitate the color design process used in these traditional design fields. In fact, the problem of creative people being forced to work with technical design tools carries over into many other fields of computer aided design and computer aided art. As a result, there are endless opportunities for using computer science, computer graphics, and engineering to serve artists, designers, and other creative people.

Bibliography

1. Sameer Agarwal, Ravi Ramamoorthi, Serge Belongie, and Henrik Wann Jensen. Structured Importance Sampling of Environment Maps. In *Proceedings of SIGGRAPH '03*, Pages 605–612, 2003.
2. David H. Alman. Directional Color Measurement of Metallic Flake Finishes. In *Proceedings of the ISCC Williamsburg Conference on Appearance*, Pages 53–56, 1987.
3. Ken-Ichi Anjyo, Shuhei Wemler, and William Baxter. Tweakable Light and Shade for Cartoon Animation. In *Proceedings of NPAR '06*, Pages 133–139, 2006.
4. Michael Ashby and Kara Johnson. *Materials and Design: The Art and Science of Material Selection in Product Design*, Pages 41–42, Butterworth-Heinemann, Oxford, 2002.
5. Aner Ben-Artzi, Ryan Overbeck, and Ravi Ramamoorthi. Real-time BRDF Editing in Complex Lighting. In *Proceedings of SIGGRAPH '06*, Pages 945–954, 2006.

6. Seth Berrier, Gary Meyer, and Clement Shimizu. Creating Metallic Color Sequences for an Architectural Wall. In *Proceedings of ACADIA '08*, Pages 308–313, 2008.
7. Carole Bouchard, Jean Francois Omhover, Celine Mougenot, Ameziane Aoussat, and Stephen J. Westerman. Trends: A Content-based Information Retrieval System for Designers. In *Proceedings of Design Computing and Cognition '08*, Pages 593–611, 2008.
8. David H. Brainard and Laurence T. Maloney. Perception of Color and Material Properties in Complex Scenes. In *Journal of Vision*, Volume 4, Issue 9, Pages 2–4, 2004.
9. Mark Colbert, Sumanta Pattanaik, and Jaroslav Krivanek. BRDF-shop: Creating Physically Correct Bidirectional Reflectance Distribution Functions. In *IEEE Computer Graphics and Applications*, Volume 26, Issue 1, Pages 30–36, 2006.
10. Forrester Cole, Aleksey Golovinskiy, Alex Limpaecher, Heather Stoddart Barros, Adam Finkelstein, Thomas Funkhouser, and Szymon Rusinkiewicz. Where do People Draw Lines? In *Proceedings of SIGGRAPH '08*, Pages 1–11, 2008.
11. Robert L. Cook and Kenneth E. Torrance. A Reflectance Model for Computer Graphics. In *ACM Transactions on Graphics*, Volume 1, Issue 1, Pages 7–24, 1982.

12. Paul Debevec. Rendering Synthetic Objects into Real Scenes: Bridging Traditional and Image-based Graphics with Global Illumination and High Dynamic Range Photography. In *Proceedings of SIGGRAPH '98*, Pages 189–198, 1998.
13. Paul Debevec and Chris Tchou. *HDR Shop*. Online at <http://www.hdrshop.com>, Accessed 2001.
14. Ron Dror, Edward H. Adelson, Alan S. Willsky. Recognition of Surface Reflectance Properties from a Single Image under Unknown Real-World Illumination. In *Proceedings of the IEEE Workshop on Identifying Objects Across Variations in Lighting*, Pages 1–8, 2001
15. DuPont Performance Coatings. *Spectramaster Solid, Metallic, and Pearl Color Library*. Online at <http://www.performancecoatings.dupont.com>, Accessed 2005
16. Sergey Ershov, Konstantin Kolchin, and Karol Myszkowski. Rendering Pearlescent Appearance Based on Paint-composition Modelling. In *Proceedings of Eurographics '01*, Pages 227–238, 2001.
17. Roland W. Fleming, Ron O. Dror, and Edward H. Adelson. Real-world Illumination and the Perception of Surface Reflectance Properties. In *Journal of Vision*, Volume 3, Issue 5, Pages 347–368, 2003.
18. Saul I. Gass. *Linear Programming*, Page 395. McGraw-Hill, New York, 1984.

19. Johannes Günther, Tongbo Chen, Michael Goesele, Ingo Wald, and Hans-Peter Seidel. Efficient Acquisition and Realistic Rendering of Car Paint. In *Proceedings of 10th International Fall Workshop - Vision, Modeling, and Visualization*, Pages 487–494, 2005.
20. Wolfgang Heidrich and Hans-Peter Seidel. Realistic, Hardware-accelerated Shading and Lighting. In *Proceedings of SIGGRAPH '99*, Pages 171–178, 1999.
21. Richard S. Hunter and Richard W. Harold. *The Measurement of Appearance*, Pages 68–94. Wiley-IEEE, New York, 1987.
22. Rafal Jaroszkiewicz and Michael D. McCool. Fast Extraction of BRDFs and Material Maps from Images. In *Proceedings of Graphics Interface*, Pages 1–10, 2003.
23. Joe Marks, Brad Andalman, Paul A. Beardsley, William T. Freeman, S. Gibson, Jessica K. Hodgins, T. Kang, Brian Mirtich, Hanspeter Pfister, Wheeler Ruml, Kathy Ryall, J. Seims, and Stuart M. Shieber. Design Galleries: A General Approach to Setting Parameters for Computer Graphics and Animation. In *Proceedings of SIGGRAPH '97*, Pages 389–400, 1997.
24. Jan Kautz and Michael D. McCool. Interactive Rendering with Arbitrary BRDFs using Separable Approximations. In *Proceedings of the Tenth Eurographics Workshop on Rendering*, Pages 281–292, 1999.

25. Jan Kautz and Michael D. McCool. Approximation of Glossy Reflection with Prefiltered Environment Maps. In *Proceedings of Graphics Interface '00*, Pages 119–126, 2000.
26. Jan Kautz, Peter-Pike Sloan, and John Snyder. Fast, Arbitrary BRDF Shading for Low Frequency Lighting Using Spherical Harmonics. In *Proceedings of the 13th Eurographics Workshop on Rendering*, Pages 291–296, 2002.
27. Jan Kautz, Pere-Pau Vázquez, Wolfgang Heidrich, and Hans-Peter Seidel. A Unified Approach to Prefiltered Environment Maps. In *Proceedings of Eurographics Workshop on Rendering Techniques '00*, Pages 185–196, 2000.
28. Eric P. F. Lafortune, Sing-Choong Foo, Kenneth E. Torrance, and Donald P. Greenberg. Non-linear Approximation of Reflectance Functions. In *Proceedings of SIGGRAPH '97*, Pages 117–126, 1997.
29. Daniel Fylstra, Leon Lasdon, John Watson, and Allan Waren. Design and Use of the Microsoft Excel Solver. In *Interfaces*, Volume 28, Issue 5, Pages 29–55, 1998.
30. Jason Lawrence, Aner Ben-Artzi, Christopher DeCoro, Wojciech Matusik, Hanspeter Pfister, Ravi Ramamoorthi, and Szymon Rusinkiewicz. Inverse Shade Trees for Nonparametric Material Representation and Editing. In *Proceedings of SIGGRAPH '06*, Pages 735–745, July 2006.

31. Hendrik P. A. Lensch, Jan Kautz, Michael Goesele, Wolfgang Heidrich, and Hans-Peter Seidel. Image-based Reconstruction of Spatially Varying Materials. In *Proceedings of the Eurographics Rendering Workshop '01*, Pages 103–114, 2001.
32. Robert R. Lewis. Making shaders more physically plausible. In *Proceedings of the Eurographics Rendering Workshop '94*, Pages 109–120, 1994.
33. William R. Mark, R. Steven Glanville, Kurt Akeley, and Mark J. Kilgard. Cg: A System for Programming Graphics Hardware in a C-like Language. In *Proceedings of SIGGRAPH '03*, Pages 896–907, 2003.
34. Wojciech Matusik, Hanspeter Pfister, Matt Brand, and Leonard McMillan. A Data Driven Reflectance Model. In *Proceedings of SIGGRAPH '03*, Pages 759–769, 2003.
35. David K. McAllister, Anselmo Lastra, and Wolfgang Heidrich. Efficient Rendering of Spatial Bi-directional Reflectance Distribution Functions. In *Proceedings of Graphics Hardware '02*, Pages 79–88, 2002.
36. Michael D. McCool and Wolfgang Heidrich. Texture Shaders. In *Proceedings of the SIGGRAPH/EUROGRAPHICS Workshop on Graphics Hardware '99*, Pages 117–126, 1999.

37. Gary W. Meyer. Computer Aided Color Appearance Design. In *CGIP '00: The First International Conference on Color in Graphics and Image Processing*, Pages 195–200, 2000.
38. Gary W. Meyer and Clement Shimizu. Computational Automotive Color Appearance. In *Proceedings of Computational Aesthetics '05*, Pages 217–222, 2005.
39. Gary W. Meyer, Clement Shimizu, Alan Eggly, David Fischer, Jim King, and Allan Rodriguez. Computer Aided Design of Automotive Finishes. In *Proceedings of AIC Colour '05*, Pages 685–688, 2005.
40. Ren Ng, Ravi Ramamoorthi, and Pat Hanrahan. All-frequency Shadows Using Nonlinear Wavelet Lighting Approximation. In *Proceedings of SIGGRAPH '03*, Pages 376–381, 2003.
41. Addy Ngan, Fredo Durand, and Wojciech Matusik. Image-driven Navigation of Analytical BRDF Models. In *Proceedings of the 17th Eurographics Workshop on Rendering*, Pages 399–408, 2006.
42. Peter Notebaert, Michel Berkelaar, and Kjell Eikland. *Lp Solve, An Open Source Linear Programming System*. Online at <http://www.geocities.com/lpsolve>, Accessed 1995.

43. Romain Pacanowski, Xavier Granier, Christophe Schlick, and Pierre Poulin. Sketch and Paint-based Interface for Highlight Modeling. In *Eurographics Workshop on Sketch-based Interfaces and Modeling '08*, Pages 17–23, 2008.
44. Fabio Pellacini and Jason Lawrence. Appwand: Editing Measured Materials Using Appearance-driven Optimization. In *Proceedings of SIGGRAPH '07*, Pages 54.1–54.9, 2007.
45. Bui Tuong Phong. Illumination for Computer Generated Pictures. In *Communications of the ACM*, Volume 18, Issue 6, Pages 311–317, 1975.
46. William H. Press, Saul A. Teukolsky, William T. Vetterling, and Brian P. Flannery. *Numerical Recipes in C: The Art of Scientific Computing (2nd ed.)*. Cambridge University Press, Cambridge, England, 1992.
47. Ravi Ramamoorthi and Pat Hanrahan. A Signal-processing Framework for Inverse Rendering. In *Proceedings of SIGGRAPH '01*, Pages 117–128, 2001.
48. Allan B. J. Rodrigues. Measurement of Metallic and Pearlescent Finishes. In *Die Farbe*, Volume 37, Pages 65–78, 1990.
49. Allan B. J. Rodrigues. Color and Appearance Measurement of Metallic and Pearlescent Finishes. In *ASTM Standardization News*, Volume 23, Issue 10, Pages 68–72, 1995.

50. Jose Manuel Medina Ruiz. Proposed Metameric Indices for Goniochromatic Objects. In *Color Research & Application*, Issue 27, Volume 6, Pages 382–390, 2002.
51. Helge Seetzen, Wolfgang Heidrich, Wolfgang Stuerzlinger, Greg Ward, Lorne Whitehead, Matthew Trentacoste, Abhijeet Ghosh, and Andrejs Vorozcovs. High Dynamic Range Display Systems. In *Proceedings of SIGGRAPH '04*, Pages 760–768, 2004.
52. Clement Shimizu and Gary W. Meyer. Computer Aided Color Appearance Design Using Environment Map Based Lighting. In *Proceedings of Computational Aesthetics '05*, Pages 223–230, 2005.
53. Clement Shimizu and Gary W. Meyer. Predicting and Fixing Geometric Color Mismatches. To appear in *Proceedings of AIC Colour '09*, 2009.
54. Clement Shimizu, Gary W. Meyer, and Joseph P. Wingard. Interactive Goniochromatic Color Design. In *Proceedings of the 11th Color Imaging Conference*, Pages 16–22, 2003.
55. Peter Shirley and Kenneth Chiu. Notes on Adaptive Quadrature on the Hemisphere. *Department of Computer Science Technical Report TR-411*, Indiana University, 1994

56. Peter-Pike Sloan, Jan Kautz, and John Snyder. Precomputed Radiance Transfer for Real-time Rendering in Dynamic, Low-frequency Lighting Environments. In *Proceedings of SIGGRAPH '02*, Pages 527–536, 2002.
57. Peter-Pike J. Sloan, William Martin, Amy Gooch, and Bruce Gooch. The Lit Sphere: A Model for Capturing NPR Shading From Art. In *Proceedings of Graphics Interface '01*, Pages 143–150, 2001.
58. Roberta Gordon Smith. *Trompe L'Oeil: Creating Decorative Illusions With Paint*. David and Charles Publishers, Newton Abbot, UK, 2001.
59. Roberta Gordon Smith. *Trompe L'Oeil Home*. Watson-Guptill Publications, New York, 2001.
60. Twyla Tharp. *The Creative Habit: Learn It and Use It for Life*. Simon & Schuster, New York, 2005.
61. Mihran Tuceryan and Anil K. Jain. Texture Analysis. In *Handbook of Pattern Recognition & Computer Vision*, Pages 235–276, 1993.
62. Susumu Umemura. Innovative Color Development Procedure for Automobiles. In *Journes Internationales D'etude sur la Nition des Carrosseries Automobiles*, 2007.
63. William H. Venable. A Model for Interpreting Three-angle Measurements of Flake Finishes. In *Proceedings of the ISCC Williamsburg Conference on Appearance*, Pages 57–60, 1987.

64. Gregory J. Ward. Measuring and Modeling Anisotropic Reflection. In *Proceedings of SIGGRAPH '92*, Pages 265–272, 1992.
65. Harold B. Westlund and Gary W. Meyer. Applying Appearance Standards to Light Reflection Models. In *SIGGRAPH '01*, Pages 501–510, 2001.
66. Peter Wissling. *Metallic Effect Pigments: Basics and Applications*, Page 27, Vincentz Network, Hanover, Germany, 2006.
67. Tsung-Yi Wu, Wan-Chun Ma, Yung-Yu Chuang, Bing-Yu Chen, and Ming Ouhyoung. Image-based BRDF Acquisition for Non-spherical Objects. In *Proceedings of CVGIP '05*, 2005.
68. Yizhou Yu, Paul Debevec, Jitendra Malik, and Tim Hawkins. Inverse Global Illumination: Recovering Reflectance Models of Real Scenes From Photographs. In *Proceedings of SIGGRAPH '99*, Pages 215–224, 1999.